NTIS #PB96-129101

# SSC-385

# Hydrodynamic Impact on Displacement Ship Hulls

## *An Assessment of the State of the Art*

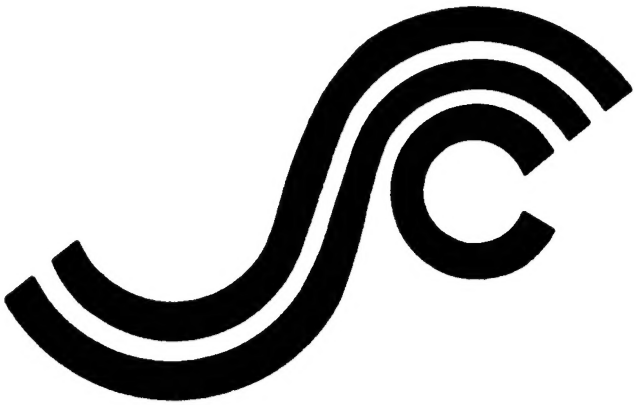



This document has been approved for public release and sale; its distribution is unlimited

**SHIP STRUCTURE COMMITTEE**

**1995**

## SHIP STRUCTURECOMMITTEE

The SHIP STRUCTURE COMMITTEE is constituted to prosecute a research program to improve the hull structures of ships and other marine structures by an extension of knowledge pertaining to design, materials, and methods of construction.

RADM J. C. Card, USCG (Chairman)
Chief, Office of Marine Safety, Security
and Environmental Protection
U. S. Coast Guard

Mr. Thomas H. Peirce
Marine Research and Development
Coordinator
Transportation Development Center
Transport Canada

Mr. Edwin B. Schimler
Associate Administrator for Ship-
building and Technology Development
Maritime Administration

Dr. Donald Liu
Senior Vice President
American Bureau of Shipping

Mr. Robert McCarthy
Director, Survivability and Structural
Integrity Group (SEA O3P)
Naval Sea Systems Command

Mr. Thomas Connors
Acting Director of Engineering (N7)
Military Sealift Command

Dr. Ross Grahm
Head, Hydronautics Section
Defence Research Establishment-Atlantic

EXECUTIVE DIRECTOR

CDR Stephen E. Sharpe, USCG
U. S. Coast Guard

CONTRACTING OFFICER TECHNICAL REPRESENTATIVE

Mr. William J. Siekierka
Naval Sea Systems Command

## SHIP STRUCTURESUBCOMMITTEE

The SHIP STRUCTURE SUBCOMMITTEE acts for the Ship Structure Committee on technical matters by providing technical coordination for determinating the goals and objectives of the program and by evaluating and interpreting the results in terms of structural design, construction, and operation.

MILITARY SEALIFT COMMAND

Mr. Robert E. Van Jones (Chairman)
Mr. Rickard A. Anderson
Mr. Michael W. Touma
Mr. Jeffrey E. Beach

MARITIME ADMINISTRATION

Mr. Frederick Seibold
Mr. Richard P. Voelker
Mr. Chao H. Lin
Dr. Walter M. Maclean

U. S. COAST GUARD

CAPT George Wright
Mr. Walter Lincoln
Mr. Rubin Sheinberg

AMERICAN BUREAU OF SHIPPING

Mr. Glenn Ashe
Mr. John F. Conlon
Mr. Phillip G. Rynn
Mr. William Hanzelek

NAVAL SEA SYSTEMS COMMAND

Mr. W. Thomas Packard
Mr. Charles L. Null
Mr. Edward Kadala
Mr. Allen H. Engle

TRANSPORT CANADA

Mr. John Grinstead
Mr. Ian Bayly
Mr. David L. Stocks
Mr. Peter Timonin

DEFENCE RESEARCH ESTABLISHMENT ATLANTIC

Dr. Neil Pegg
LCDR Stephen Gibson
Dr. Roger Hollingshead
Mr. John Porter

## SHIP STRUCTURE SUBCOMMITTEE LIAISON MEMBERS

SOCIETY OF NAVAL ARCHITECTS AND MARINE ENGINEERS
Dr. William Sandberg

CANADA CENTRE FOR MINERALS AND ENERGY TECHNOLOGIES
Dr. William R. Tyson

U. S. NAVAL ACADEMY
Dr. Ramswar Bhattacharyya

U. S. MERCHANT MARINE ACADEMY
Dr. C. B. Kim

U. S. COAST GUARD ACADEMY
LCDR Bruce R. Mustain

U. S. TECHNICAL ADIVSORY GROUP TO THE INTERNATIONAL STANDARDS ORGANIZATION
CAPT Charles Piersall

NATIONAL ACADEMY OF SCIENCES - MARINE BOARD
Dr. Robert Sielski

NATIONAL ACADEMY OF SCIENCES - COMMITTEE ON MARINE STRUCTURES
Dr. John Landes

WELDING RESEARCH COUNCIL
Dr. Martin Prager

AMERICAN IRON AND STEEL INSTITUTE
Mr. Alexander D. Wilson

OFFICE OF NAVAL RESEARCH
Dr. Yapa D. S. Rajapaske

MASSACHUSETTS INSTITUTE OF TECHNOLOGY
CAPT Alan J. Brown

STUDENT MEMBER
Mr. Jason Miller
Massachusetts Institute of Technology

Member Agencies:

*American Bureau of Shipping*
*Defence Research Establishment Atlantic*
*Maritime Administration*
*Military Sealift Command*
*Naval Sea Systems Command*
*Transport Canada*
*United States Coast Guard*

**Ship Structure Committee**

An Interagency Advisory Committee

Address Correspondence to:

Executive Director
Ship Structure Committee
U.S. Coast Guard (G-MMS/SSC)
2100 Second Street, S.W.
Washington, D.C. 20593-0001
Ph:(202) 267-0003
Fax:(202) 267-4816

SSC-385
SR-1342

2 January 1996

# HYDRODYNAMIC IMPACT ON DISPLACEMENT SHIP HULLS

The ability of the naval architect to optimize the structural design of a ship is limited by both our understanding of, and our ability to predict hydrodynamic loads. In addition to having to account for the random nature of wave induced loads, transient loadings such as slamming, wave slap and frontal impacts must also be addressed. Failure to account for these impulsive loads and how best to combine these loads with ever present slow varying wave induced loads can result in, at best, reduced ship operational time and, at worst, catastrophic failure.

In order to address these concerns, a critical review of the state of the art in predicting hydrodynamic impact forces has been completed. This report identifies numerous theories of hydrodynamic impact loading that have been developed over the years by many researchers. These theories are evaluated to identify which are most applicable for use in design with example calculations presented. Recommendations for future research are given.

J. C. CARD
Rear Admiral, U.S. Coast Guard
Chairman, Ship Structure Committee

**Technical Report Documentation Page**

| 1. Report No. | 2. Government Accession No. | 3. Recipient's Catalog No. |
|---|---|---|
| SSC-385 | PB96-129101 | |

**4. Title and Subtitle**

HYDRODYNAMIC IMPACT LOADING ON DISPLACEMENT SHIP HULLS
- AN ASSESSMENT OF THE STATE OF THE ART -

**5. Report Date**
April 15, 1995

**6. Performing Organization Code**

**8. Performing Organization Report No.**
SR-1342

**7. Author(s)**
Dr. John C. Daidola and Dr. Victor Mishkevich

**9. Performing Organization Name and Address**
M. ROSENBLATT & SON, INC.
350 Broadway
New York, NY 10013

**10. Work Unit No. (TRAIS)**

**11. Contract or Grant No.**
DTCG23-92-C-E01088

**13. Type of Report and Period Covered**
Final Report

**12. Sponsoring Agency Name and Address**
SHIP STRUCTURE COMMITTEE
U. S. COAST GUARD
2100 Second Street, S.W.
Washington, D.C. 20593

**14. Sponsoring Agency Code**
G-M

**15. Supplementary Notes**
Sponsored by the Ship Structure Committee. Jointly funded by its member agencies.

**16. Abstract**

This report provides a comprehensive assessment of the state of the art of hydrodynamic impact loading on displacement ship hulls. The subject is considered in light of the three distinct phenomena of slamming, wave slap, and frontal impact. Factors leading to hydrodynamic impact are defined in terms of environmental and vessel characteristics. The theories of impact are reviewed in sub-categories of two and three dimensional analytical hydrodynamic models, hydroelastic models, seakeeping theory, model tests, and full scale data. The techniques and procedures identified which lend themselves to analysis and potential design application are identified and described, the characteristics of each summarized, and example calculations relating the techniques and procedures presented. The report concludes with recommendations for future research.

| 17. Key Words | 18. Distribution Statement |
|---|---|
| Hydrodynamic, Frontal Impact, Displacement Ships, Slamming, Hydroelastic, Seakeeping, Impact, Wave Slap, Model Tests, Theory | Distribution Unlimited, Available from: National Technical Information Service U.S. Department of Commerce Springfield, VA 22151 |

| 19. Security Classif. (of this report) | 20. Security Classif. (of this page) | 21. No. of Pages | 22. Price |
|---|---|---|---|
| Unclassified | Unclassified | 204 | $36.50 Paper $17.50 Micro |

Form DOT F 1700.7 (8-72) Reproduction of completed page authorized

United States Department of Commerce
Technology Administration
National Institute of Standards and Technology
Metric Program, Gaithersburg, MD 20899

# METRIC CONVERSION CARD

## Approximate Conversions to Metric Measures

| *Symbol* | *When You Know* | *Multiply by* | *To Find* | *Symbol* |
|---|---|---|---|---|
| | **LENGTH** | | | |
| in | inches | 2.5 | centimeters | cm |
| ft | feet | 30 | centimeters | cm |
| yd | yards | 0.9 | meters | m |
| mi | miles | 1.6 | kilometers | km |
| | **AREA** | | | |
| $in^2$ | square inches | 6.5 | square centimeters | $cm^2$ |
| $ft^2$ | square feet | 0.09 | square meters | $m^2$ |
| $yd^2$ | square yards | 0.8 | square meters | $m^2$ |
| $mi^2$ | square miles | 2.6 | square kilometers | $km^2$ |
| | acres | 0.4 | hectares | ha |
| | **MASS** (weight) | | | |
| oz | ounces | 28 | grams | g |
| lb | pounds | 0.45 | kilograms | kg |
| | short tons (2000 lb) | 0.9 | metric ton | t |
| | **VOLUME** | | | |
| tsp | teaspoons | 5 | milliliters | mL |
| Tbsp | tablespoons | 15 | milliliters | mL |
| $in^3$ | cubic inches | 16 | milliliters | mL |
| fl oz | fluid ounces | 30 | milliliters | mL |
| c | cups | 0.24 | liters | L |
| pt | pints | 0.47 | liters | L |
| qt | quarts | 0.95 | liters | L |
| gal | gallons | 3.8 | liters | L |
| $ft^3$ | cubic feet | 0.03 | cubic meters | $m^3$ |
| $yd^3$ | cubic yards | 0.76 | cubic meters | $m^3$ |
| | **TEMPERATURE** (exact) | | | |
| °F | degrees Fahrenheit | subtract 32, multiply by 5/9 | degrees Celsius | °C |

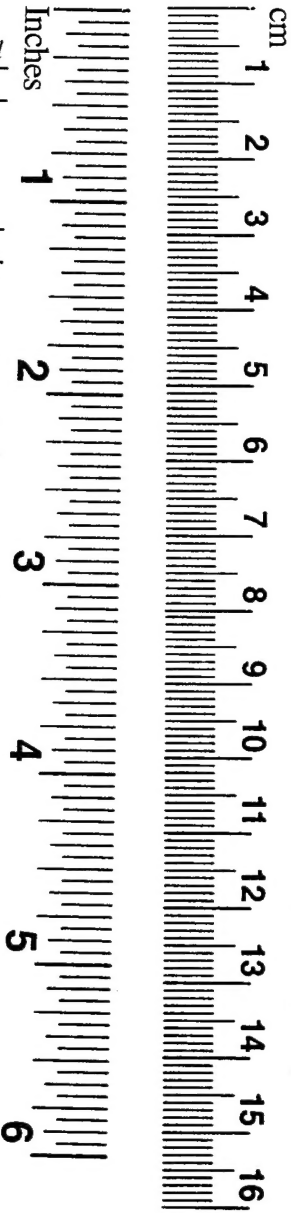


## Approximate Conversions from Metric Measures

| *Symbol* | *When You Know* | *Multiply by* | *To Find* | *Symbol* |
|---|---|---|---|---|
| | **LENGTH** | | | |
| mm | millimeters | 0.04 | inches | in |
| cm | centimeters | 0.4 | inches | in |
| m | meters | 3.3 | feet | ft |
| m | meters | 1.1 | yards | yd |
| km | kilometers | 0.6 | miles | mi |
| | **AREA** | | | |
| $cm^2$ | square centimeters | 0.16 | square inches | $in^2$ |
| $m^2$ | square meters | 1.2 | square yards | $yd^2$ |
| $km^2$ | square kilometers | 0.4 | square miles | $mi^2$ |
| ha | hectares ($10{,}000\ m^2$) | 2.5 | acres | |
| | **MASS** (weight) | | | |
| g | grams | 0.035 | ounces | oz |
| kg | kilograms | 2.2 | pounds | lb |
| t | metric ton (1,000 kg) | 1.1 | short tons | |
| | **VOLUME** | | | |
| mL | milliliters | 0.03 | fluid ounces | fl oz |
| mL | milliliters | 0.06 | cubic inches | $in^3$ |
| L | liters | 2.1 | pints | pt |
| L | liters | 1.06 | quarts | qt |
| L | liters | 0.26 | gallons | gal |
| $m^3$ | cubic meters | 35 | cubic feet | $ft^3$ |
| $m^3$ | cubic meters | 1.3 | cubic yards | $yd^3$ |
| | **TEMPERATURE** (exact) | | | |
| °C | degrees Celsius | multiply by 9/5, add 32 | degrees Fahrenheit | °F |

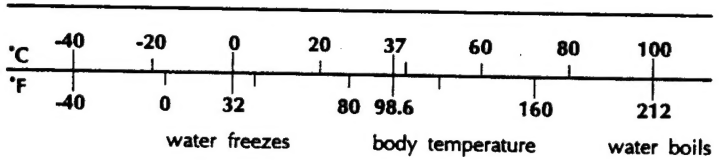

## TABLE OF CONTENTS

## LIST OF FIGURES

## LIST OF TABLES

## ACKNOWLEDGEMENT

The authors wish to thank the SSC Project Technical Committee for its guidance during the conduct of this study.

At M. Rosenblatt & Son, Inc., Messrs. Anthony Bromwell and Christopher Reyling contributed to the technical effort. Mrs. Evelyn Goodman painstakingly prepared the text allowing for the authors' indulgences.

Several references and literature sources were provided by Dr. Alfred Tunik, Senior Engineer, American Bureau of Shipping; Dr. Ephraim Suhir, Member of Technical Staff, AT&T Bell Laboratories; Dr. Vladimir Ankudinov, Vice-President, Designers and Planners, Inc.; and Mrs. Leslie Mitchell, Administrative Assistant, Science Applications International Corporation. The authors appreciate helpful suggestions provided by Dr. P. Kaplan, Chairman, Hydromechanics, Inc.; Mr. D. Lavis, Chief Executive Officer, Band, Lavis, and Assoc., Inc.; Prof. Armin Troesch, University of Michigan; and the Survey of Russian/Soviet Studies results and data on hydrodynamic load estimation by Drs. O. Ravinovitch, D. Rostovtsev, and I. Stepanov at the St. Petersburg State Marine Technical University, St. Petersburg, Russia.

# 1. INTRODUCTION

## 1.1 General

The procedures for the estimation of hydrodynamic impact loads have been under development for decades and vary considerably in their approach, required effort for application, and results. The Ship Structure Committee (SSC) has identified the need for accurate impact load estimation techniques. The SSC's first objective is assessing the state-of-the-art in estimating forebody hydrodynamic impact loading, which is the subject of this project.

In the Ship Structure Committee Long-Range Research Plan [1]* covering the years 1990-2000, the Research and Development (R&D) tasks in slamming and bow flare impact are ranked as having the "greatest value" of structural improvement and as "top value" of importance.

The extreme forces exerted on a ship's hull are the principal drivers of the structural arrangement and scantlings of a vessel. The forces which exert the greatest loads are the results of hydrodynamic impact which has been termed the least understood area of ship structural design [2]. This phenomenon has been defined in terms of three categories of loading which manifest themselves in different ways and at different locations on a ship's hull: Slamming, Wave Slap, and Frontal Impact.

These extreme environmental forces drive structural design in one direction, towards more substantial and heavier structure. The unfortunate consequences to a vessel include the effects of weight addition, reduced payload, increased construction costs, and reduced vessel speed. This is a particularly acute problem in high-speed combatants and patrol craft, which are highly weight critical. Accordingly, a conservative approach to estimating the impact loads can result in an extremely heavy penalty to the vessel under construction where weight is a problem.

A more rigorous design approach involves the complete determination of the loads and responses on the basis of scientific data rather than by use of empirical procedures. The design of the main hull girder has long ago resulted in standard procedures for still water and wave bending loads. These procedures have been able to model the wave bending phenomena as a quasi-static process and the results have proven to be adequately accurate. They have become standard and accepted practices. On the other hand, reliable means for the estimation of hydrodynamic impact loads, which are necessary to design and optimize the hull structure forward, have not been identified. It is only when these impact loads can be estimated with reasonable accuracy that design, maintenance, and repair decisions can be made rationally.

* Number in brackets indicate references in Section 10, References.

Hydrodynamic impact loading cannot be modeled as a quasi-static phenomenon as wave bending. It is an impulse phenomenon involving extreme pressures acting over a body surface during very short time periods relative to the natural rate of response of the structure. It is the lack of understanding with regard to the chain of events occurring during the impulse time that presents the greatest problem. Furthermore, impulse loading can involve complex mathematics dealing with three-dimensional fluid modeling. The formulas for this type of model at present are only solved by making assumptions about the temporal and spatial distribution of forces, and it is these assumptions that may introduce inaccuracies.

The presence of assumptions in hydrodynamic impact theories is well recognized and traditional approaches to structural design and performance assessment have consequently relied on deterministic and empirical safety factors to account for the possible variabilities. These safety factors vary significantly and are not founded on a uniform rational philosophy. Furthermore, associated with a given nominal safety factor, no matter how conservative it may be, there is invariably some underlying probability of failure which is accentuated by the large loads that accompany hydrodynamic impact. There is, therefore, a dire need to develop accurate prediction methods for hydrodynamic loads in order to reduce the probability of structural failure.

The dynamic response of structure to extreme hydrodynamic loadings is a highly transient and non-linear process. The damage sustained by a vessel due to hydrodynamic impact loading can manifest itself in many forms, from deformed shell plating, to distorted and buckled longitudinals and frames, and to fatigue cracking. For the most part damage is sustained by the vessel's tertiary structure at the location of impact, but the secondary and primary structures are affected as well. The secondary structure can be damaged by the direct action of impulse forces or by the high frequency whipping forces that accompany hydrodynamic impact. The primary structure is usually only affected by the whipping forces.

The safe and economical operation of engineering structures demands that technical capabilities exist for the estimation of hydrodynamic impact loads. This report touches on broad technical areas as the study of hydrodynamic impact loading is a hydro-elastic phenomenon, yet at the same time it will concentrate on the specific aspect of impact load prediction as related to high speed weight critical vessels. First, all types of theories that have been developed over the years are identified. Next, these theories and prediction methods are evaluated to pinpoint the most accurate. In addition, the gaps or assumptions that exist in current technology are addressed. In order to verify the accuracy of these prediction methods, they are applied to two vessels for correlation. In conclusion, possible future research is identified where the gaps and assumptions previously addressed are considered. A total of 222 references were reviewed in the process of preparing this report. The distribution of publications over years is shown in Figure 1-1.

The sections that follow address each type of hydrodynamic impact subject area in more depth. As there are some distinct differences in their interpretation, it is the

purpose here to clearly define each as they have been identified in the literature, and as they will be used in the subsequent sections of this report. Correlation with the recently published Society of Naval Architects and Marine Engineers (SNAME) notes on ship slamming [3] has been emphasized.

The original intent was to publish all numerical data in this report in SI units. However, the great diversity of analyses of previous investigations reported in both British and metric units made this task sufficiently difficult to effect a change in approach. Accordingly, there is a variation of units reported and the reader should be certain of the units currently in use throughout the text.

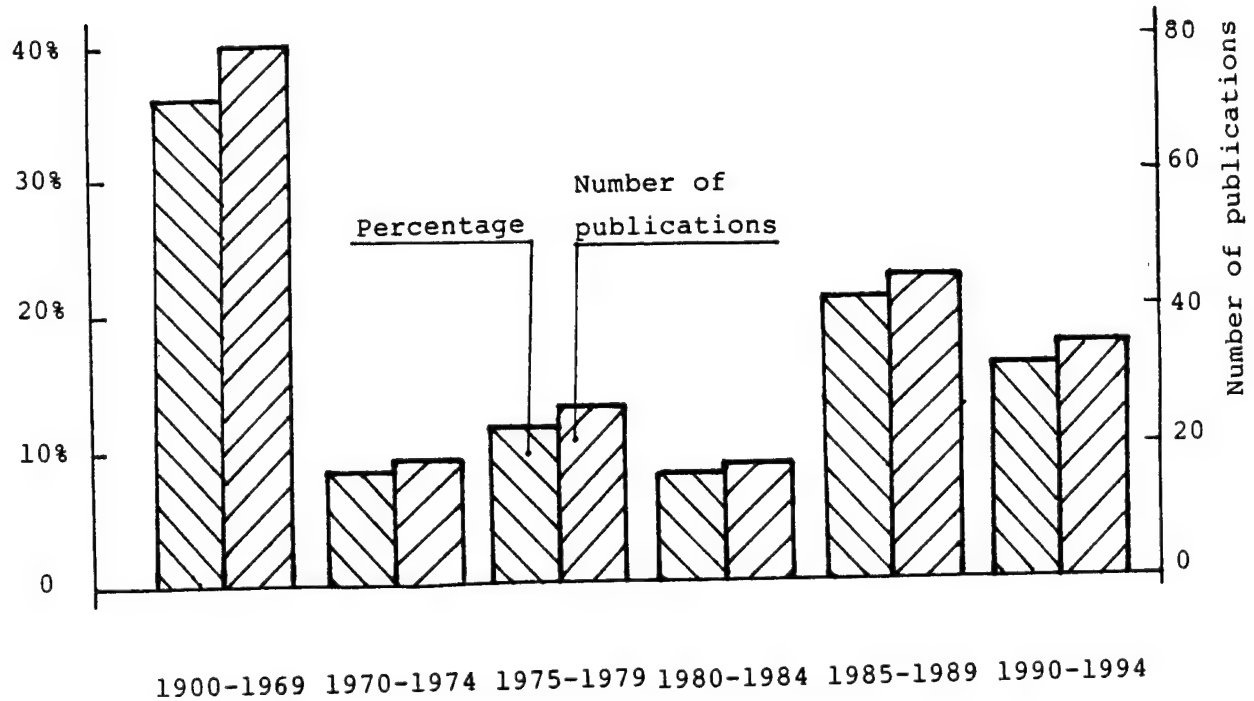


**Fig. 1-1 Number of Publications Covered by Present Review (Total of 222 References)**

## 1.2 Description Of Impact Phenomena Experienced By A Ship At Sea

When a ship navigates in rough seas it frequently experiences various types of impacts from the waves which give rise to a shudder or elastic vibration throughout the hull. The descriptions or definitions of these wave impact and vibration phenomena have been many, but to date, none have gained universal acceptance. For example, the terms "slamming" and "pounding" have been associated with these phenomena, but considerable confusion exists in the literature as to the definition of these terms.

The term "pounding" has been used to mean many different things, such as: (1) a blow applied at the ship's hull; (2) an impact when the ship approaches the water; (3) a rapid or sudden application of a load due to contact with a shoal or rocks; (4) a blow received by the hull of a fast motor craft due to planing action at high speed; or (5) a wave slap resulting in a jarring load which is abrupt but not severe. Quite frequently, the word "pounding" is loosely considered synonymous with "slamming". Yet, the definition of the word "slamming" is no clearer. For example, "slamming" has been used to mean: (1) an impact when the water approaches the ship; (2) an impact at the ship bow; (3) an impact on the bow flare; (4) an impact of the bottom of a large displacement vessel (as contrasted to small craft); or more generally, (5) any impact between any part of the side or bottom of a ship and the water surface which generates a shock-like blow to the ship. The literature has also failed to agree on the prerequisites for slamming. Some investigators believe forefoot emergence is necessary, while others suggest that damage can occur without forefoot emergence [3].

The foregoing should give the reader some idea of the confusion which is prevalent in the interpretation of "wave impact and vibration phenomena." The need for clarification should be apparent. In what follows, the various types of wave impact will be discussed in more detail, and attempts will be made to clearly differentiate between them.

### 1.2.1 Slamming

The term Slamming will be used to describe Forward Bottom Impact [3]. During higher sea states, when a vessel experiences large pitch and heave motions, the forefoot of a vessel can rise above the water surface. As the vessel re-enters the water large impulse pressures are imparted to the hull structure due to the relative motions of the sea and ship. The hull literally slams into the water surface. At this time the vessel experiences heavy impulse pressures to the local forefoot structure and subsequent whipping forces to the entire hull structure [2]. It is these large impulse pressures and whipping forces that cause extensive local damage to and high frequency stresses in the ship's structure.

It is generally reasoned that these loadings are associated with the short time exchange of momentum between the ship and the sea; such exchanges can only take place in the vicinity of the free surface of the fluid. The duration of slamming pressure measured at one position on the structure is in the order of milliseconds [4] and very localized in space. Furthermore, the position where high slamming pressures occur changes with time

and slamming pressures are sensitive to the manner in which the water impacts the structure. The loadings generated, because of their short duration, excite dynamic response of the local structure and hull girder. Damage to the local structure and support structure is the most frequent occurrence but deckhouse connections have been known to rupture and main hull girder strength failures have been initiated [2].

### 1.2.2 **Wave Slap**

The term Wave Slap will be used to describe any Bow-Side Impact between a wave system and a marine structure. In general wave slap involves the act of a severe wave system imparting its energy to a relatively stationary structure. Although somewhat of an ambiguous definition, wave slap is uncharacteristic of other forms of hydrodynamic impact loading. For example, for wave slap to occur, the large pitch and heave motions associated with both bottom and flare slamming (frontal impact) need not be present. In addition, forefoot emergence and forward speed are not necessarily present. An important factor of wave slap, as similar to other impact forces, is wave severity [2]. Evidence of wave slap damage can be found at or near the operating waterline, and usually affects the lighter structure at the forward end of a vessel. It is usually the least severe of the three forms of hydrodynamic impact.

### 1.2.3 **Frontal Impact**

Frontal Impact will be used to describe the occurrence of Flare Slamming [3] and/or Shipping of Water (a.k.a. Green Water on Deck). For those two types of hydrodynamic impact mentioned the following descriptions will apply.

The term Flare Slamming will describe the impact forces applied to the bow flare of a vessel. As a result of large ship motions, an impact force is generated on the bow flare as it enters an oncoming wave system. This impact produces not only high forces, but also the intense shudder and high frequency vibrations associated with bottom slamming. While similar to bottom slamming, some major differences exist between bow flare and bottom slamming. One is the speed of impact which is slower with flare slamming than with bottom slamming. This reduces the peak impulse pressure applied to the structure; furthermore, the pressure is spread across the rapidly increasing cross-sectional area of the blow flare, potentially causing larger total forces on the structure. This is the main reason why the prediction methods for bottom slamming tend to inaccurately predict the forces caused by bow flare slamming. The second difference is that forefoot emergence is a characteristic of bottom slamming while it is not for flare slamming [3]. Also, the duration of the impact force is relatively long for the flare impact as compared to that for forward bottom impact.

To fully describe the impact force on the bow flare and the resulting structural response, a number of variables (entrapped air, hydro-elastic interaction, and non-linear free surface mechanics) must be correctly taken into account. In addition, a three-dimensional solution to the fully non-linear boundary value problem has not yet been found. The

complexities of the non-linear free surface and body boundary conditions require that simplifying assumptions be made in order to calculate the impact forces [5].

The term Shipping of Water will be used to describe the following: As a result of large ship motions and forward speed, the bow of a vessel can travel below the surface of an oncoming wave system and plunge into it, causing the water to break over the bulwark and onto the deck of the vessel. Large pressures are applied to the deck structure causing damage. This phenomenon is generally associated with bow flare impact, and is therefore grouped with it [3].

### 1.3 Impact On Dynamically Supported Craft Including Planing and SES Types

At high speeds, the forward bottom of dynamically supported craft rides clear of the water surface and the hull is mainly supported by planing action of the aft body or lift provided by the air cushion on Surface Effect Ships (SES). When the craft fails to maintain dynamic equilibrium in encountering waves, it plunges onto the water surface and an impact is applied to the bottom. This impact causes a shudder throughout the hull. The sea condition, and pitch and heave motions are not necessarily severe. The location of the impact and structural damage (if any) is on the craft bottom and or cross structure of SES.

### 1.4 Impact On Aircraft Landing On Water

Aircraft landing on water are usually supported by planing action of the fuselage bottom or pontoons under the wings. The dynamic phenomena are then identical to those for planing craft.

Interestingly, the first efforts in describing and predicting hydrodynamic impact were directed to aircraft and the interest has continued over the years. Consequently, the literature contains numerous references specifically for aircraft but which have been useful for ships and craft.

# 2. PHENOMENA FOR OCCURRENCE OF AND RESULTING FROM HYDRO IMPACT

## 2.1 General

Hydrodynamic impact in displacement ships does not occur in calm water. Rather, the vessel must be travelling in a seaway of some relative magnitude. This combined with inherent and operational characteristics of the vessel can result in a combination of phenomena which will provide the opportunity for hydrodynamic impact loading. Once this occurs the results may be the generation of significant impact forces applied to the hull. These in turn will generate a structural response in the hull. For small craft the effect of impact on heave and pitch is significant enough that the two problems should be coupled [6,7]. The interrelationships are shown in Figure 2-1 [8].

The sections which follow address these phenomena separately for bottom slamming, bow flare impact and frontal impact, respectively.

## 2.2 Factors Leading To Proper Conditions For Slamming

Szebehely [9], and Akita and Ochi [10,11] have found from tests in regular waves that slamming generally occurred when the ship model and the impact surface were nearly parallel. Szebehely showed that three conditions must exist for a slam to occur; (1) bow emergence, (2) a certain magnitude of relative velocity between the bow and wave surface, and (3) unfavorable phase between bow motion and wave motion. A fourth criterion mentioned by Szebehely affecting the severity of slamming was the angle between the wave surface and keel. Ochi [12] examined the condition leading to slamming from tests in irregular waves and found that bow emergence was a prerequisite for bottom slamming. However, bow emergence was not sufficient cause for slamming and it appears that a critical relative velocity exists between bow and wave, below which slamming does not occur. This critical relative velocity equals to $0.096(g*L)^{0.5}$, where L is the ship length in meters, and $g=9.81$ m/sec$^2$ is gravitational acceleration.

Perhaps the most significant factors which govern or influence slamming conditions are the length of ship, sea severity, ship speed, and course angle relative to predominant sea, ship loading condition, overall ship form as it affects ship motion, and also fullness or flatness of bottom forward.

### 2.2.1 Sea State

Ochi [12] has shown that model test results suggest that slamming severity increases with wave severity, if other conditions remain equal.

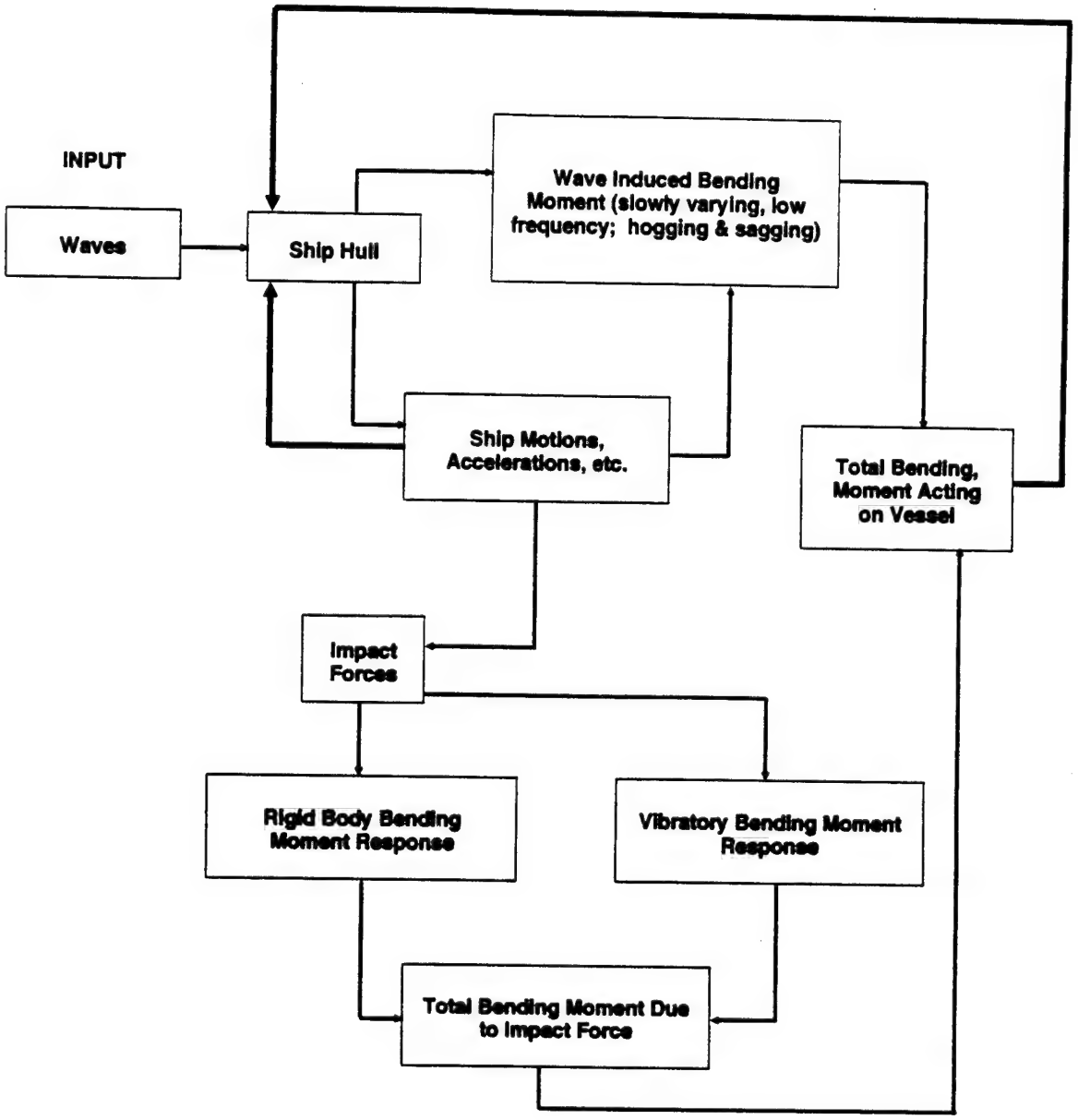


**Fig. 2-1. Combined Loads on Ship Hull in Waves (From Kaplan and Dalzell [8])**

### 2.2.2 Speed

The forward speed of a vessel has a significant effect upon the severity of slamming [3]. In regular waves the primary effect of speed is to change the period of encounter and, therefore, the tuning factor which has a significant effect on the motions and hence bow emergence and relative velocity. Thus, for a given ship, there are certain dangerous speeds associated with certain waves. Prudent ship masters normally reduce the speed of a ship to avoid slamming. An often used criterion for "voluntary speed reduction" is that a typical ship master reduces the speed if slams occur for more than three out of 100 waves that pass the ship [4]. If slamming occurs in very short waves and low ship speeds, the probability of slamming may be reduced by increasing speed somewhat. In waves of length equal to and greater than ship length, however, a speed reduction is necessary if slamming becomes severe.

The principles of slamming in regular waves may also apply in irregular waves. Ochi [12] has shown that model tests indicate that with increasing speed, the probability of slamming and the pressure magnitude increases, and the location of maximum pressure shifts aft. At very high speeds, the so-called supercritical speed, it can be expected that the impact pressure could be reduced since the ship motions will be reduced above these supercritical speeds.

### 2.2.3 Heading

Ochi [12] has shown from model tests that the most severe condition for slamming occurs when the predominant direction of the oncoming waves is from head-on to about 30 degrees off the bow. This can be attributed to the fact that pitch and heave, the major contributors to the relative motion between wave and ship, are maximum for this range of headings. The severity of slamming decreases significantly for waves with heading angles greater than 30 degrees off the bow, and there is virtually no slamming for waves with heading angles greater than 60 degrees off the bow.

### 2.2.4 Draft

Ochi [12] has shown as well that model tests indicate that increasing the draft of a ship generally decreases the probability of slamming, as well as reduces the pressure magnitudes. Ochi [13] showed that the reduced slamming occurrence for deep draft may be attributed more to the less frequent forefoot emergence than to reduced vertical motion at the bow. The ship motions which have a close relation to slamming are not significantly different for light and heavy draft conditions; however, the reduced draft at the bow for ballast condition results in more frequent bow emergence. These findings are also in agreement with those reported by Lehman in [14] and Society of Naval Architects of Japan [15]. It may therefore be concluded that increasing the ship draft is advantageous in minimizing the amount and extent of slamming pressure, thereby reducing bottom structural damage.

### 2.2.5 Ship Form

Results of model experiments in waves by Dillon and Lewis [16] indicates that substantial changes in transverse section shape, while maintaining forebody design waterline configuration, results in negligible change in pitch amplitude and bow acceleration regardless of the variation in wave height and length. On the other hand, it has been established by Ochi [13] that there is a small increase in the pitch, heave, and bow acceleration amplitudes when the forebody design waterline configuration is increased in beam in way of the forward most stations. However, as a result of improved phase relationship between the motion of the ship bow and the water surface, an overall decrease in the relative bow motion was observed for the ship with the increased forebody waterline configuration. This reduced relative bow motion, and the more "V" shaped underwater bow, which automatically resulted from increasing waterline beam while maintaining sectional area, resulted in less keel slam pressure.

This conclusion is confirmed by Ochi [17], during experiments with two vessels of vastly dissimilar forebody shape, but with quite similar forebody design waterline configuration. One model had modified "U-V" sections and a cutaway forefoot, and the other had extreme "U" shaped sections, a bulb and a vertical stem below the design waterline. Within the possible range of variation for afterbody forms with conventional single and twin screw propulsion, the afterbody form has significantly less influence on the incidence of slamming than the forebody form.

Lacey [18] reported the higher incidents of localized bow structural damage caused by slamming for ARCO tankers with blunter, more stubby entrance. His conclusion was made on the basis of analysis of damages of 10 tankers with different hull fullness serving the same route between Alaska and the lower United States West Coast ports.

## 2.3 Factors Leading to Proper Conditions for Wave Slap

When a ship is navigating in rough oblique seas, waves slap the side plating at the bow and vibration is excited in the hull. Large pitching or heaving motions are not necessarily associated with this phenomenon although rolling may be. The location of impact and any structural damage will be on the bow side plating.

### 2.3.1 Sea State

Sea state (sea severity) is the important factor which governs the wave slap phenomenon [3]. The intensity of wave slap increases with wave severity.

### 2.3.2 Speed

The forward speed of a vessel has no significant effect on severity of wave slap [2].

### 2.3.3 Heading

The course angle is the important factor for wave slap [3]. For fine bow entrance (near the waterline and above) the most severe condition for wave slam occurs when the predominant direction of the oncoming waves is close to 90 degrees off the bow. For larger entrance angles the critical course angle decreases. For example, the Soviet tanker "Krim" with traditional block coefficient of 0.80 experienced severe wave slaps due to extremely blunt fore lines above the operating waterline [19] while in head seas.

### 2.3.4 Draft

Ship draft is unrelated to the wave slap and forefoot emergence is not required.

### 2.3.5 Ship Form

As was mentioned in the Section 2.3.3, the ship fore lines near and above the operating waterline has a significant effect on direction of critical heading angles and intensity of wave slap loads.

## 2.4 Factors Leading to Proper Conditions for Frontal Impact

The frontal impact phenomenon is very similar to slamming. One can assume the same factors leading to proper conditions as for slamming (see Section 2.2). The significant difference between these two is that the forward bottom impact is always associated with the emergence of the forefoot, while frontal impact (bow flare and green water on deck) is not. The duration of the impact force is relatively long for frontal impact as compared to that for slamming. This phenomenon appears to be serious only for a ship having large bow flare such as an aircraft carrier and other naval combatants or container ships and with increasing speed the seriousness of this problem is intensified (see, for example, Vulovich, Hirayama [20]).

For Sea State, Speed, Heading, Draft, Ship Form conditions see Sections 2.2.1 through 2.2.5.

## 2.5 Structural Response

There are three main facets to vessel hull strength analysis, namely:

(1) Determination of the hull loadings;
(2) Determination of the structural responses resulting from the loads;
(3) Determination of the ability of the material and structure to withstand the resulting stresses.

Solutions to the first two of these problems have been the primary concern of structural seaworthiness studies. This report on hydrodynamic impact concerns mostly the first one, although there are methods coupling the second.

When a ship is exposed to ocean waves without hydrodynamic impact present, it is subject to three types of hydrodynamic forces:

- hydrostatic force
- inertial and damping forces
- wave excitation forces (the simplified form of which is known as the Froude-Krylov force).

Determination of these forces is sufficient to provide one with predictions of rigid body ship motions, [3], [21]. Ship motions and wave loads can be predicted by linear or nonlinear approaches. Whereas linear theory of wave loads on ships is a very valuable tool for fatigue investigation, it can only give a rough indication of load ranges and of differences between different ships, loading cases and locations in the structure for determining extreme loads during the lifetime of a ship; this is so because nonlinear effects are very important in extreme weather conditions [21,22,23,24,25]. Figure 2-2 (calculated according to [26] gives an indication of growing non-linear effects with increasing wave heights [7].

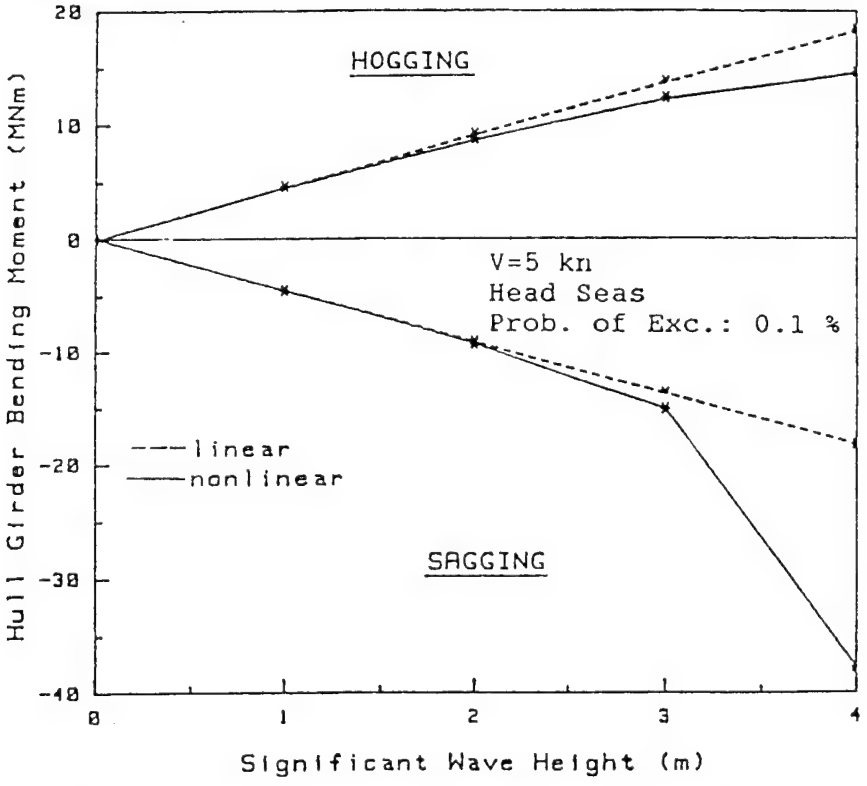


**Fig. 2-2. SES-600 Hullborne Hull-Girder Bending Moments. Slamming occurs at $h_{1/3}$ = 3m [7]**

Hydrodynamic impact loads are dynamic impulse loads resulting from slamming or wave impact on the forefoot, bow flare and other parts of the hull structure, including the effects of green water on deck. In response to hydrodynamic impact in heavy or moderate seas, a ship can develop substantial elastic hull stresses. This includes flexural vibration of the hull girder including transient hull vibration that is termed whipping and persists for a large number of cycles, the rate of decay being small, and can be analyzed using a linear elastic model [27]. Local hull response under these same loads may require use of analysis based on an inelastic behavior approach. The effect may be bottom and bow damage above the waterline. The bottom plating may experience fatigue, local damage may be inflicted due to overstressing and equipment, particularly sonar domes, may suffer as a result of the "shock" loading.

The slamming pressure is distributed over an area of the ship bottom in the immediate vicinity of the point of re-entry, and is typically a maximum on the centerline at any instant of time. As the ship forefoot re-enters the water, the point of maximum pressure tends to move toward the bow. The position of maximum pressure is about 15-25% of ship length aft of the forward perpendicular. As a result of the movement of the re-entry location, the pressure pulse moves also, meanwhile maintaining its peak intensity.

The duration of slamming pressure measured at one place of the structure is of the order of milliseconds, in contrast with wave-induced loads which have significantly higher periods. Due to the movement of the re-entry location, the total duration of the force pulse that the ship experiences will be several times as great as the pulse duration at a single station. This space-time behavior of the force is illustrated in Figure 2-3 from Ochi and Motter [28].

The slam-induced vibration may result in vibratory stress intensities that are equal in magnitude to the wave-induced low frequency bending stresses [6,27,29]. Examples of time history of deck stresses in amidship section are shown in Fig. 2-4 for a tanker in the ballast condition (slamming only) and in Fig. 2-5 for a containership in the full load condition (slamming and bow-flare impact). Dash lines show wave-induced stresses and solid lines correspond to total stresses. These results show that stresses due to slamming have an impulsive nature and the first stress peak coincides, as a rule, with the instant when a hogging moment is changing to sagging. Maximum dynamic stresses in this case are equal to the sum of wave-induced bending stresses and stresses occurring after impact.

The slamming stresses must be carefully evaluated and be suitably combined with the low-frequency wave-induced bending stresses. Attempts to solve the problem of combining the low-frequency wave-induced bending and the high-frequency slamming induced bending moments in ships have so far been based on a Poisson pulse train model for the occurrence of the slamming impacts. A review and revision of this approach was made by Hansen [30].

In contrast, the impulsive loads due to the bow flare impact have greater duration and coincide with maximum wave-induced sagging moment. As a result fast ships with substantial bow flare may experience a maximum sagging bending moment which is significantly larger than the maximum hogging moment. Hence, bow flare impact may be more dangerous for these types of vessels [6].

In general, whipping of a ship's hull due to impact loadings can cause large additional hull girder bending moments of a transient nature, as opposed to the more slowly varying bending moment due to buoyancy or wave-induced effects. Additional research is needed to determine how significant whipping stresses are in producing hull failures.

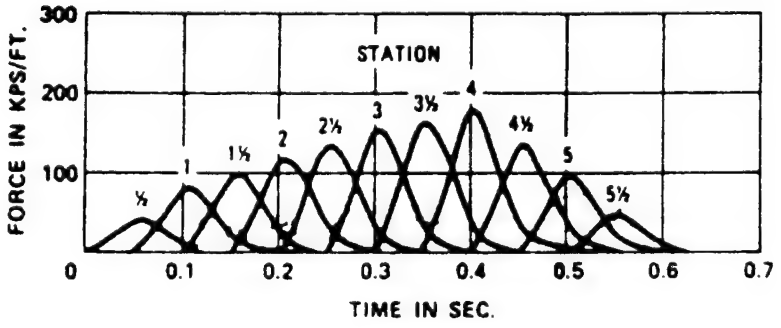


**Fig. 2-3. Calculated Force Applied at Various Stations as a Function of Time; Mariner; Sea State 7, Significant Wave Height 25 ft., Ship Speed 7.4 Knots, Light Draft [28]**

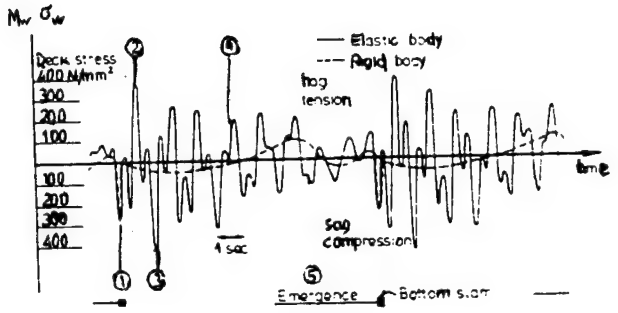


**Fig. 2-4. Time History of Bending Moment at Station 7½; Tanker in Ballast [6]**

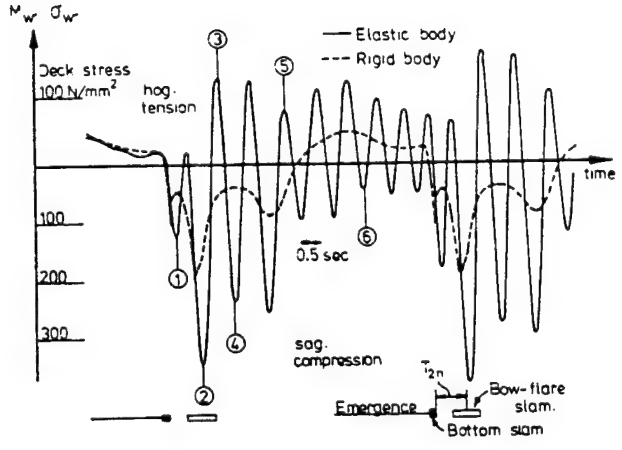


**Fig. 2-5. Time History of Bending Moment at Midships; Containership, Fn = 0.261 [6]**

# 3. HYDRODYNAMIC IMPACT

## 3.1 Introduction

### 3.1.1 General

The previous section has provided a description of the phenomena which can lead to the occurrence of hydrodynamic impact. This section addresses the predictive approaches and data which are available to determine the magnitude of the hydrodynamic impact loading under these conditions.

The variety and volume of predictive approaches and data is significant and much of the work builds upon previous efforts. Accordingly and consistent with SNAME [3], the approaches have been categorized broadly in three groups; Theoretical Approaches, Experimental Results and Empirical Formulas. The sub-sections which follow in this report will address each of these.

### 3.1.2 Slamming

The current prediction methods for bottom slamming rely on a certain level of ambiguity. Slamming impact has in the past been modeled as a quasi-static force applied to the local structure, similar to wave bending moment calculations. More recently, bottom slamming has been predicted using two-dimensional models and slender body theory and currently three-dimensional models are under development. In order to fully describe impact forces and resulting structural response, various phenomenon (entrapped air, hydro-elastic interaction, compressibility effects, and non-linear free surface mechanics) must be correctly modeled [5]. It is the lack of understanding with regard to these phenomenon that presents the largest problem. As a result, marine structures are usually designed and constructed with a considerable degree of indeterminacy or redundancy to help compensate for the complex and uncertain nature of the ocean environment. The formulae for this type of modeling at present are only solved by making assumptions about the temporal and spatial distribution of forces, and it is these assumptions that introduce inaccuracies in impact load prediction and subsequent structural design inefficiencies.

Figure 3-1 provides an overall view of the nature of the predictive approaches for slamming. This is not to imply that every procedure includes all the features noted and in fact, historically, the most work has been accomplished with 2-D theory assuming rigid bodies. The phenomena is described differently by a number of investigators. Some consider the pressures and/or forces at the instant when the hull strikes the free surface of the waves. This type of slam is of short duration and spray, compressibility and air cushioning may be important. Others consider the pressure and force variations as the hull continues to enter the water. Bishop and Price [29] have termed the former "impact slamming" and the latter "momentum slamming" noting that slamming is really a combination of the two, while frontal impact is adequately described only by the latter.

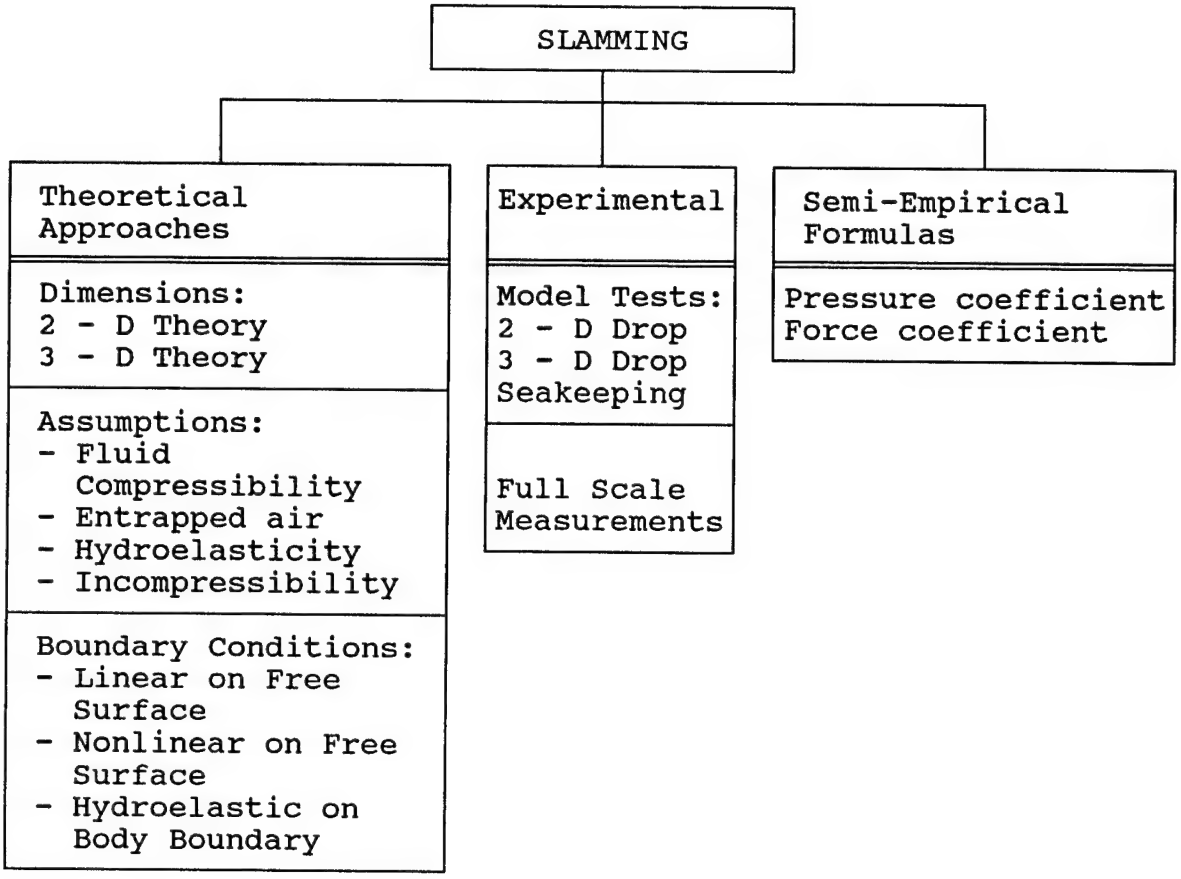


**Fig. 3-1. Overview of the Predictive Approaches for Slamming**

### 3.1.3 Wave Slap

As previously mentioned, wave slap is an impulse phenomenon, although usually the least severe of the three forms considered herein. The impulsive pressures of hydrodynamic loading in part rely on the relative motions of both the sea and the structure. Since the relative motion of the structure during wave slap approaches zero, there is a reduction in the peak impulse pressures. For the most part wave slap has received little attention. Most investigations of hydrodynamic activity have concentrated on bottom slamming and its more serious consequences. Investigations into wave impact water pressures on the hull of a ship are very difficult to address. Researchers have conducted ship model tests to study under what conditions impulsive wave pressure will occur and what part of the hull surface the wave impact will affect. In addition, experiments have been conducted to observe some aspects of water impact to clarify the roles of certain mechanisms.

Furthermore, studies on the phenomenon of breaking waves on a ship's side were performed in a series of model scale experiments in which the time and space variation of impact forces impinging on a flat vertical plate were recorded. These experiments

suggested that the temporal variation of the pressure at a specific point is a pulse that can be idealized by a function that assumes zero time rise and decays exponentially [30a].

Also, investigations of wave pressures and forces on plane vertical walls carried out in coastal design engineering are of great importance. An overview of recent works on wave loads acting on vertical wall (usually a concrete caisson which rests on a rubble-mount base), with annotated bibliography, was published by Green [31].

Finally, design procedures commonly used by naval architects employ standard wave slap pressure loadings in lbs/ft$^2$ which vary from a maximum at the vessel waterline to lower values at higher vertical elevations.

Figure 3-2 provides an overall view of the nature of predictive approaches for wave slap. This is not to imply that every procedure includes all the features noted and in fact, historically, most work has been accomplished with experiments and semi-empirical formulas.

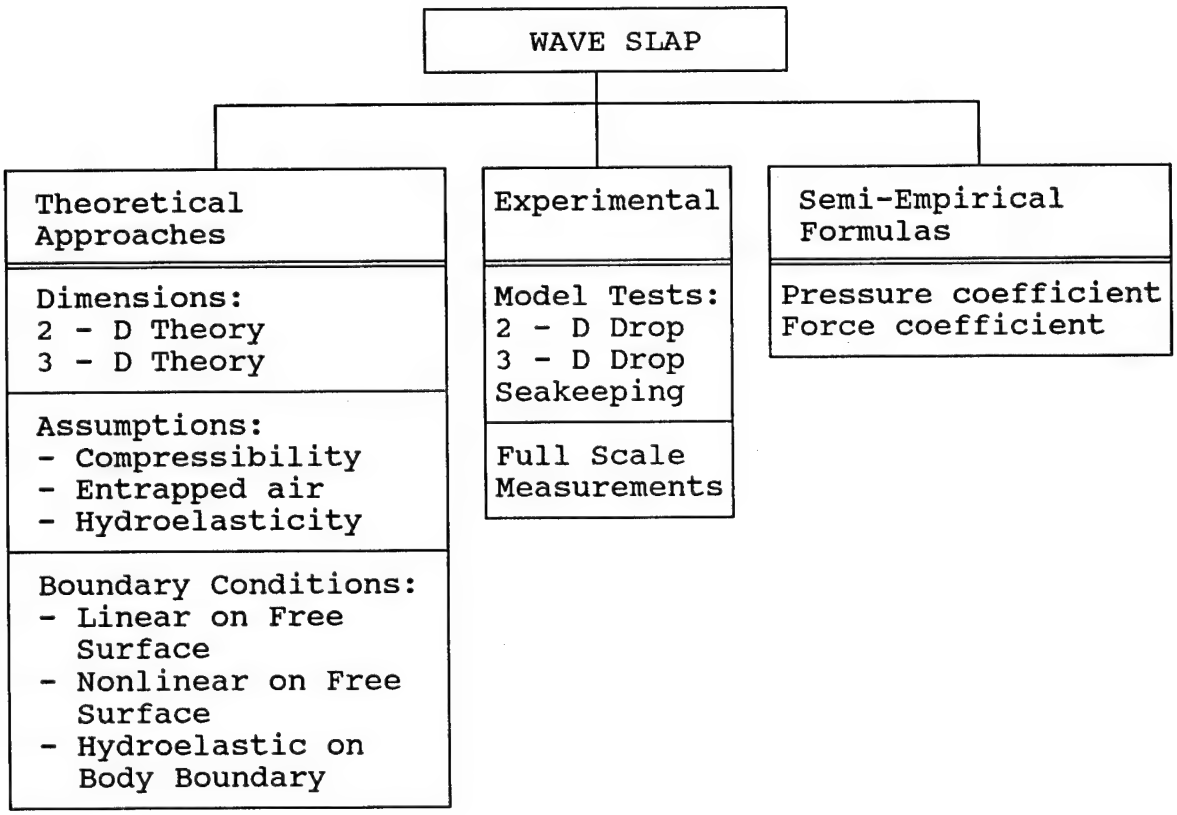


**Fig. 3-2. Overview of the Predictive Approaches for Wave Slap**

### 3.1.4 Frontal Impact

To fully describe the impact force on the bow flare and the resulting structural response, a number of variables (entrapped air, hydro-elastic interaction, and non-linear free surface mechanics) must be correctly taken into account. In addition, a three-dimensional solution to the boundary value problem has not yet been found. The complexities of the non-linear free surface and body boundary conditions require that simplifying assumptions be made in order to calculate the impact forces [5].

Most current prediction methods use two-dimensional calculations coupled with strip-theory assumptions to yield their three-dimensional results. Slender body or strip theory has long been accepted in normal linear seakeeping analysis, however the usual seakeeping quantities of interest are vessel motions and bending moments and shear forces near the middle of the ship. These forces and moments are typically less sensitive to end effects where strip-theory approximations are less valid. Bow flare impact and loads occur in places of high longitudinal curvature and the applicability of strip theory is thus more questionable. In fact there is evidence that strip-theory in these calculations may over predict the impact force by a significant amount [5].

Investigating such a problem requires investigating the relationship between ship's motion and environmental conditions. The impact problem associated with green water conditions are related to bow submergence. However, the relative bow motion depends on the environmental conditions and on the ship's characteristics. Researchers have investigated the impact strength of ships due to shipping green seas. Ship model test experiments were conducted to quantify the amount of peak pressure due to wave impact and their associated duration times. The results classified the generating mechanism of shipping green seas into three categories: dropping of piled up spray; dropping of swelled up waves; and scooping waves after submergence on the foredeck. In addition, conclusions were made that the time variation in the impact force due to shipping green seas results in the highest pressure loading during the dropping of piled up spray and swelled waves [31a]. These pressures were predicted to reach 50 tons/$m^2$ in the worst conditions.

Figure 3-3 provides an overall view of the nature of predictive approaches for frontal impact. This is not to imply that every procedure includes all the features noted and in fact, historically, the most work has been accomplished with 2-D theory.

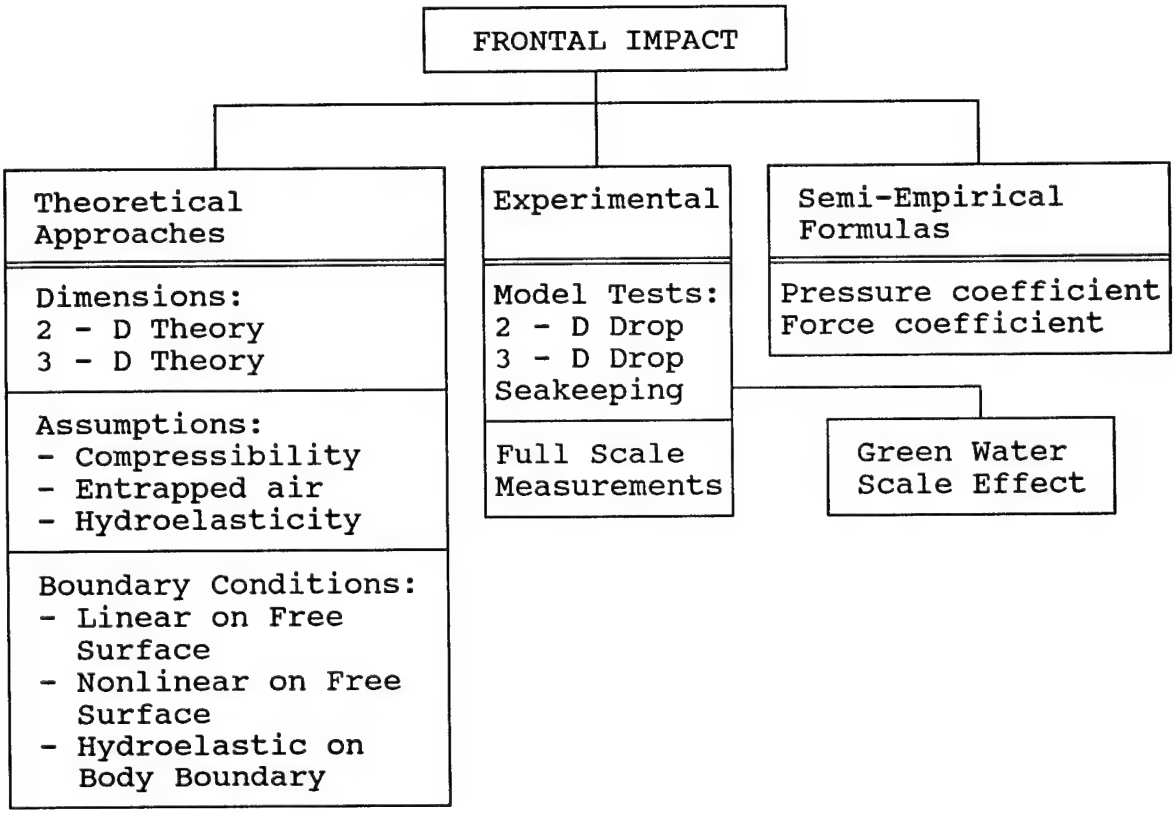


**Fig. 3-3. Overview of the Predictive Approaches for Frontal Impact**

## 3.2 Theoretical Approach

### 3.2.1 Introduction

The problem of interaction between a solid body and a liquid with a free surface is a broad subject that includes several significant sections of classical and modern hydrodynamics. In this review the attention will be paid to the analysis of processes characterized by strong unsteadiness in their development and by the existence of a contact line between the free surface of the liquid and the body surface. In the general form such processes can be described in the following manner: At the initial instant of time $t=0$, a solid body touches a free surface of liquid. At this moment the position of the body, the domain occupied by the liquid, and the velocity field of the liquid particles are assumed to be known. For $t>0$, either the law of body motion or the external forces affecting it are prescribed. The flow field and the character of its action upon the body are to be determined.

The first theories of body impact with water (the penetration theory of von Karman [32] and the impact theory of Wagner [33] and Sedov [34]) were directed at a global description of this process. Many applied problems have since been solved on the basis of these theories. But in some cases, more complete information about the process is required. For instance, it is necessary to take into account the peculiarities of the flow velocity field in order to determine the height and form of a free surface splash during impact. It should be noted that very often the global characteristics can be determined with good accuracy from only rather simplified knowledge of the interaction mechanism, and therefore a detailed description of the process in some problems is unnecessary.

The problem of a blunt body penetrating a liquid that initially occupies a lower half-space and is at rest is a typical problem considered in this Chapter. Even with further simplifications (the fluid is assumed to be ideal and incompressible, its flow to be potential, and the solid body to be rigid) the problem is still very complicated for the following reasons:

- The flow region is not predetermined;
- Division of its boundary into components (wetted part of a body surface and free boundary) is also unknown;
- Singularities can appear on the three-phase contact line.

Quantitative information about the process of interaction, even with the use of idealized models, can be obtained only on the basis of numerical methods. The expanding application of numerical modeling is the modern trend in hydrodynamics. A number of numerical techniques, combined with powerful computers, have been applied in recent years to complex problems in marine hydrodynamics, including ship resistance and propulsion [35], seakeeping and maneuvering [36,37,38]. The "Numerical Tank" approach is commonly used in science and engineering [39].

At the same time, to understand the dynamics of the process and develop an adequate computational algorithm, it is necessary to investigate analytically the qualitative nature of the phenomenon, obtaining simplified and asymptotic solutions for major stages of the process that are difficult and inexpedient to derive by numerical methods.

It should be noted that at the present time there are no mathematically rigorous results of a general character in the theory of nonlinear unsteady hydrodynamic problems with a free boundary and a contact line. Thus the following solutions and asymptotic expansions are of approximate character.

### 3.2.2 Two-Dimensional

Most theoretical studies pertaining to slamming impact which have appeared in the literature to date have treated the impact of a two-dimensional body falling onto calm water. The majority of the studies deal with incompressible fluid and are based on the earlier work of von Karman [32,40]$^x$, and later extended by Wagner [40,41]$^x$. Their work essentially involved a rigid wedge entering a fluid boundary as shown in Figure 3-4. The basic idea of von Karman was that during impact the momentum of the dropping body is imparted to the momentum of an apparent mass of water assumed to be that associated with an imaginary flat plate having the dimensions of the wedge at the intersection of the water surface. Wagner introduced the concept of pile-up water at the side of the wedge during entry, computed the pressure distribution, spray thickness, and gave the equation of a constant-force bottom.

These theories begin with the momentum conservation principle which requires that the system consisting of the body and water preserve its total momentum. Let the momentum at the instant the body touches the water surface be $M \cdot V_o$, where $M$ = mass of the body, and $V_o$ = velocity at the moment of impact. During penetration the velocity of the body is reduced ($V < V_o$), and its mass is increased due to the inertia of the water moving with it. This apparent increase of mass, $m_{zz}$, is called "added mass". If the external forces (such as buoyancy, gravity, and friction) acting on the body are represented by $F$, the equation describing the motion of the system may be written as:

$$M\dot{V} + \frac{d}{dt}(m_{zz}V) = F \qquad (3\text{-}1)$$

where, $V$ can be obtained from:

$$(M+m_{zz})V - MV_o = \int_0^t F\,dt \qquad (3\text{-}2)$$

$^x$Superscript indicates more detailed evaluation of references in Section 4, 5 and 6.

Then, the impact force at any instant is given by $d/dt\ (m_{zz}V)$. Hence, the impact force for a given $V$ is determined by the instantaneous value of $m_{zz}$ and by its derivative $dm_{zz}/dt$. Therefore, a correct estimation of the variable added mass is essential.

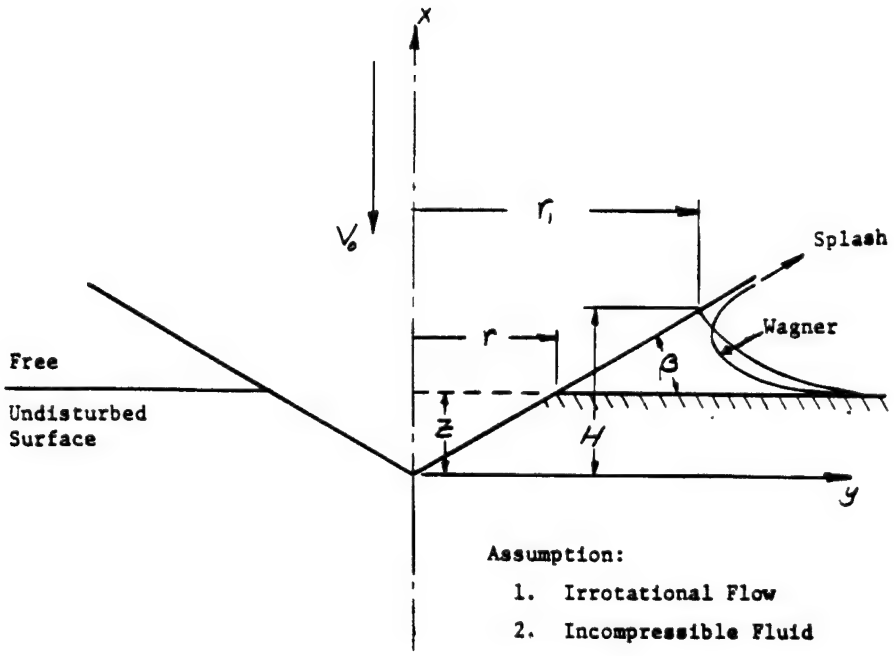


**Fig. 3-4 Wedge Entry Into Fluid Medium [32]**

If we assume that the viscosity of the fluid is negligible and the fluid is initially at rest, the motion of the fluid during impact may be considered to be irrotational and a velocity potential, $\phi$, exists.

The added (or apparent) mass due to an energy transfer of the fluid particles is related to the velocity potential according to [32]:

$$m_{zz} = \frac{\rho}{V^2} \int\int \phi \frac{\partial \phi}{\partial n}\, ds \qquad \textbf{(3-3)}$$

If furthermore, the fluid is considered to be incompressible, the velocity potential, $\phi$, satisfies the Laplace equation,

$$\nabla^2\phi = 0 \tag{3-4}$$

If the free surface condition is linearized and approximated by its initial undisturbed position away from the body, then in this region the boundary condition has been termed equipotential, which ignores the piled up water at the body:

$$\phi = 0 \tag{3-5}$$

On the body:

$$\frac{\partial\phi}{\partial n} = V_n \tag{3-6}$$

Von Karman [32][x] considered this problem for a wedge with a small wedge angle as shown in Figure 3-4 in the interest of making stress analyses of seaplane floats during landing. He took the added mass for a long plate of width 2r accelerated in a fluid as $\frac{1}{2}\rho r^2\pi$ and neglected buoyancy effects (Note that $\frac{1}{2}\rho r^2\pi$ is half the added mass in heave of the flat plate in an infinite fluid for infinite frequency. He determined the following impact force for unit length and average pressure:

$$F = \frac{V_o^2 \cot\beta}{\left(1 + \frac{\rho\pi r^2}{2M}\right)^3}\,\rho\pi r \tag{3-7}$$

$$p = \rho\frac{V_o^2}{2}\,\frac{\pi\cot\beta}{\left(1 + \frac{\rho\pi r^2}{2M}\right)^3} \tag{3-8}$$

Here M=mass of the body per unit length. The maximum pressure is equal to:

$$p_{max}(r \sim 0) = \frac{\rho V_o^2}{2}\,\pi\cot\beta \tag{3-9}$$

For $\beta = 0$ the pressure is infinite but for a seaplane with floats having $\beta = 20°$ the author obtained acceptable results.

The U.S. Federal Aviation Administration [42] has adopted a similar formula for the design pressure to be applied to the hull and main float bottom pressures of seaplanes. Frames and bulkheads, stringers, and bottom plating are considered. As an example, for a bottom without curvature the pressure at the chine is to be 0.75 times the pressure at the keel and the pressures between the keel and chine vary linearly. The pressure at the keel is:

$$p_K = C_2 (K_2 V_{SI}^2 / \tan\beta_K) \qquad \textbf{(3-10)}$$

where:

$p_K$ = *pressure at the keel, psi*
$C_2$ = 0.00213
$K_2$ = *hull station weighting factor, Figure* 3-5
$V_{SI}$ = *speed, knots*
$\beta_K$ = *angle of dead rise at keel*

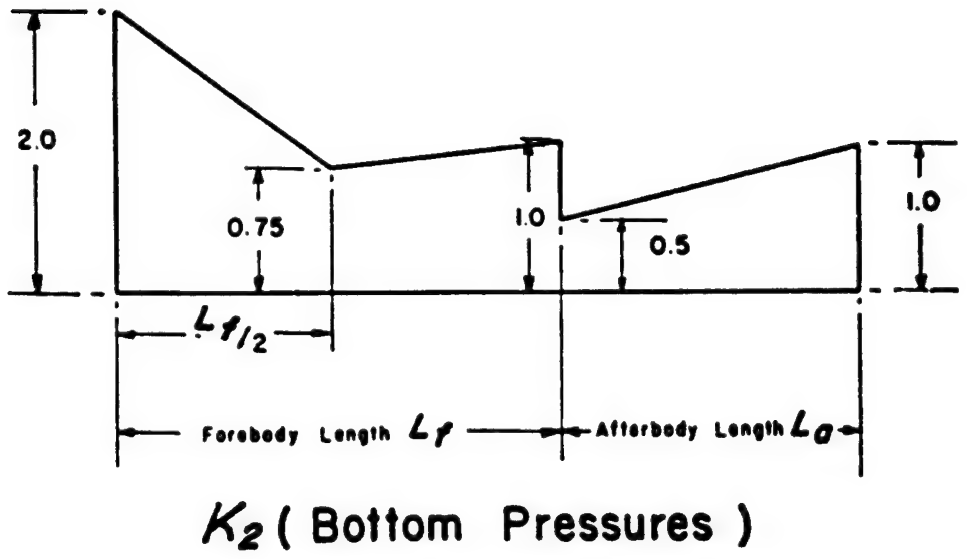


**Figure 3-5: Hull Station Weighting Factor [42]**

Wagner's linearized theory [33][x] considers pile-up of water at the free surface as shown in Figure 3-4. It significantly refines the wetted area and, hence, averaged pressure. In accordance with this solution the impact force per unit length is and maximum pressure are:

$$F = \frac{V_o^2}{\left(1 + \frac{\rho \pi r_1^2}{2M}\right)^3 u} \rho \pi r_1 \qquad (3\text{-}11)$$

$$p_{max} = \frac{\rho V_0^2}{2\left(1 + \frac{\rho \pi r_1^2}{2M}\right)^2} \frac{1}{u^2} \qquad (3\text{-}12)$$

where:

$u$ = $V/dr_1/dt$
$V$ = *The variable speed at which the section enters the water surface.*
$V_o$ = *Velocity at the moment of impact or the rate of penetration of the body into the wave.*
$r_1$ = *half-breadth of impact surface to point where spray breaks away.*

Wagner shows that $u$ is of the order of the magnitude of the keel angle $\beta$. Consequently, if the deadrise angle is small, Von Karman's Equation (3-7) for the force is identical to Wagner's Equation (3-11). Simultaneously, the pressures are equal to Equation (3-9).

Armand and Cointe [43][x] have shown that Wagner's wetting correction is valid at the instant of impact but additional terms are necessary for later time and larger depths. A number of investigators have since used Wagner's approach of "fitting" and correcting the free surface shape including Hillman [44] and Chu and Abramson [45]. In these so called expanding wedge theories as the wedge dead-rise angle, $\beta$, tends towards zero, the pressure becomes infinite [46].

Also, based on these fundamental ideas are the works of Milwitzky [47][48][49], and Mayo [50][51], Bisplinghoff [52][53], and Szebehely [54][55][56]. These studies dealt primarily with the impact of a wedge as applied to seaplane hulls. Szebehely was among the first to apply the idea to the specific problem of ship slamming. Later, Todd [57] and Bledsoe [58] computed pressures for ship-like sections following the work of Szebehely. The hydrodynamic impact problem for bodies other than the wedge has been treated by Schnitzer and Hathaway [59], and Fabula [60][61] on elliptical cylinders, by Fabula and Ruggles [62] on circular cylinders (growing circular arc), by Ochi and Bledsoe [63] on a body of general shape representing the ship bow form.

A review of various fitting techniques used in hydrodynamic impact theory to convert to ship-like bow forms may be found in the work of Chu and Abramson [45]. Figure 3-6 shows the results of utilizing various representations for the 2-D section in the corresponding 2-D theory. In each of these "fitting" techniques the velocity distribution on the free surface zero potential line is taken to be that of the circumscribing flat plate, ellipse or circle. The authors conclude that fitting methods are adequate for bodies for reasonably large deadrise angle during later stages of the impact process. For bodies of small deadrise angle, more typical of ship bottom structures, more accurate formulations that avoid linearization of the free surface boundary conditions are probably required, but will involve somewhat lengthy numerical procedures. They do acknowledge, as shown in Figure 3-6, that Von Karman's theory is good for low deadrise angles when the body is almost a flat plate.

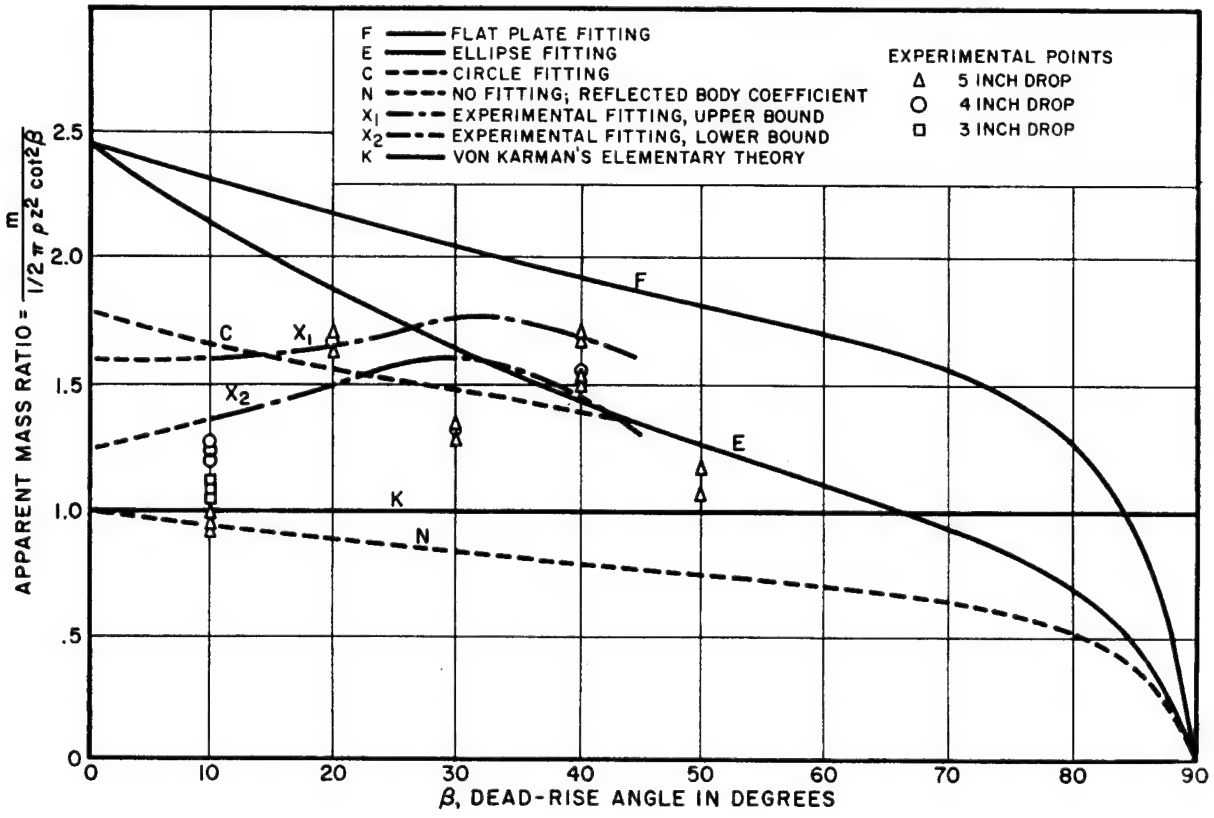


**Figure 3-6: Ratio of Apparent Mass to Von Karman Apparent Mass Versus Deadrise Angle [45]**

Gran et al [64]$^{x}$ in considering bow flare hydrodynamic forces conclude that the solutions to Equation (3-3) for the time varying added mass are few but include the circular cylinder which by means of conformal mapping can be extended to a variety of different forms. An expression for the instantaneous impact force is given as:

$$F = \pi \rho r C_v V_o^2 \frac{dr}{dx} \tag{3-13}$$

$$M = \frac{\pi}{2} \rho C_v b^2 \tag{3-14}$$

where $C_v$ is the ratio between hydrodynamic mass of the actual hull form section shape and hydrodynamic mass of a circular cylinder of the same beam. $C_v$ coefficients are given which are said to include a correction for piled-up spray, Table 3-1.

| Section Area Coeff: = (SA)/2d B | 0.5 | 0.6 | 0.7 | 0.8 | 0.9 |
|---|---|---|---|---|---|
| 0.2 | 0.90 | 0.93 | 0.97 | 1.01 | 1.05 |
| 0.4 | 0.85 | 0.89 | 0.94 | 1.01 | 1.10 |
| 0.6 | 0.82 | 0.87 | 0.93 | 1.02 | 1.13 |
| 0.8 | 0.80 | 0.85 | 0.92 | 1.02 | 1.16 |
| 1. | 0.78 | 0.83 | 0.91 | 1.02 | 1.19 |
| 1.5 | 0.76 | 0.81 | 0.89 | 1.02 | 1.23 |
| 2. | 0.76 | 0.80 | 0.88 | 1.03 | 1.26 |
| 2.5 | 0.75 | 0.79 | 0.87 | 1.03 | 1.26 |
| 3. | 0.75 | 0.78 | 0.87 | 1.03 | 1.29 |
| 4. | 0.75 | 0.77 | 0.86 | 1.03 | 1.31 |

**Table 3-1: Added Mass Coefficients, $C_v$, for Lewis Two-Parameter Forms [64]**

The statement of the entire boundary value problem in three dimensions, including non-linear boundary conditions, is given in Section 3.2.2. The two-dimensional cases just discussed had simplified or linearized boundary conditions. Troesch and Kang [5]x have developed a computer based three-dimensional integral equation technique satisfying the exact body boundary and the equipotential free surface conditions. They determined that the results compare well with the equivalent two-dimensional strip theory when the beam to draft ratio exceeds 2.0 and that adequate engineering predictions are obtained for slamming but that bow flare slamming was over-predicted by about 30% at peak, Figures 3-7 and 3-8. They ascribe this to the simplified free surface boundary condition which neglects the jet-like behavior of the water above the mean waterline. It should also be noted that in the case of the vertical slam of a sphere they found consistent over-prediction of the force by about 40% by the two-dimensional method compared to the three-dimensional.

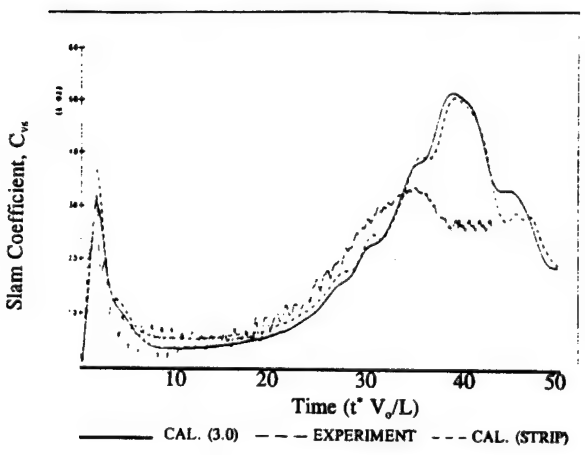


**Figure 3-7: Experimental and Theoretical Comparison of the Vertical Slam Coefficient for the Flared Body. (Zero degree trim, 61 cm (2.0 ft) drop height) [5]**

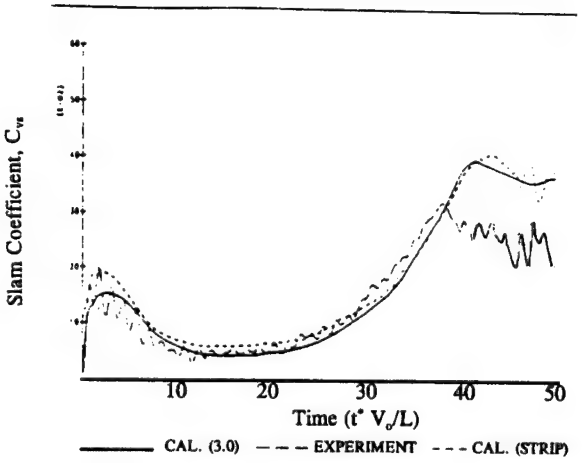


**Figure 3-8: Experimental and Theoretical Comparison of the Vertical Slam Coefficient For the Flared Body. (Ten degree trim, 61 cm (2.0 ft) drop height) [5]**

The rapid increase in computer computational power has resulted in attempts to solve the two-dimensional equivalent of the non-linear boundary value problem. Greenhow [65], Greenhow and Lin [66] and Yim [67] have made use of the Cauchy integral theorem including the rigid body boundary and a mixed Eulerian-Lagrangian description of the free surface. Calculations have shown some agreement for pressure distribution on small to moderate wedge angles below the mean free surface.

A numerical method for studying water entry of a two-dimensional body of arbitrary cross-section was presented by Zhao and Faltinsen [68]. In this solution the exact nonlinear free-surface condition without gravity is satisfied. Important features of the

solution method are how the jet flow occurring at the intersection between the free surface and the body is handled, and how conservation of fluid mass is satisfied in areas of high curvature of the free surface. The method confirms that conservation of mass, momentum and energy are satisfied. It was also verified by comparisons with similarity solution results for wedges with deadrise angles varying from 4 deg. to 81 deg.

In this method water is assumed incompressible and the flow is irrotational. That means that impact velocity is not so high that compressibility effects in the water matter. In practice this is not a severe limitation. Korobkin and Pukhnachov showed that the effects of gravity, viscosity, and capillarity are negligible in the initial stage of impact [69]. It is assumed that no air pocket is created during impact. This means that deadrise angle has to be larger than 2-3 deg.

Under these assumptions the velocity potential satisfies the Laplace equation (3-4) in the fluid domain. The pressure is set equal to a constant atmospheric pressure on the free surface. The kinematic free surface condition is that a fluid particle remains on the free surface. Hence the motion of the free surface may be found by integrating the fluid velocity. The dynamic free surface condition (applied to the exact free surface) can be written as:

$$\frac{D\phi}{Dt} = \frac{1}{2}\left[\left(\frac{\partial\phi}{\partial x}\right)^2 + \left(\frac{\partial\phi}{\partial y}\right)^2\right] \qquad \textbf{(3-15)}$$

where D/Dt is the substantial derivative. The body boundary condition on the wetted body surface can be expressed in form of Eq. (3-6).

It is assumed that a jet flow is created at the intersection between the free surface and the body surface as shown in Figure 3-9. The pressure is set equal to atmospheric pressure in the upper part of the jet (lines AB and CD) where fluid motion is assumed to be a one-dimensional.

The unknown velocity potential $\phi$ for the flow inside the fluid domain is represented by Green's second identity, i.e.

$$2\pi\phi(x,y) = \int_S \left[\frac{\partial\phi(\xi,\eta)}{\partial n(\xi,\eta)}\log r - \phi(\xi,\zeta)\frac{\partial \log r}{\partial n(\xi,\eta)}\right] ds \qquad \textbf{(3-16)}$$

where $r = [(x-\xi)^2 + (y-\eta)^2]^{1/2}$. The surface S consists of AB, CD, $S_B$, $S_F$ and $S_\infty$, where $S_\infty$ is a control surface far away from the body.

In the numerical evaluation of Equation (16), the free surface $S_F$ and body surface are divided into a number of straight line segments, on which $\phi$ and $\partial\phi/\partial n$ is constant and $\phi$ has a linear variation over AB and CD.

The integral equation is satisfied at the midpoint of each segment. In the time integration of the free-surface position, it is important to satisfy conservation of fluid mass carefully.

Typical pressure distribution along a body surface is shown in Fig. 3-10. Fig. 3-11 shows numerical predictions of pressure distribution and free-surface elevation around wedges that are forced with constant vertical velocity $V_o$ through and initially calm free-surface.

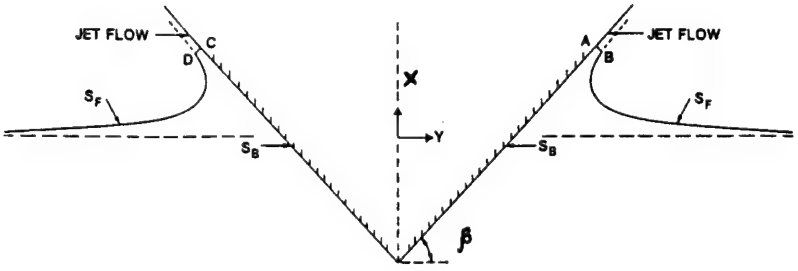


**Fig. 3-9. Definitions of Coordinate System and Control Surfaces Used in Numerical Solution of Water Entry of a Wedge by a Boundary Element Method [68]**

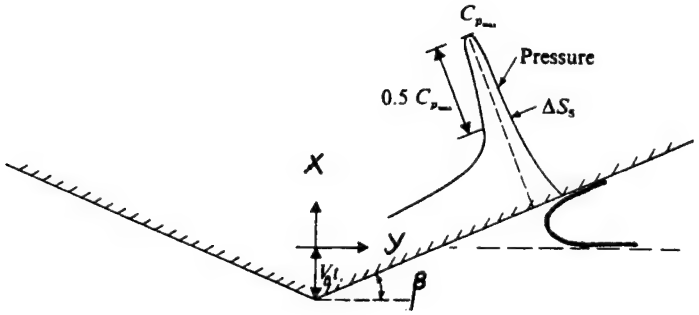


$C_p$ = pressure coefficient.
$\Delta$ $S_s$ = spatial extent of the slamming presure.

**Fig. 3-10. Definitions of Parameters Characterizing Slamming Pressure During Water Entry of a Blunt Two-Dimensional Body [68]**

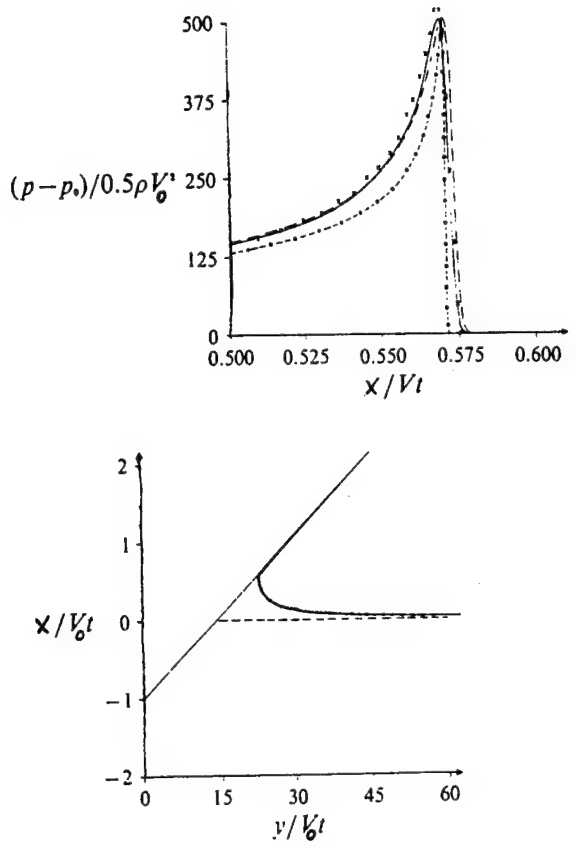


**Fig. 3-11. Prediction of the Pressure Distribution and Free Surface Elevations During Water Entry of a Wedge ($\beta$ = 4°) With Constant Vertical Velocity**

The pressure distribution for different deadrise angles of wedges is shown in Fig. 3-12. When the deadrise angle $\beta$ is larger than about 45 deg., the maximum pressure occurs at the apex of the wedge. Comparison for maximum pressure coefficient $C_{p\,max}$ with Wagner's formula is shown in Fig. 3-13. For very large $\beta$-values Wagner's formula underpredicts the maximum pressure. For $\beta$ <45 deg. agreement with Wagner's formula is excellent.

Another way to obtain a numerical solution to the nonlinear problem with free surface is based on the analysis of so-called similarity solution. Dobrovol'skaya [71] has presented similarity solutions for flow around symmetrical wedges. In the similarity flow the fluid velocity can be written as

$$\nabla\phi = V_o F\left(\frac{x}{V_o t}, \frac{y}{V_o t}\right), \tag{3-17}$$

where F is a function that should be found by solving the special integral equation. Zhao and Faltinsen [68] reviewed the Dobrovol'skaya solution [71] and presented numerical results for different deadrise angles, see Fig.3-12. It is shown that when the deadrise angle of the wedge is larger than about 45 deg., the maximum pressure occurs at the apex of the wedge. In other words, for this values of $\beta$ the pressure distribution on the body surface does not show the typical slamming behavior of high impulse pressures concentrated over small surface areas.

Very good results, close to "exact" numerical solution were derived by Zhao and Faltinsen [68] on the basis of the method using matched asymptotic expansions. The flow is divided into an inner and outer flow domain. In the inner flow the details of the jet flow at the intersection between the free surface and the body surface are studied by means of Wagner local jet flow analysis. In the outer flow the body-surface conditions and the free-surface conditions are transferred to a horizontal line and the body corresponds to a flat plate. The velocity potential is set equal to zero in the free-surface conditions. The inner and outer solutions are matched, which enables one to set up a composite solution for pressure distribution. This technique was shown by Armand and Cointe [43], Cointe [72], and Howison et al [73]. Relationships between inner, outer and composite solutions are shown in Figure 3-14.

According to asymptotic solution the vertical coordinate of maximum pressure is equal to

$$x = \left(\frac{\pi}{2} - 1\right) V_o t, \tag{3-18}$$

and the maximum pressure (slamming pressure) coefficient is equal to

$$C_{pmax} \equiv \frac{Pmax - Po}{0.5\ \rho V_o^2} = \frac{\pi^2}{4} cotan^2 \beta \tag{3-19}$$

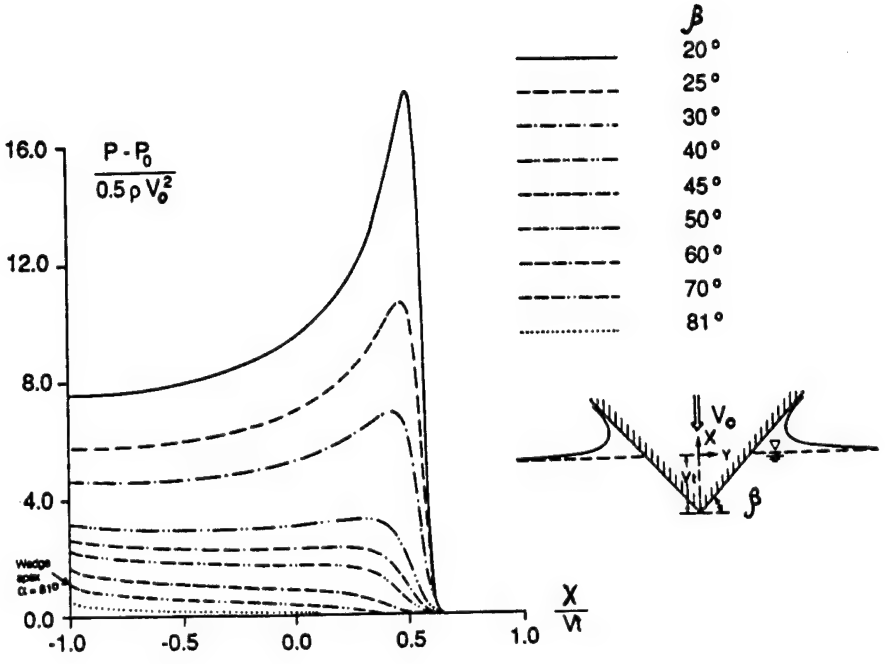


**Fig. 3-12. Predictions of Pressure Distribution During Water Entry of a Wedge With Constant Vertical Velocity $V_o$ By Means of the Similarity Solution [68]**

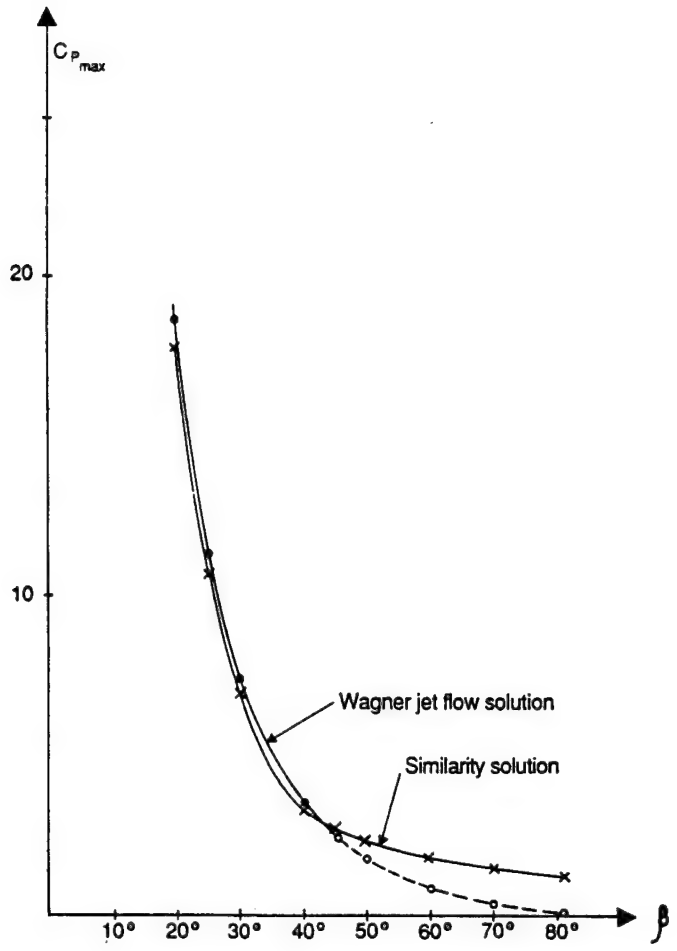


**Fig. 3-13. Prediction of Maximum Pressure Coefficient $C_{p\,max}$ During Water Entry of a Wedge with Constant Vertical Velocity $V_o$ by Means of Similarity Solution and Wagner's Jet Flow Solution (Asymptotic Solution) [68]**

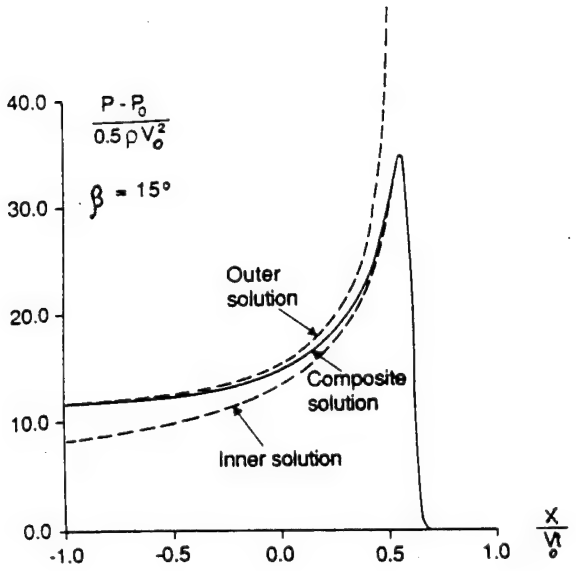


**Fig. 3-14. Prediction of Pressure Distribution During Water Entry of a Wedge with Constant Vertical Velocity $V_o$ by Means of Asymptotic Method Described by Zhao & Faltinsen (68)**

The jet thickness is

$$\delta = \frac{1}{4} V_o t \tan \beta \qquad \textbf{(3-20)}$$

The asymptotic solution is shown in Figure 3-13. For small and moderate deadrise angles the agreement with the similarity solution is very good.

Watanabe [70] has also provided a solution based on matched aymptotic expansions and local jet flow analysis. However, his analysis of the jet flow, the matching, and the final results are not the same as Zhao and Faltinsen [68].

A two-dimensional potential-flow model was employed to predict the flow fields generated by a wedge penetrating a still fluid at constant velocity [74]. The model includes the full nonlinear free-surface boundary conditions on a boundary-fitted coordinate system. The model equations were solved using a second-order finite-difference technique with a modified Euler method for the time domain and a successive overrelaxation procedure for the spatial domain. The mathematical model gives pressure distributions and force coefficients in excellent agreement with observations and theoretical results.

Hydrodynamic impact pressures, both on the hull bottom and on the wet-deck, are of particular interest in multi-hull and SES hydrodynamics [7]. These pressures can be calculated by using methods well established for the conventional ships. Based on classical hydrodynamics, Toyama [75] developed an improved two-dimensional method for calculating hydrodynamic impact pressures on an arbitrary ship section. The author applied this method to SES hull sections.

In concluding on the analysis of the 2-D incompressible solutions, it should be pointed out that designer must be careful in applying results for wedges to other cross sections. The local deadrise angle is not the only important body parameter. For instance, the local curvature also matters. Further, the assumption of constant body velocity does not account for accelerations that may have importance, in particular for drop test experiments. This will be discussed later.

All the above mentioned theories for incompressible fluid, however, are not applicable at the instant of impact. This is due to the fact that the velocity potential instantaneously jumps from zero to a finite value and thereby the magnitude of the impact pressure becomes infinite. This situation can be eliminated if the compressibility of water is included in the theory. For this case, the velocity potential must satisfy the wave equation instead of Equation (3-4). That is:

$$\nabla^2\phi = \frac{1}{c^2}\frac{\partial^2\phi}{\partial t^2} \qquad \textbf{(3-21)}$$

where:

$c$ = velocity of sound in the fluid.

The effect of compressibility of water on the impact of a flat plate was studied by Von Karman [32], Egorov [76] and Ogilvie [39], and of a wedge by Skalak and Feit [78]. In the latter two studies, supersonic flow theory was applied to the impact problem. That is, if the expansion rate of the area of contact between the water and the body exceeds the sound velocity, then the compressive wave will not propagate outward from the edges of the contact surface and hence the free water surface beyond the contact surface will not be disturbed. An acoustic pressure is applied to the contact surface in this case. Immediately after contact, the expansion rate decreases; then, the acoustic pressure is dissipated and only the hydrodynamic pressure remains. Although these theories give a finite magnitude of pressure at the moment of impact, the magnitude is still very high in comparison with that expected to occur in ship slamming. In addition, the theories on compressibility show that the pressure is linearly proportional to the impact velocity which is contradictory to the results observed in ship slamming which show instead the pressure to be approximately proportional to the square of the velocity. Hence, the notion of compressibility of water may not be appropriate to the slamming problem.

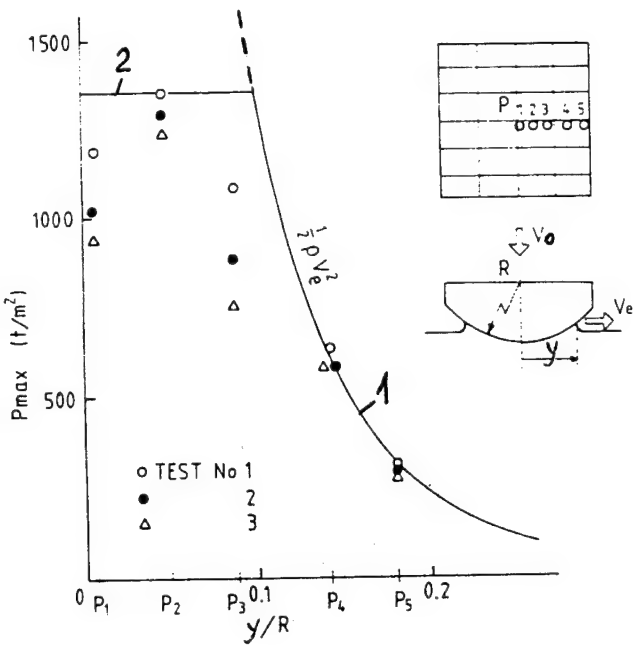


1 - Wagner's formula
2 - Acoustic pressure $\rho C V_o$
(Cp = 375)

**Fig. 3-15. Maximum Impact Pressures on a Circular Cylinder as a Function of Time After Initial Impact ($V=8ms^{-1}$, R=5m) (Hagiwara & Yuhara, [79])**

The acoustic pressure, or limit for pressure in water under impact, is equal to

$$p_{ac} = \rho\ C\ V_o \qquad (3\text{-}22)$$

With no air content C varies typically between 1450 m/s and 1540 m/s. In rough seas, air bubbles will be in the water altering the speed of sound dramatically. The importance of the acoustic pressure is illustrated in Figure 3-15 where pressure results from forcing a vertical cylinder with radius 5 m through the free-surface with velocity $V_o$ = 8 m/s are presented, Hagiwara and Yuhara [79]. As it is shown from this figure, the acoustic pressure is about 125 times the atmospheric pressure and the maximum pressure occurs close to the centerline of the cylinder. When $y \geq 0.5$ m the slamming pressure is determined from Wagner's analysis. As pointed out earlier, the slamming pressures are very local in time and space and the maximum slamming pressure does not occur simultaneously around the cylinder surface.

Other considerations in the theoretical treatment of the impact problem are the effect of entrapped air between the body and the water at the moment of impact, and

the effect of body elasticity. Kamel [80] concluded that shock pressures resulting from the impact between a solid and a liquid, as in his specific investigation of waves breaking against coastal structures, can best be described as a water hammer phenomenon where the compressibility of the liquid and the elasticity of the solid are the governing factors. He expects that in most cases the pressure will be reduced due to the presence of some air. The effect of deformation of the hull cross section (plate) on impact was studied by Weinig [81], Meyerhoff [82] and Chuang [83]. In Meyerhoff's study, the general formulation of Wagner's theory for a wedge including elasticity was developed. Sellers [84] has developed a solution for maximum impact pressure taking into account structural elasticity and entrapped air:

$$p_{max} = S_T \rho_S C_w V_o \qquad \textbf{(3-23)}$$

where:

$S_T$ = *a function of the structural impedance*

$\rho_S, C_w$ = *mass density and speed of shock wave in water–air mixture*

$V_o$ = *relative velocity of impact*

Sellars found that in full scale with high relative velocities the effects of structure can be important and reduce the impact pressure as flexibility of the structure increases. Equation (3-23) results in conservative predictions of full-scale pressure and the effect of air entrapment on the maximum pressure does not appear significant.

### 3.2.3 Three-Dimensional

The application to three-dimensional cases has been less significant to date due to the increased complexity of the mathematical problem. The theories which have been developed predominantly rely on potential flow. The impact pressures and loads are assumed to be due to a rigid body entering otherwise calm water. Viscosity, surface tension, air entrapment, compressibility of air or water and vessel forward speed are ignored. Hydro-elasticity is considered in some cases which are identified in Section 3.2.4.2 herein.

Relatively few attempts have been made to rigorously solve impact problems dealing with three dimensional bodies. Examples are Shiffman and Spencer [85], Chuang [86], and Miloh [87]. Shiffman and Spencer and Chuang developed general expressions for the pressure distributions and slamming forces on a cone. Using similar assumptions, Miloh analytically derived the added mass coefficients for a double spherical bowl. From these coefficients the impact force on a sphere was calculated assuming that the free surface is represented by an equi-potential surface.

Of practical engineering interest are the impact forces in the bow region of a ship. Due to complexities associated with the three-dimensional boundary value problems, it has been common practice to use simplifying assumptions that reduce the calculations of hydrodynamic forces to a two-dimensional strip theory. Examples of this are given by Ochi

and Motter [88], [28], Yamamoto, et al [89], Belik, et al [90], and Oliver [91]. These types of hydrodynamic theories assume that the ship is of sufficient length and cross-sectional uniformity to allow the hull to be divided into segments, each of which is assumed to act independently of any other, Figure 3-16. A number of two-dimensional solutions are then summed to yield the total impact force. Techniques such as these are not precise in the bow region where the assumed two-dimensionality of the flow may not be valid. An illustration of the relative error of the two-dimensional approximation for three-dimensional bow loads can be seen in Figure 3-17. There the nondimensional impact force for a sphere, defined by $C_s$ = 2 (impact force)/$\rho\pi$ $R^2V_o^2$ is calculated using results similar to Miloh [87] for three-dimensional theory and a strip theory based on Kaplan and Silbert's [92] or Sarpkaya and Isaacson's [93] formulas for a circular cylinder. The slam coefficient is plotted as a function of z/R, the normalized vertical distance. In both cases the free surface is represented by an equipotential surface and the velocity of the body is constant. While the strip theory approximation of the sphere represents an extreme example, it demonstrates the need to exercise caution when applying two-dimensional solutions in areas where three-dimensional effects are large.

The following is the formulation of the three-dimensional potential impact problem with non-linear free surface condition Troesch, Kang [5].

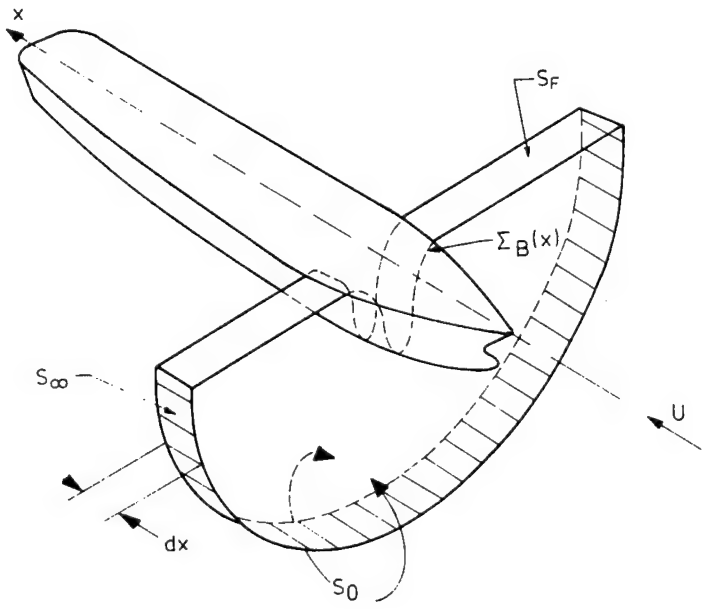


**Fig. 3-16. Use of Strip Theory to Calculate Loads on Sections of Ships [4]**

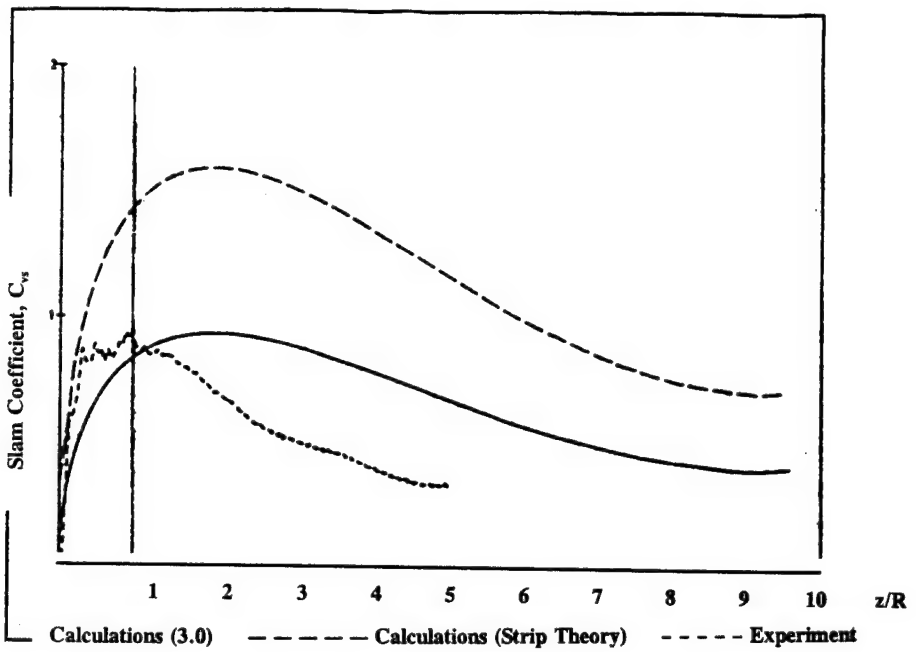


**Fig. 3-17. Experimental and Theoretical Comparison of the Vertical Slam Coefficient For a Sphere (Drop height - 61 cm (2.0 ft.))[5]**

Consider an ideal fluid where a rigid body passes through the free surface. The boundary value problem for the three-dimensional case has been described by Troesch and Kang [5]:

The free surface is defined by

$$z = \varsigma(x,y,t) \tag{3-24}$$

where $(x,y,z)$ is a right-handed coordinate system with $z$ positive upwards and the origin located at the mean free surface. The governing field equation is the 3-D Laplace Equation, Equation (3-4). Newman [94], among others, derived the complete free surface boundary condition, including both kinematic and dynamic considerations as

$$\frac{\partial^2\phi}{\partial t^2} + g\frac{\partial\phi}{\partial z} + 2\nabla\phi \cdot \nabla\frac{\partial\phi}{\partial t} + \frac{1}{2}\nabla\phi \cdot \nabla(\nabla\phi \cdot \nabla\phi) = 0 \tag{3-25}$$

which must be satisfied on the surface defined by Equation (3-24). Here g is the gravitational constant. The body boundary condition, satisfied on the instantaneous body surface, is expressed as

$$\frac{\partial \phi}{\partial n} = V \cdot n \tag{3-26}$$

where $\underline{V}$ is the velocity vector of the body and $\underline{n}$ is the outward unit normal. To complete the statement of this boundary value problem, radiation conditions must be given.

$$\phi = 0 \qquad x,y = \infty \tag{3-27}$$

If a velocity potential satisfying the above conditions can be found, then the pressure may be determined from Bernoulli's equation as

$$\frac{p}{\rho} + \frac{\partial \phi}{\partial t} + \frac{1}{2} \nabla\phi \cdot \nabla\phi + gz = constant \tag{3-28}$$

Once the pressure distribution becomes known, it can be integrated and the force found in a straight-forward manner.

If only vertical motion is considered. The velocity vector, $\underline{V}$, used in the body boundary condition is determined from the solution of the equations of motion in the vertical plane shown below:

$$F_z = m\ddot{z} = -\int\int p n_z \, dS - mg \tag{3-29}$$

The vertical velocity, $\dot{z}(t)$, and displacement, $z(t)$, are found through the usual integration formulas of:

$$\dot{z}(t) = \int_o^t \ddot{z}(t)dt \tag{3-30}$$

$$z(t) = \int_o^t \dot{z}(t)dt \tag{3-31}$$

A general three-dimensional solution to the boundary value problem posed by Equations (3-24) - (3-27) has not yet been found. The complexities of the non-linear free surface and body boundary conditions have resulted in assumptions being made in order to calculate the impact forces as have been reviewed by Greenhow [65]. Troesch and Kang [5] have noted it is possible to catalogue the various existing theories based upon their

approximations of the boundary conditions and their assumptions regarding rigid body dynamics and there are extensive literature surveys on the subject available as part of the publications of The International Ship Structures Congresses (ISSC) [22,23,24,95]. The simplification of the problem to two-dimensional theory is treated in Section 3.2.1 herein.

Troesch and Kang [5]* developed both two-dimensional strip and three-dimensional panel methods for the solution of the impact boundary value problem satisfying the body boundary condition and the simplified equipotential free surface condition ($\phi = 0$). In order to investigate the validity of the assumptions listed in the previous paragraphs, the hydrodynamic impact forces acting on two different body shapes were examined [5]. The body shapes are shown in Figure 3-18. One has circular cross sections with a cylindrical parallel midbody. The ends are halves of hemispheres. The other body has a bow flare shape with elliptical water lines. Both shapes have length-to-beam ratios of 2.0. The cylindrical shape has a beam-to-draft ratio of 2.0, while the flared body has a beam-to-draft ratio of 1. Theoretical pressures were calculated by both two- and three-dimensional boundary integral methods. Experimental results were obtained in the Ship Hydrodynamics Laboratory at the University of Michigan. These results were representative of time histories of a series of impact experiments. The bodies shown in Figure 3-18 were dropped from three drop heights, with three different trim angles, 0, 5, and 10 degrees.

The vertical impact force as function of time for the cylindrical body is shown in Figure 3-19 for zero trim angle and Figure 3-20 for a 10 deg. trim in the form of the vertical slam coefficient, $C_{vs}$.

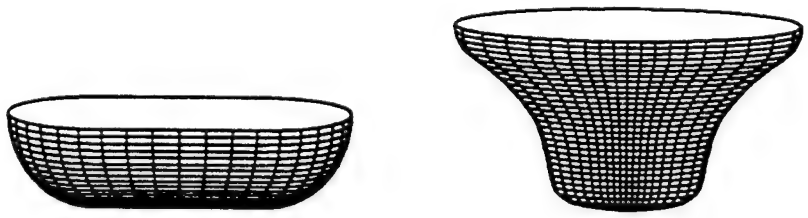

**Fig. 3-18. Panel Distributions for the Cylindrical and Flared Bodies.**

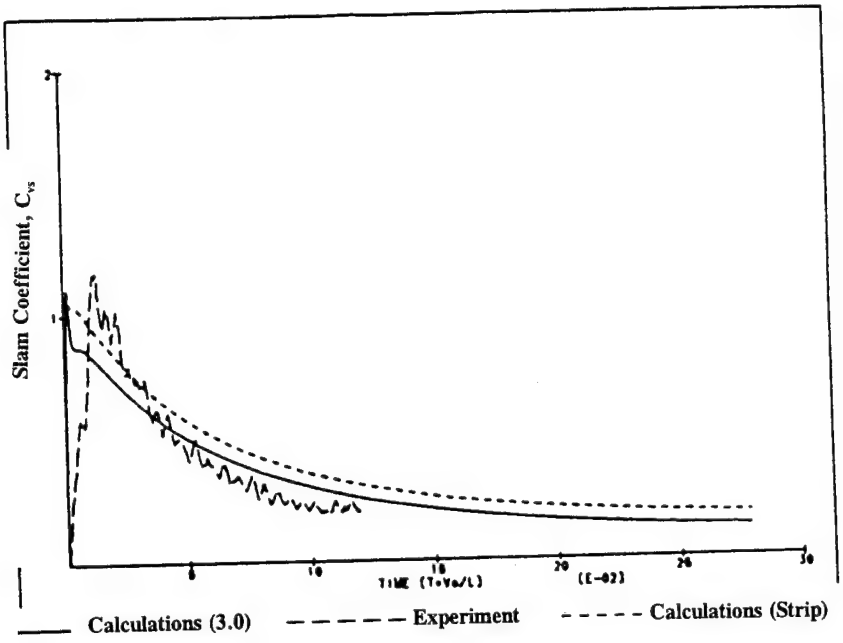


**Fig. 3-19. Experimental and Theoretical Comparison of the Vertical Slam Coefficient for the Cylindrical Body (Zero Degree Trim, 61 cm (2.0 ft.) Drop Height) [5]**

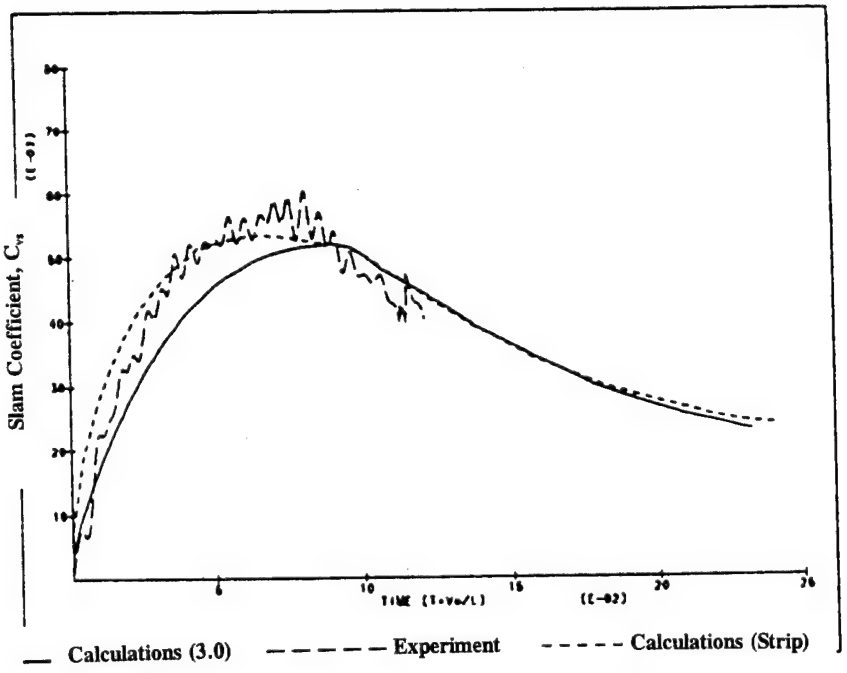


**Fig. 3-20. Experimental and Theoretical Comparison of the Vertical Slam Coefficient for the Cylindrical Body (Ten Degree Trim, 61 cm (2.0 ft.) Drop Height) [5]**

$$C_{vs} = \frac{2m\ddot{z}}{\rho\pi\left(\frac{L}{2}\right)^2 V_o^2} \qquad (3\text{-}32)$$

where:
- m = mass
- $\ddot{z}$ = vertical acceleration
- $\rho$ = water density
- L = representative length (for the sphere L is the diameter, for the cylindrical body or the flared body it is the overall length)
- $V_o$ = is the initial impact velocity

Theoretical calculations based upon the three-dimensional and two-dimensional methods are shown by the solid and short dashed lines respectively. The experimentally measured force is given by the intermediate dashed line. The data for the flared body is shown in Figures 3-7 and 3-8.

Based upon the information displayed in these figures, the following observations may be made:

- The 2-D and 3-D theoretical curves are surprisingly close when compared to the results for the sphere, a body with a beam to draft ratio of 1.0, shown in Figure 3-17. It is interesting that experimental curves for cylindrical body are close to the 2-D solution for the initial phase of impact, while the 3-D theory predicts maximum force coefficient well.

- The slam coefficient for the flared body is characterized by two maxima, one occurring during the initial contact between body and water, and the other when the flared sections pass through the surface. The second maxima due to flare has a value equal to or greater than the first maximum.

- The variation of the trim angle from 0 to 10 degrees produces a significant decrease in the maximum value of slam coefficient for the cylindrical shape and for the first maximum in the flared body curve. Those values decrease by approximately a factor of two over this range of trim. The decrease due to trim angle change in the second maximum for the flared body is not as large. In fact, the experimental value remains essentially equal for trim angles from 0 to 5 degrees and then decreases slightly at 10 degrees.

- The comparison between theory and experiment for the slam coefficient maximum of the cylindrical shape and for the first maximum of the flared body is good. However, the second maximum for the flared body was consistently overpredicted, with the largest error occurring at a trim angle of 0 degrees and the smallest at 10 degrees.

- The nondimensional time coordinates for the slam force coefficient maxima were underpredicted depending upon the body and trim considered.

- These results are applicable to both slamming and bow flare impact.

The solution to the three-dimensional problem of submersion of an object of an arbitrary form in ideal incompressible flow was gained by Stepanov for free-fall life boats [96], [97]. The numerical solution to the boundary value problem with a nonlinear condition on the free surface was performed by using the integral equation method. The general problem was transformed into some sequence of problems for fixed instances in time separated by small intervals. The integral equation was reduced to a system of linear algebraic equations. To determine the vertical resultant force the Lagrangian formula for changing of the kinematic energy of fluid expressed in generalized coordinates was used.

The analysis of the kinematic energy of fluid was also used by Chuvikovsky for evaluation of slam forces acting on a 2-D section of a ship [98], [99]:

$$q(x,t) = m(\zeta,x)\ddot{\zeta} + K\dot{\zeta}^2 \frac{\partial m(\zeta,x)}{\partial \zeta} \qquad \text{(3-33)}$$

where: m = added mass of the immersed part of 2-D section;
$\zeta$ = relative vertical motion of this section during pitch and heave.

The factor K depends on the section deadrise angle $\beta$ (degrees):

$$K = 1 - \frac{1}{2}\left(\frac{\beta}{90}\right)^{1.5} \qquad \text{(3-34)}$$

The kinematic energy approach was commonly used by Russian engineers to calculate dynamic bending moments [96], [98].

Kaplan and Malakhoff [100] have applied the expanding wedge work of von Karman [32] to the bows of SES craft. They utilize a formulation of the 2-D added mass to represent the 3-D added mass of the bow. In carrying out this work for higher speed vessels than displacement hulls, the effect of forward speed is considered in the framework of an analytical model proposed by Smiley [101] using the concept of equivalent planing velocity. They show the resultant slamming pressure as:

$$p_{slam} \approx \frac{\rho}{2}\left[u + W_r\, Cot(\tau + \theta)\right]^2 \qquad \text{(3-35)}$$

where $u$ is forward velocity, $W_r$ is the vertical velocity, $\tau$ relates to hull geometry and $\theta$ is pitch. They conclude that this expression indicates the quadratic variation of slam pressure

with vertical velocity when the forward speed is relatively low, as in the case of a surface ship where the large velocity at the bow influencing impact pressure is the relative vertical velocity between the vessel and the sea surface. For the SES case the expressions indicate both linear and quadratic variation with relative vertical velocity, together with a forward speed effect.

Kaplan [102] has applied a similar approach to predict impacts on the water surface of the flat of bottom of centerbody surfaces of multi-hull vessels such as SWATH and catamarans. Von Karman's technique is applied however in taking the 2-D section in the longitudinal plane rather than the transverse where the flat exists and as a result the singular (i.e., infinite) behavior associated with the time rate of change of the sectional added mass is avoided. As an example, the added mass of the flat wetdeck is taken as:

$$m_s = \rho \frac{\pi}{8} b c^2 \qquad \textbf{(3-36)}$$

where $b$ is the beam of the flat wetdeck and $c$ is the changing wetted length which has a finite angle with the wetdeck surface. Kaplan reasons that the wetdeck beam is generally large compared to the wetted length and hence Equation (3-36) is a valid expression of the three-dimensional added mass.

Ohtsubo and Fukumura [103] and also Tanizawa [104] applied boundary elements to solve the self-symmetrical problem of a rigid symmetrical wedge entering vertically and with constant speed into initially calm water. Comparison of the pressure distributions with Wagner's expanding plate theory showed good agreement for small deadrise angles, up to about 10 degrees. For larger deadrise angles the comparison with Wagner is not good. However, a comparison with expanding prism results would have been more appropriate. Good agreement is achieved with Hughes' [105] numerical results for a large deadrise.

The problem of oblique wedge entry into initially calm water was investigated by Greenhow [65]. The study allows nonsteady speed, gravity and suction on the "backside". The author shows that for sharp wedges satisfactory results are obtained with deadrise of up to about 30 degrees and fair results for a deadrise angle of 45 degrees.

Arai and Matsunaga [106], [107] applied finite difference methods to solve the problem of a cross section with considerable flare entering into an initially calm water surface at constant speed, and at an angle. The effect of gravity is included. Comparison of computed and measured time histories show remarkable agreement. The authors conclude that the numerical approach is well suited to predict the high pressure region, which extends over a considerable area of the flare when the flare comes into contact with the water.

The water entry of a rigid circular cylinder into a compressible fluid was studied by Radev [108]. Results are presented for a cylinder of 0.15 m diameter and two

entry velocities. Results show that the elevation of the fluid surface tends to reduce the pressure with increasing time.

The cushioning effect of layers of elastomeric material bonded to the undersurface of a flat bottom falling on calm water was investigated by Ando [109]. It was shown that a layers of optimum elasticity could significantly reduce the slamming forces for flat bottoms striking the water vertically. Such layers tended to increase the slamming force for wedge-shaped bottoms. However, the peak impact forces for the wedges were considerably smaller than those for the flat bottom under identical drop conditions.

The effect of the three-dimensionality of the ship hull and the wave was calculated by Watanabe [110], by means of matched asymptotic expansions assuming small immersion and neglecting gravity. The calculated results were compared with experimental results obtained in free-running tests with a bulk-carrier model. Agreement between calculation and experiment was satisfactory only when the measured motion response was used instead of a theoretical prediction.

A theoretical method for the prediction of impact pressures of arbitrary ship-like 2-D forms was presented by Song et al [111]. The flow around the two-dimensional shape immersing at constant speed was approximated by a multi-coefficient conformal transformation technique applied to the instantaneous immersion. Piled-up water during immersion was considered. Two typical sections, a fishing vessel midship section and a containership forebody section were investigated.

Although most theoretical studies involving wave slamming have considered the case of regular waves, Isaacson and Subbiah [112] have recently analyzed the application of a suitable force formulation to the case of random waves impacting on a horizontal cylinder. An expression is developed for the probability distribution of the force maxima, based on the assumption of a narrow-band spectrum.

### 3.2.4 Hull Response

#### 3.2.4.1 Response of Structure to Water Impacts

Slamming damages have been a matter of concern for more than 60 years and for the past 30 years, hull structure damages due to heavy weather vessel operations have fairly consistently been 10-12% of vessel claims, about the same as for collisions [24].

The ability to predict forces acting on the ship forebody and stern surfaces and the resulting dynamic hull girder response has been of long standing concern. As ship fatigue life came into question during the sixties, the manner in which slamming induced dynamic hull girder response superimposed on the quasi-static wave load response took on interest that remains today.

In accordance with the general approach (see, for example, Lewis and Gerard [113]) ship structural response to slamming may be grouped into three categories; i.e., localized response, transitional response, and overall response. During and immediately after slamming, there is a period of localized response when the hull-plate panels respond immediately because of direct contact with the slamming load. Since keel, floors, and nearby frame structures function as supports to the hull plating, they also react without delay. This is followed by a period of transition during which momentum imparted to the outer hull in the slamming area is transferred to the nearby outer hull, as well as to interior hull structural members, but the entire ship hull is not yet aware of the slamming load. Finally, there follows a period of overall response. If the exciting force, i.e., the slamming load, has produced sufficient momentum, the hull may vibrate vertically, horizontally, longitudinally, torsionally, or in any combination of these, depending on what portion or locality of the ship hull has been affected. This hull vibration is sometimes referred to as whipping. In addition, impact loads and the dynamic structural response contribute to fatigue.

Only the overall effects can normally be noticed by those aboard the ship. As both the loadings of the local and of the overall structure may well exceed the limits of safe operations, an assessment solely on the basis of the overall response is unsatisfactory. Methods to describe the limits of safe operation of ships with respect to impact loads in severe seas have so far only been developed for the risk of the bottom slamming. For example, Lipis [114] relates sea state to vessel proportions, draft, engine power, and speed. Such an approach seems to be insufficient for ships with fine hull lines and a minimum of flat bottom [115].

When a ship is exposed to ocean waves, it is subjected to three types of hydrodynamic forces. These force components are the hydrostatic force, inertial and damping forces (characterized by added mass and damping coefficients); and wave excitation forces (the simplified form of which is known as the Froude-Krylov force). Determination of these forces are sufficient to provide one with predictions of rigid body ship motions. However, in response to slamming in heavy or moderate seas, a ship can develop hull stresses associated with the flexural vibration (whipping) of the hull girder. This high frequency excitation may be generated when either there is an emersion of the ships keel (at either the bow or stern) followed by a significant impact upon reentry, or for ships with pronounced bow flare when a sudden increase in submerged area results in a rapid increase in added mass with associated increases in local pressure. Kline and Daidola [116] have shown slam-induced and bow flare frontal impact induced vibratory response appears to vary measurably with ship stiffness and the trends are uniform and consistent, i.e., increased stiffness increases response, and decreased stiffness lowers response.

It should be noted that impact loads of high performance vehicles (ACV, SES, SWATH, high-speed catamarans, planing or semiplaning monohulls) are basically of the same nature as on conventional ships and even seaplanes. Stavovy and Chuang [117] gave a procedure to compute slamming impact pressure of high performance vehicles (HPV), in

which they provided an empirical formula based on two- and three-dimensional model test data. Nevertheless, the HPV's have some special features.

Weight is a critical matter of all HPV's, and every precaution must be taken, therefore, to reduce weight to a minimum. This leads to the consideration of alternative materials to steel to minimize structural weight. To achieve a lightweight and safe structure, not only must the structural design loads be as realistic as possible, but also the structural response analysis should be of high reliability and accuracy. However, in the case of aluminum (the material for many HPV structures) even more careful attention must be given to fatigue loads as the allowable fatigue stress in comparison to yield is generally lower than that for steel.

The high hydrodynamic loads due to high speed and the unconventional geometry of means of support cause unusual load distributions. For example, for the case of a catamaran cross deck the two sidewalls tend to seal off the escape of water when contact is made with the free surface. Thus, the cross structure may be more vulnerable to a hydrodynamic impact than the bottom of a ship bow. This also implies that the threshold velocity associated with cross-structure slamming should be somewhat lower than used for normal monohull applications. Hadler, et al [118] assumed a zero value of the threshold velocity for slamming pressure calculations connected with the catamaran USNS HAYES. They found good agreement between calculated values of slamming pressure and measured results.

There are two main approaches to predict the overall structural loading of ships due to hydrodynamic impact:

- Based on estimation of the local pressure distribution;
- Based on the analysis of relative motion and momentum without predicting the local pressure distribution.

The following sections discuss the coupled hydrodynamic and structural techniques developed to address overall or hull response to hydrodynamic impact. As such, they consider theoretical 2-D, 3-D and experimental hydrodynamic impact loading theories as well.

#### 3.2.4.2 **Hull Response Theory**

In the early 1960s, Jasper [119] developed a theoretical analysis of hull whipping induced by bow-flare type of frontal impact. It utilizes measured or calculated rigid-body motion at each transverse section of a ship to compute the instantaneous waterline as well as the velocity of the section relative to the water and computes the added mass for each section at each waterline. The hydrodynamic force at each section is calculated as the time rate of change of the momentum imparted to the water and is added to the buoyancy and damping forces to give the total force. Finally, it computes response

of the elastic ship, thus giving the desired bending moments and shear forces in the vertical plane for a ship operating in a head sea. The theory was first programmed for analog computers (SAC: Seaworthiness Analog Computer) and later for digital computers (ROSAS: Response of Ship at Sea). As discussed in Section 3.3.2 the comparison with full scale results from the ESSEX was encouraging.

Chuang [120,121,122] expanded ROSAS to ROSAS3 [123] incorporating the effects of both lateral and torsional bending. Due to lateral symmetry in a ship the problem is subdivided into two independent sub-problems. That is, one sub-problem for the vertical motion identical to the two-dimensional analysis and one additional sub-problem for the horizontal motion coupled with the torsional motion. However, while bottom slamming forces are included for the vertical plane they are not taken into account for the coupled horizontal and torsional components.

ROSAS [120]$^x$ accepts the wave data as input in the form of sinusoidal continuous or discrete trains which move without change in form and at constant wave velocity from the bow to the stern of a moving ship. The moving waterline is then considered at each of 21 discretized stations along the ship. The forces generated by the moving wave consist of added mass ($P_1$), buoyancy ($P_2$) including Smith correction, hydrodynamic damping ($P_3$), and bottom slamming ($P_4$). The total force then becomes:

$$P(x,t) = P_1 + P_2 + P_3 + P_4 \tag{3-37}$$

where:

$$P_1 = \frac{d}{dt}(m_v V_r) \tag{3-38}$$

$$P_2 = \rho A\left(g + \frac{dV}{dt}\right) - \rho g A_o \tag{3-39}$$

$$P_3 = C(\omega)V_r \tag{3-40}$$

$P_4$ = *bottom slamming force due to triangular pressure distribution computed by Chuang* [124]
$\omega$ = *wave frequency*
$V_r$ = *relative vertical velocity* (3-41)

The added mass $m_v$ and submerged area $A$ are repeated into linear and nonlinear terms:

$$m_v = m_o + \overline{m_v} \tag{3-42}$$

$$A = A_o - b_1 Y_r + \overline{A} \tag{3-43}$$

where $m_o$ is the added mass associated with the still waterline, and $m_v$ is the time varying portion of the added mass as shown in Figure 3-21, which are computed by the method of Wagner [33]. $A_o$ is the cross sectional area up to the mean waterline (still waterline).

When the force function $P(x,t)$ acts on the flexible ship the governing equations of ship response for deflection $Y$ which are solved in the time domain:

$$m \frac{\partial^2 Y}{\partial t^2} + C \frac{\partial Y}{\partial t} + \frac{\partial V}{\partial x} = P \tag{3-44}$$

$$\textit{Inertia} + \textit{damping} + \textit{shearing} = \textit{excitation} \tag{3-45}$$

Kaplan and Sargent have developed procedures to perform time domain analysis at relatively high execution speed [125][x]. The approach utilizes motions through the use of the linear, frequency domain, ship motion theory used, along with fluid momentum analysis techniques, to provide for an initial estimate of impact forces. Once determined, the effects of non-linear buoyancy and momentum changes are estimated similar to Jasper [119] and Chuang [120]. Results are fed back as corrections to the initial estimate. The procedure is repeated until the solution converges. Structural responses are determined by assuming the hull to be a non-uniform Timoshenko beam. However, rather than solving for the governing differential equation a digital filtering technique is used to determine the flexural response of the first elastic mode only. As seakeeping theory is used to determine the impact force, the details of the force prediction technique are discussed in 3.2.4.2 Seakeeping Hydrodynamics.

Bishop, Price, et al [29][90][126][127] have performed extensive work in the area of hydro-elastic response of ships. Initial efforts began with investigations of responses in the vertical plane only and was later expanded to include not only lateral responses but asymmetric hull shapes as well. All these approaches are based on linear strip theory and assume that the ship can be represented as a non-uniform Timoshenko beam. The authors are of the opinion that a rigid body model for the hull girder will not result in the same response forces as when the stiffness and vibratory character of the hull is considered.

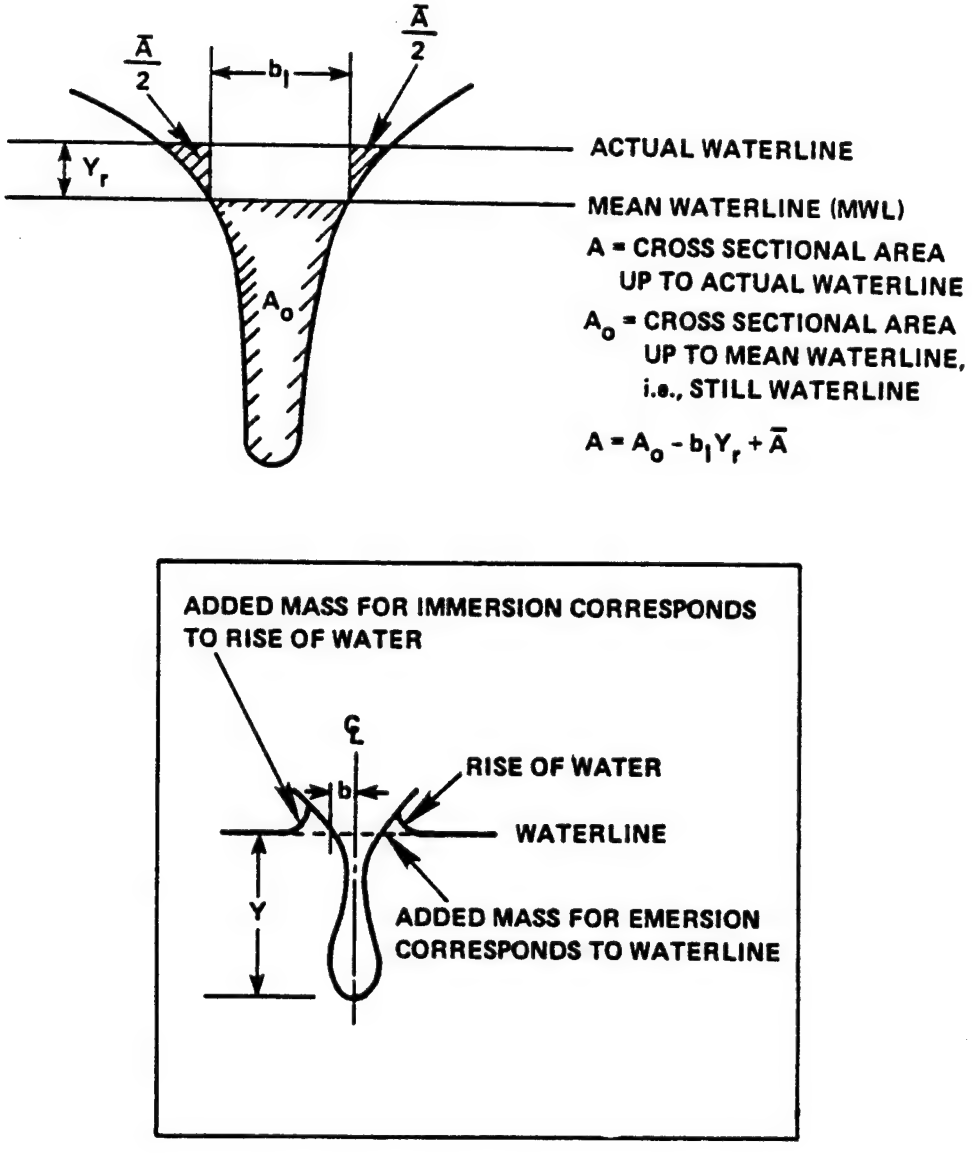


**Fig. 3-21. Method for Determining Added Mass for Immersion and Emersion**

The authors consider slamming as a combination of initial impact, for which they use the method of Stavovy and Chuang [117] to calculate pressures and forces, and subsequent momentum slamming as the hull plunges further in the water, for which they use the method of Leibowitz [128][129] for the added mass and buoyancy. They also consider frontal impact (flare slamming) using the latter approach. The time history of the force at each section is estimated by the techniques of Ochi and Motter [28] and Kawakami, Michimoto and Kobayashi [130]. More recently, work [131] has centered on applying a linear finite element approach to describe the elastic hull model and a hydrodynamic model based on translating pulsating sources and sinks and extending their approach to three dimensions [132].

The American Bureau of Shipping [133], [134] predictions for the vertical hull girder bending moments of a flexible ship can be performed by using the computer program ABS/BOWSLAM. The procedure treats the hull girder as a non-uniform Timoshenko beam and a modal analysis approach is used to determine structural responses. Inputs required for this analysis include ship mass, added mass and damping coefficients, relative motion and velocity at ship sections ahead of midships, and the first five or more modal shapes and corresponding natural frequencies. These parameters are determined by the computer programs ABS/SHIPMOTION and ABS EIGEN - V.

Although the procedure which is used is applicable to both regular and irregular waves, the model currently in use is limited to regular waves. Hence predictions of structural response of irregular seas must be represented by an equivalent regular wave system. Calculations can be performed for head seas only.

Mitsubishi Heavy Industries [135]: A time domain non-linear program, MSLAM, for predicting ship response to slamming has been developed by the Nagasaki Experimental Tank of Mitsubishi Heavy Industries [20]. The procedure allows for the prediction of time histories for vertical motion (heave and pitch), shear and bending moments as well as the effects of whipping due to both bow flare and keel slamming.

Strip theory is used to determine hydrodynamic coefficients for added mass, damping and wave exciting force. Non-linear effects are accounted for by calculating the change in added mass at each time step. Structural responses are determined by representing the ships hull as a non-uniform Timoshenko beam. Results can be obtained for either regular or irregular long-crested waves.

Chou, S. K., Chiu, F. C. and Lee, Y. J.: Have performed studies on non-linear motions and wave loads, including whipping of high speed craft [3]. The general approach utilizes a modified strip theory in order to predict sectional hydrodynamic coefficients at each time step and represents the ships hull as either an Euler or Timoshenko beam. Structural responses are determined by either modal superposition or finite element methods.

Most of Russian studies of hull response to the hydrodynamic impact deal with semi-empirical formulas for the dynamic bending moments due to bottom or bow flare slamming [96,98]. According to this approach, the amplitude value of the bending moment amidship due to bottom slamming can be calculated as:

$$M_{max} = 0.0028\ \gamma\ \frac{h_{3\%}}{\sqrt{C_B}\rho m}\ (h_{3\%}/L - 2T_2/a_* L)a_*^2(\bar{b}_2^*\ \beta_2^{*0.5})_*^{4/3}$$
$$\bar{\sigma}_1 \nu(\bar{\tau})(1+10Fr)(1-\psi L/3T)B^2L^2/10T, \qquad (3\text{-}46)$$

where

$\gamma$ = *specific weight of water, t/m*$^3$;
$h_{3\%}$ = *wave's height with probability 3% that random function h exceeds* $h_{3\%}$,*m*; $h_{3\%} = 1.33h_{1/3}$;
$L,B,T$ = *respectively length, beam, and draught amidship, m*;
$T_2$ = *the draught at the section* $X_2 = 0.1L$, *m*;
$\psi$ = *trim angle, positive if* $T_2 > T$, *rad.*;
$\bar{b}_2^*$ = *the relative beam of the section at* $0.1L$ *above base line at* $0.1B$, $\bar{b}_2^* = b_2^*/B$,(*Fig.* 3-22);
$\beta_2^*$ = *area coefficient for the section at* $0.1L$ *between base line and* $0.1\ B$;
$\bar{\sigma}_1 = \sigma_1\sqrt{L/g}$;
$\bar{\tau} = \dfrac{0.1(1-0.8\beta_2^*)\bar{\sigma}_1}{1+2.5Fr}$;
$\sigma_1$ = *frequency of the first flexural mode (natural)*;
$Fr$ = *Froude number*;
$a_*$ = *RAO value for vertical motion of section at* $0.1L$:

$$a_* = K(C_B)(1.3+6.5Fr)(2.4-1.75\alpha)(0.7+\frac{10T}{L})(0.3+3\rho_m) \qquad (3\text{-}47)$$

$K(C_B)$ = $1-12(C_B-0.67)^2m$, *but not less than* 0.80 *for* $C_B > 0.67$ *and* 0.9 *for* $C_B < 0.67$;
$C_B$ = *ship hull block coefficient*;
$\alpha$ = *waterplane area coefficient*;
$\rho_m$ = *relative radius of inertia.*

$$\rho_m = \frac{1}{L}\left[\frac{\int_o^L x^2 m(x)dx}{\int_o^L m(x)dx}\right]^{0.5};$$

$\nu(\bar{\tau})$ = *coefficient taking into account the impact impulse duration (Fig.3-23).*

$m(x)$ = *ship mass distribution including added mass of water*

The formula (3-47) is valid for Froude number $Fr \leq 0.2$ and $0.6 \leq \alpha \leq 0.9$.

A similar formula is valid for the dynamic bending moment due to bow flare lamming:

$$M_{max} = 0.003\ \gamma \frac{K_M(\bar{x})}{\sqrt{C_B \rho_m}} \cdot \frac{h_{3\%}^2}{H_f} a_*^2 (1+2.5Fr)_*^2 \left[(\bar{b}_f)^{1.5}\sqrt{1-\left(\frac{1.5H_f}{h_{3\%}a_*}\right)^2} - (\bar{b}_2^{\nu})^{1.5}(\bar{b}_5^{\nu})^{0.5}\right] B^2 L \qquad (3\text{-}48)$$

where

$K_m(\bar{x})$ = *coefficient taking into account distribution of the bending moment (Fig.3-24);*

$H_f$ = *freeboard at cross section* $0.1L$, *m;*

$\bar{b}_2^f$ = *relative beam of the upper deck at cross section* $0.1L$, $\bar{b}_2^f = b_2^f/B$;

$b_2^{\nu}$ = *relative hull beam on the waterline at the section* $0.1L$;

$\bar{b}_5^{\nu}$ = *the similar value for the cross section* $0.25L$.

If value in the brackets is negative, the bending moment equals to zero.

The comparison of theoretical results obtained by using of the Equations (3-46) and (3-48) and experimental data is shown in Figures 3-25 and 3-26. The data represented in the form of nondimensional bending moment $M_{max} = M_{max}/(0.5\ \gamma\ h_{3\%}\ BL^2)$ correspond to the tanker "Sofia" . The Figure 3-25 demonstrates the effect of Froude number on bending moment due to the bottom slamming. Figure 3-26 shows the behavior of the nondimensional bending moments for the bottom slamming (curve 1) and for bow flare slamming (curve 2) as a function of bow draught ration for constant Froude number Fr = 0.25. These data were obtained for the general cargo ship "Leninskyi Komsomol". It should be noted that the bending moment increases considerably with Froude number.

Equations (3-46) and (3-48) are quite informative. They enable the designer to evaluate the effect of ship motions parameters, environmental factors and main dimensions on the magnitude of the bending moments due to bottom and bow flare impact.

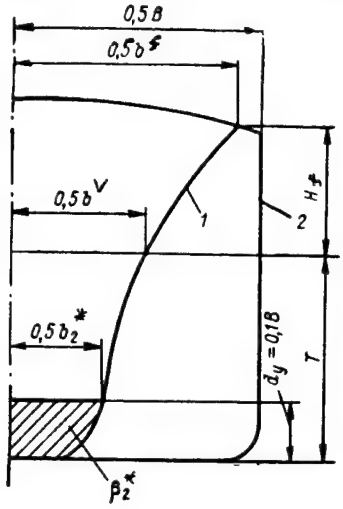


**Fig. 3-22. Cross Sections at 0.1L (1) and Amidships (2) [98]**

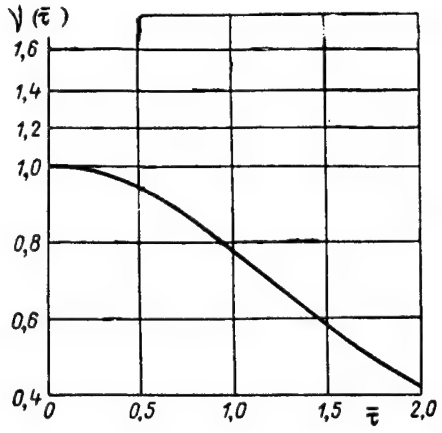


**Fig. 3-23. The v value as a function of the impact duration $\tau$ [98]**

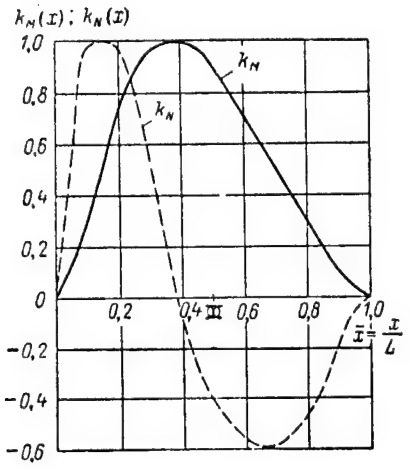


**Fig. 3-24. Longitudinal Distribution of a Coefficient $K_M$ for Bending Moment and $K_N$ for Vertical Force Due to Bow Flare Slamming [98]**

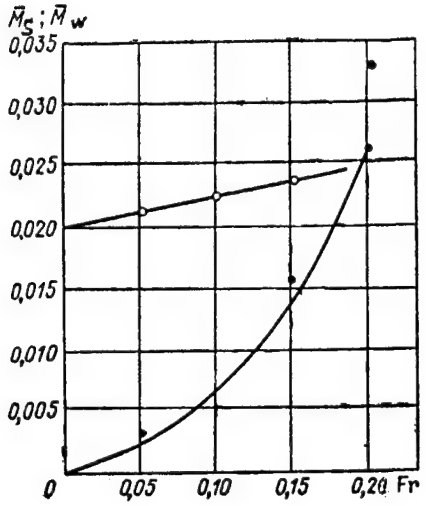


$T_f/L = 0.032$; $h_{3\%}/L = 1/20$; $\lambda/L = 1$;
——— formula (3-46 ) for maximum bending moment due to bottom slamming $M_s$;
experiment;
—o— wave bending moment $M_w$.

**Figure 3-25. Comparison of Theoretical and Experimental Results for Model of a Tanker "Sofia" [98]**

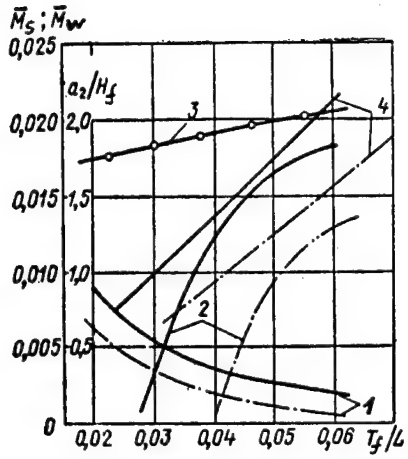


——— $h_{3\%}/L$ = 1/15
—•— $h_{3\%}/L$ = 1/20
3 Wave bending moment $M_w$
4 ratio of wave height at section 0.1L to freeboard.

**Figure 3-26. Theoretical Data for Bending Moments Due to Bottom Slamming (1) and Bow Flare Slamming (2) for the General Cargo Ship "Leninskyi Komsomol" [98]**

In addition to those mentioned here, other computer codes have been developed by Mansour and d'Oliveira [27], Antonides [136], Yamamoto, Fujino and Fukasawa [89], Schlachter [26]. The procedures and programs selected for review above have been based on availability of reference material. Others may also be suitable for mention, but sufficient detail and computer codes are proprietary. A sample list of possible sources of other potential procedures, partly based on a U.S. Navy report [137], can be mentioned:

- David Taylor Model Basin (Generalized Bending Response Code GBRC);
- BMT International, Inc., Columbia, MD (now Designers & Planners, Inc.);
- Kockums Computer System AB, Sweden (program HULLTECH for simulating of ships' motion in frequency and time domains);
- Det Norske Veritas (ship motions programs SWAN-I and SWAN-II);
- Hydromechanics, Inc., Delray Beach, Fl (programs for simulation of wave induced responses and slamming SCORES II SLAM);
- Science Applications International Corporation, Annapolis, MD (Small Amplitude Motion Program SAMP and Large Amplitude Motion Program LAMP);
- Analytical Methods, Inc., Redmond, WA (Wave-Hull Interaction Program WHIP);
- Offshore Technology Research Center, College Station, TX;
- Future Technology, MTG Marin Technik GMBH, Hamburg, Germany;
- MARIN, Wageningen, The Netherlands;
- Advanced Multi-Hull Designs Pty. Ltd., Sidney, Australia

#### 3.2.4.3 **Classification Society Rules**

Classification society rules for hull structure have considered special strengthening requirements pertinent to slamming. These do not explicitly address the loading but instead are generally implemented under the subject of strength of forward structures of the vessel.

In general, all societies require stiffer floors and girders, closely spaced stiffeners and, in some cases, intermediate stiffeners or intercostals. The bottom platings are increased; however, some rules have allowed less increase in plating thickness if certain additional stiffeners are added. A comparison of various rules is shown in Table 3-2 [3].

### 3.2.5 Seakeeping

#### 3.2.5.1 General

The analytical evaluation of seakeeping has long made successful use of slender body and linear two-dimensional strip theory.

| Classification Society | Extent of Forward Strengthening | Limits of Forward Draft at FP for Bottom Plating | Ship Speed |
|---|---|---|---|
| American Bureau of Shipping | 0.25L if $C_b \leq 0.6$<br>0.30L if $C_b \geq 0.8$ | Bottom plating strengthening procedure is provided | Subject to special consideration |
| Bureau Veritas | 0.25L | Bottom plating strengthening procedure is provided | |
| China Corporation Register of Shipping | 0.2L if machinery amidships, 0.25L if machinery aft of comparatively broad flat-of-bottom forward | Bottom plating strengthening procedure is provided | Extend strengthening to 0.25L from the fore-end in ship's of relatively high speed |
| Det Norske Veritas | Depends on forward ballast draft, breadth of bottom, and ship's length | Strengthening method is based on estimating slamming pressure | Embedded in slamming pressure |
| Germanisher Lloyds | 0.25L if machinery amidships, if machinery aft,<br>0.3L if L < 100 m<br>0.25L if L > 150 m<br>(0.4 - 0.001L) if<br>100 m ≤ L ≤ 150 m | Bottom plating strengthening procedure is provided.<br>Full strengthening if draft is < 0.03L.<br>No strengthening at all if draft is > 0.04L.<br>L should not be taken more than 200 m. | If speed > $1.6\sqrt{L}$ kts, strengthening extends aft.<br>If speed > 10 kts or $1.2\sqrt{L}$ kts, bottom plate thickness increases by 0.5 mm for each extra knot of speed and not to exceed 2 mm |
| Korean Register of Shipping | From 0.15L to 0.3L according to $V/\sqrt{L}$ | Strengthening method is based on estimating slamming pressure | Embedded in slamming pressure |
| Lloyd's Register of Shipping | 0.3L | Strengthening method is based on estimating slamming pressure | |
| Nippon Kaiji Kyokai | From 0.15L to 0.3L according to $V/\sqrt{L}$ | Strengthening method is based on estimating slamming pressure | Embedded in slamming pressure |
| Registro Italiano Navale | Between 0.25L and 0.05L | Bottom plating strengthening procedure is provided | |
| Register of Shipping USSR/Romanian | 0.25L | Bottom plating strengthening procedure is provided | $V/\sqrt{L} > 1.25$ bottom strenghtening area shall extend aft from the section located at 0.25L from FP by 0.03L for each additional knot, but in any case, the length of strengthening area shall not exceed 0.5L |

**Table 3-2: Classification Society Rule Features Pertinent to Slamming [3]**

The usual seakeeping quantities of interest are global hydrodynamic forces or bending moments and shear forces in the main body of the hull. These forces and moments are typically insensitive to end effects where strip theory approximations are less valid. However, Troesch and Kang [5] have shown that in some cases two-dimensional and three-dimensional bow flare slam theoretical results compare well to each other.

Some approaches to the analysis of slamming substitute the frequency-dependent added mass computed for seakeeping analysis for the infinite fluid added mass resulting from the impact boundary value problem as discussed by Beukelman [137a]. The impact pressure or impact force is determined for the predominant frequency of encounters for the vessel in a seaway. Armand and Cointe [43] have discussed the use of infinite frequency added mass under circumstances of shallow drafts and small time scales. Troesch and Kang [5] indicate concern for the general use of frequency dependent coefficients which are derived from linear frequency domain hydrodynamics which are derived from a different boundary value problem than the impact added mass.

#### 3.2.5.2 **Seakeeping Hydrodynamics**

Kaplan et al [125]$^{x}$ and [138,139] have developed a procedure for vertical plane motion slamming and bow flare impact utilizing 2-D ship motion theory and impact momentum theory for the prediction of hull girder bending moments and shear forces. Local pressures are not determined. The slam force $P(x,t)$ is made up of two terms, one of which is of inertial nature considering momentum and the other is due to buoyancy. Both are the result of the continuing submergence of the hull during a slam event.

$$P(x,t) = P_1(x,t) + P_2(x,t) \tag{3-49}$$

$$P_1(x,t) = -\frac{D}{Dt}(m_{nl} w_r) \tag{3-50}$$

where the operator

$$\frac{D}{Dt} = \frac{\partial}{\partial t} - V\frac{\partial}{\partial x} \tag{3-51}$$

$m_{n\ell}$ is the additional added mass at a 2-D section that is determined from the instantaneous immersion geometry of the ship section. This added mass is frequency dependent. (The authors note a high frequency limit is used to arrive at frequency independence.) The relative velocity $w_r$ is determined from the 2-D linear seakeeping theory solutions of the rigid body motions.

$$P_2(x,t) = \rho g A_{nl}(Z_r,x) \qquad (3\text{-}52)$$

Where similar to Jasper [119] and Chuang [120], Equation (3-39), $A_{nl}$ is the additional cross-sectional area at a section due to the difference between the area corresponding to the instantaneous submerged portion of the ship section and that corresponding to the still waterline, and after eliminating the linear buoyance force terms.

Kaplan [102]$^x$ has extended this procedure to predict slamming of twin hull vessels with centerbody or cross structure such as SES, SWATH and catamarans by introducing forces due the cross structure and adding them to the flare effects considered for monohulls. The author's approach to determining the centerbody impact forces are discussed in Section 3.2.3 herein.

#### 3.2.5.3 **Seakeeping Events**

Ochi and Motter's analysis technique is developed through a series of publications spanning a number of years [for example 11,12,28,88,140,141,142]. The culmination appears to be a method taking into account the entire spectrum of phenomena surrounding slamming [28]$^x$. The heart of the method describing the hydrodynamic impact itself is based on the empirical and widely used pressure relation for two-dimensional sections, which is discussed further in Section 3.3.1:

$$p = kV^2 \qquad (3\text{-}53)$$

Seakeeping events are then considered to identify the frequency of occurrence of slamming and the relative velocity between the ship and the wave at the occurrence. The seakeeping events are assumed to be Raleigh distributed. Since the amplitude of relative velocity follows the Raleigh probability law, it can be shown that the impact pressure has a truncated exponential probability distribution. A comparison between the theoretical probability density function and the histogram of impact pressure obtained from model experiments shows some discrepancy at lower pressures, but overall agreement appears reasonable. From the probability density function, the average and ⅓ highest pressure can be obtained.

It is assumed the magnitude of impact pressure varies randomly from one impact to the next following the truncated exponential probability distribution. The statistical prediction of the extreme values of impact pressure can be achieved by application of order statistics. The desired slamming pressures are obtained for two-dimensional strips of the hull and the results are added to provide an integration along the length of the vessel.

## 3.3 Experimental Results

### 3.3.1 Model Tests

#### 3.3.1.1 Results

Experimental study on slamming impact is generally divided into two types; one being the two-dimensional drop of a body onto the water surface, the other being the model experiment conducted in either regular or irregular waves generated in the towing tank. In both cases, the common purpose of these studies is to obtain the relationship between the pressure magnitude and the velocity at the instant of impact for a given body. The two-dimensional test results are useful to evaluate qualitatively the effect of hull form on impact or to evaluate the structural response of bottom plate to an impact load if a structural model is employed in the test. This can be seen in Szebehely [143], Ochi [144], Clevenger [145], and Chuang [146][147]. A review of the literature published in various fields on hydrodynamic impact and water entry may be found in the work of Szebehely and Ochi [143] Chuang [148], as well as 11th ISSC [24,115].

Pressure measurements on the bottoms of two types of planning hulls were published by Hirano, et al [149,150]. These measurements were performed on the models of a wedge-form hull and of a prismatic bottom with 13 degrees of deadrise and vertical sides. Tests were performed in calm water and the primary objectives were measurements of lift, drag and moment.

Watanabe, *et al.* [151] observed the bottom impact phenomena on a flat bottomed tanker model by means of high speed video and a transparent model. The model was towed in regular waves and was free to heave and pitch. One camera was set to monitor the impact through the hull, the other camera was used to record the pressure shown by an oscilloscope. Three types of slamming events were observed. They were called, (a) oblique impact, (b) trapped-air impact, and (c) normal impact. The videos showed that the high peak pressure occurs for the trapped air impact when the pick-up is in the region of the trapped air. In the case of "normal" impact the tests confirm that the pressure peak is related to the rapid expansion of the wetted area. The authors conclude that in every case three-dimensionality plays an important role.

The effect of bow flare on wave loads of a container ship was investigated by Watanabe, *et al.* [152]. A model with two types of bow flare shapes was tested in regular and irregular waves. The model was built of synthetic resins simulating the bending stiffness of the ship. Test measurements were analyzed for impact pressures at the bow, frequency of deck wetness and green seas as well as the asymmetry of the vertical wave bending moment.

Chiu, et al [153] had earlier presented a method to predict vertical motions and vertical wave loads on high speed craft which are assumed rigid. The authors determined that as the size of high-speed vessels increases the influence of fluid-structure

interaction needs attention. A rigid and an elastic model for the craft were used, and in addition, tests were carried out to measure vertical motions of two wooden models of different scale ratio. Another test series was carried out to measure the vertical bending moment along ship's length incorporating an elastic "backbone". The conclusion was that the two methods for predicting the vertical loads were satisfactory for practical purposes. The correlation between the maxima of vertical bow acceleration and bending moment was confirmed also for high speed craft of larger size.

Nagai and Hashimoto [154] address the problem of longitudinal stress and local pressure load in the bottom structure subjected to impact loads. Tests carried out comprised drop tests of flat fiber reinforced plastic (FRP) plates horizontally on a water surface and of measurements during sea trials of FRP high speed craft.

Sawada and Watanabe [155] compared two approaches to construct elastic ship models which simulate the elastic response of a ship at model scale, viz: (1) using synthetic resin for the shell; (2) using aluminum bars as the hull "backbone" while urethane foam is utilized for shaping the hull. Three models were built and tested: A container ship and a high speed patrol craft in accordance with method (1); and a bulk carrier following method (2). Comparison with sea trial results is said to show excellent agreement.

The results obtained from experiments on models representing various sectional shapes are compiled in SNAME [3] and information concerning these tests is given in Table 3-3, and the data are plotted in Figure 3-27. The following remarks are provided relative to Figure 3-27:

- Magnitudes of impact pressure are the maximum values during impact.
- All lines showing the relationship between pressure and velocity were drawn such that the impact pressure is proportional to the square of the velocity. Impact pressure is expressed by:

$$p = kV_t^2 \qquad \textbf{(3-54)}$$

  where $k$ is a constant which depends on the body cross section shape, and $V_t$ is the velocity at the moment of impact. Van Karman [32,40] and Wagner [33,41] originally used 2C for what later became $k$. Here pressure p is in psi (lbs/sq.in.), and velocity is in ft/sec.
- There is no significant effect of ship speed on the $k$-value for low and medium speed ships.
- The $k$-value for regular or irregular waves is virtually identical.
- The $k$-value is virtually identical for different sea states

| Ident.. | Test | | Model | | k-value psi-sec$^2$/ft$^2$ | Reference |
|---|---|---|---|---|---|---|
| | Drop Test | Seaworthiness Test | Two-Dimensional | Ship Form | | |
| AM-1 | | Irregular waves | | 12.7-ft. MARINER, Station 2 | 0.086 | 74 |
| AM-2 | | Regular waves | | 5.5-ft. MARINER, Station 2 | 0.086 | 7 |
| AM-3 | | Regular waves | | 5.5-ft. MARINER, Station 3 1/2 | 0.145 | |
| AM-4 | Open water | | | 5.5-ft. MARINER, Station 3 1/2 | 0.305 | |
| AV-1 | | Regular and Irregular waves | | 17.5-ft. Modified MARINER, Station 2 | 0.033 | 73 |
| AV-2 | | Irregular waves | | 12.7-ft. Modified MARINER, Station 3 1/2 | 0.077 | |
| AC-1 | | | | 17.5-ft. CHALLENGER, Station 2 | 0.053 | 11 |
| AC-2 | | | | 17.5-ft. CHALLENGER, Station 3 1/2 | 0.125 | |
| AT-1 | | | | 17.5-ft. TOWNSEND, Station 2 | 0.021 | |
| AT-2 | | | | 17.5-ft. TOWNSEND, Station 3 1/2 | 0.077 | |
| MF-1 | Test channel (2-dimensional flow) | | 10.2 x 7.7 ft Flat bottom Structural model (22,500 lbs) | | 0.365 | 69 |
| MF-2 | | | (28,800 lbs) | | 0.420 | |
| MF-3 | | | (39,300 lbs) | | 0.495 | |
| OS-1 | | | U-form (190 lbs) | | 0.950 | 70 |
| OS-2 | | | UV-form (190 lbs) | | 0.780 | |
| OS-3 | | | V-form (190 lbs) | | 0.580 | |
| UE-1 | Open water | | 7.5 x 6.6 ft Wedge(10 deg) Structural model | | 0.150 | 71 |
| UE-2 | | | 7.5 x 6.6 ft Flat bottom Structural model | | 0.210 | 41 |
| CB-1 | Test channel (2-dimensional flow) | | 26.5 x 20 in. Flat bottom | | 0.660 | |
| CB-2 | | | 26.5 x 20 in. Wedge( 6 deg) | | 0.190 | 72 |
| CB-3 | | | (10 deg) | | 0.125 | |
| CB-4 | | | (15 deg) | | 0.031 | |

**Table 3-3. Models Used in Slamming Impact Study [3,142]**

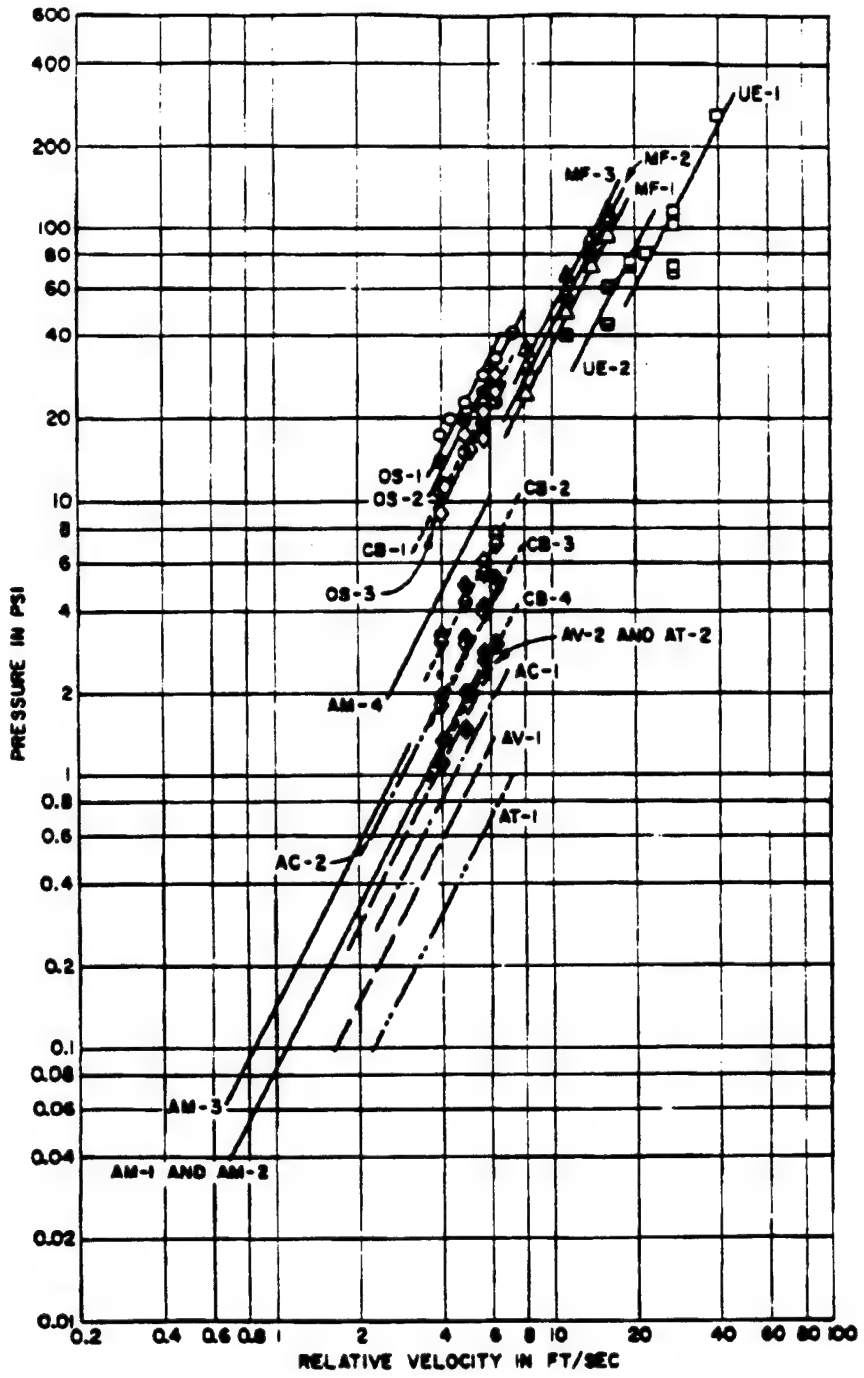


**Fig. 3-27. Slamming Impact Pressure-Velocity Relationship Obtained From Experiments on Models Representing Various Section Shapes [3]**

- The critical portion of the impact process is over when the section is submerged to a depth of 1/10 its calm water draft, or .005 the vessel length.

The generalized form of the impact pressure-velocity relationships for different model tests was published in Principles of Naval Architecture [156] and is presented in Fig. 3-28.

Comparing Figure 3-27 amd 3-28 with Table 3-3, it can be seen that all pressure magnitudes obtained from the seaworthiness tests are smaller than those obtained from the two-dimensional tests for the same velocity. It is of particular interest to compare the k-values for AM-3, AM-4, and OS-2 since the section shapes for which the pressure-velocity relationships were obtained are the same, (Station 3-1/2 of the MARINER), but the test conditions are entirely different. That is, AM-3 was obtained from seaworthiness tests in regular waves on a 5.5 foot model at a speed corresponding to 10 knots full scale. AM-4 was obtained from drop tests of the same model onto a calm water surface from various heights and OS-2 was obtained from a drop test of a two-dimensional model having a constant cross section. As can be seen in Figure 3-27, the k-values are significantly different and become larger in sequence of AM-3, AM-4, and OS-2.

Sikora and Disenbacher [157] have carried out model tests of the 3500-ton TAGOS 19 SWATH ship with the model instrumented on the wet deck, the haunch, and the inner and outer strut to determine slam, frontal impact and wave slap pressures.

Wahab, et al [158] report on model tests of the ASR Catamaran in waves. These data, plus full scale measurements obtained on the T-AGOR-16 in the Atlantic, are further analyzed by Giannotti and Fuller [159].

For models used in two-dimensional drop tests, Figure 3-27 also shows some trend on the effect of bottom rigidity on pressure magnitude. The OS-group models have a 2.5 inch thick wood bottom reinforced with 1 inch aluminum bar and appear to have the highest rigidity as compared to Model CB-1 (small model with flat bottom, steel plate 1/2 inch thick). Model MF-1 (large model with flat bottom, steel plate 1/2 inch thick), and UE-2 (large model with flat bottom, HTS steel plate 1/8 inch thick). Pressure magnitudes for the same velocity gradually decrease in sequence following the above listed order. Chuang [147] made an interesting comparison of pressure magnitudes between the two-dimensional rigid and pressurized inflatable model, and found that the latter showed considerably less pressure than the former for the same impact velocity.

The trapped air phenomenon appears to occur in reality for two-dimensional impact of a flat body on the smooth water as evidenced by underwater photographs shown by Chuang [160]. Fujita [161], Lewison and Maclean [162], and Johnson [163] also studied this problem.

Whitman and Pancione presented a "scaling law" for maximum pressure on a flat plate with entrapped air due to hydrodynamic impact [164]. Under the assumption that air compression is polytropic and the inertia terms are small compared with the viscous terms, they found that the maximum pressure varies directly with the leakage of the trapped air. Thus, circular plate of diameter $\ell$ should experience a maximum pressure only 83

percent of that of a square plate of edge $\ell$ for the same weight and drop height. They derived a "similarity" parameter scaling impact pressures which consider several variables addressed in experiments performed by Gerlach [165], including air content.

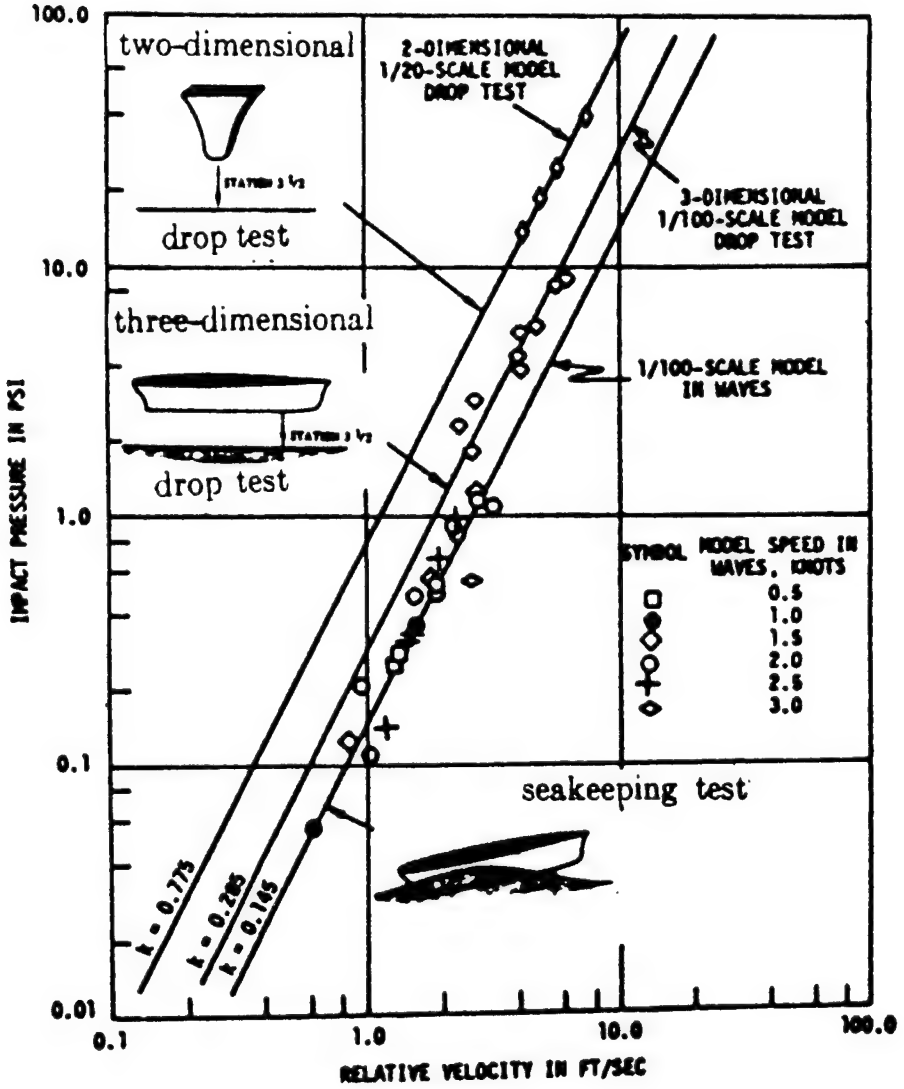


**Fig. 3-28. Comparison of Pressure-Velocity Relationships Obtained in Three Different Types of Slamming Experiments [156]**

Nott [166] has confirmed by model tests that in general for the non-uniform hydrodynamic pressures on sonar domes, a simulation by multiple static loads and the influence-coefficient method of Lunchick et al [167] leads to stresses equivalent to those resulting from three-dimensionally applied steady state hydrodynamic loads.

Garcia [168] has carried out tests concerning shock pressures created by water waves breaking against vertical barriers. These wave pressures were studied using small-scale oscillatory waves in a flume fitted with a beach slope and test wall. The variation of pressure with both time and position on the wall were determined for several wave heights, wave periods, water depths, and beach slopes. The variation of pressure with time was found to be similar to that reported by previous investigations. The pressure-time variation can be divided into two parts; namely, initial shock pressure which occurs as the wave strikes the wall and a secondary pressure which is associated with the run up of the wave on the wall. The shock pressure is characterized by a very intense pressure peak of short duration as shown in Figure 3-29 which also notes data from the work of Ross [169], Denny [170], DeRouville et al [171], Nagai [172] and Rundgren [173]. This is followed by the much less intense but longer duration secondary pulse. Equations 3-64 through 3-66 define the terminology. The maximum shock pressure that occurred for each wave condition was localized over a small region of the test wall between the still-water level at the wall and the elevation of the crest of the wave striking this wall. Above the region of maximum shock pressure the magnitude of pressure decreases to zero and below to one-tenth of the maximum.

#### 3.3.1.2 **Model Scale Effects**

In any attempt to determine the slamming pressure of a ship by means of model tests, the laws of similitude are of prime importance. These include modelling and scale effects on size, weight, two-dimensional versus three-dimensional models, and drop tests versus tests on waves.

The publications in the literature discussed in the previous section demonstrate the progress achieved in the understanding and modeling of impact phenomena. Nevertheless, the International Ship Structures Congress listed a number of issues which still need clarification [115]. Among these are:

- Scale effect between model tests and full scale for the different forms of hydrodynamic impact; there are indications that there ought to be a scale effect when air entrapment is involved;

- Randomness of impact pressures due to small scale water surface deformations (ripples) and possibly other effects, even for similar relative configurations in the macroscopic sense. In this context, the water surface after ship bottom emersion or in the splash zone is never smooth.

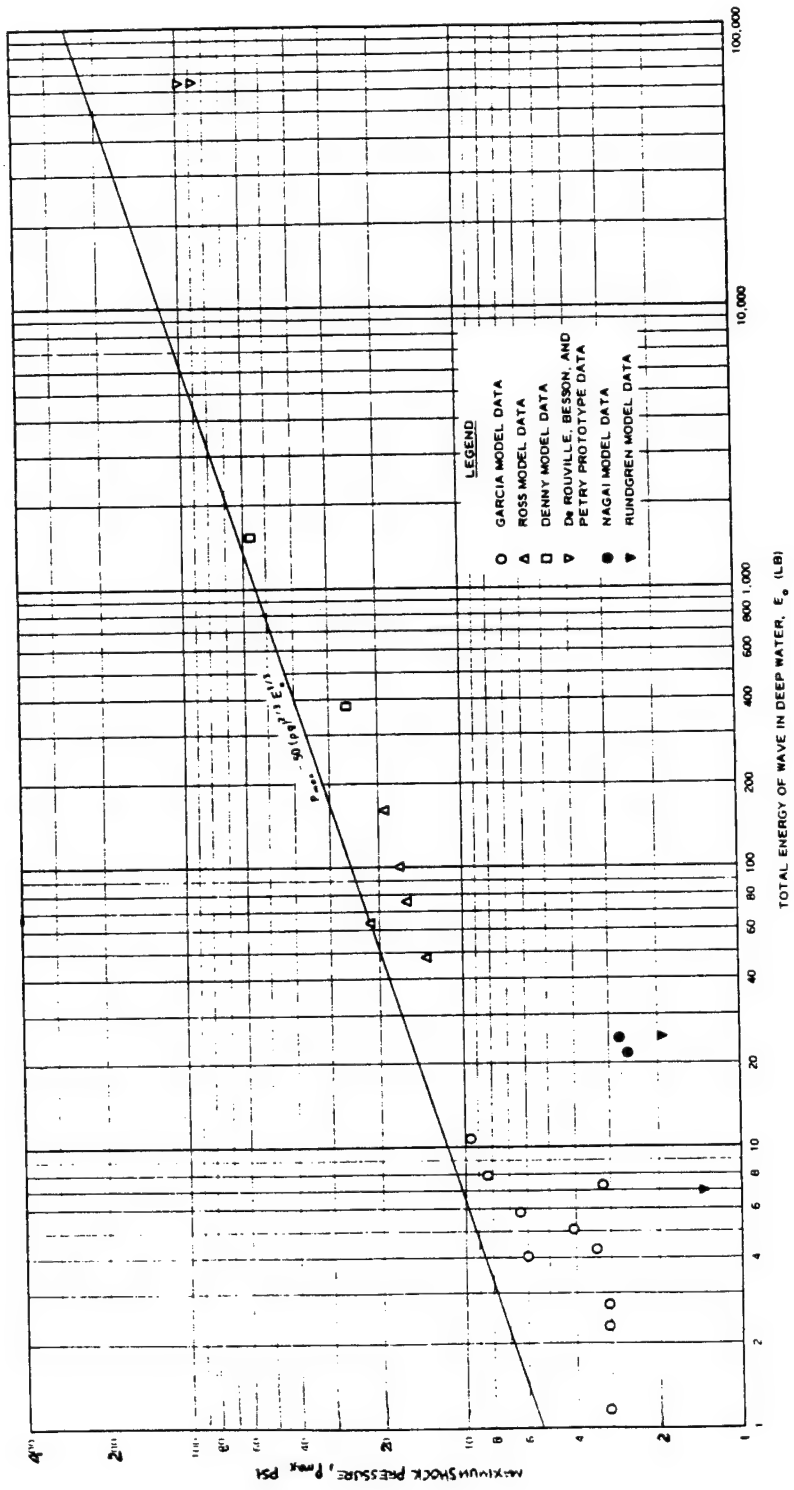


**Figure 3-29: Maximum Shock Pressure Versus Total Energy of Wave in Deep Water [168]**

A discussion and analysis of modelling scale effects is provided in SNAME [3] and it is concluded that in slamming tests of models, the differences in impact pressure may be caused by the following:

- Froude scaling applies.
- Mass per unit impact area are different between model and full-scale.
- Fluid can flow more easily in three-dimensional flow than in two-dimensional flow.
- Impact of the flat-of-bottom generates the maximum impact pressure at its center with gradually reduced pressure away from the center, and zero pressure at the edges, hence measurements must be comprehensive.
- $p = kV^2$ can be applied to both the model and the ship regardless of their sizes, i.e., $k$ depends on body cross sectional shape only.

However, as the phenomena of hydrodynamic impact loads are multi-variable, model tests provide a means to determine these loads taking into account the interrelated effects. SNAME [3]$^x$ notes that the model must be fitted with pressure panel sensors whose design is based on Froude scaling and match the structural configuration, scantlings and the corresponding dynamic frequencies to be investigated. Sellars [84] has identified the necessary structural scaling as equivalence of the Cauchy number giving the relative magnitude of inertial forces to elastic forces. The sensors may represent a plate panel or a grillage. It is suggested the model be constructed of polyvinyl chloride (PVC) sheets mounted on a support frame. The panels and grillages should be instrumented with strain gauges to provide a direct means of relating measured structural response to an equivalent uniform impact load. A similar problem was investigated by Band [174]. He found that for the determination of wet-deck slamming loads the local structure in question (plates, stiffeners, etc.) must be modeled with scaled rigidity. Specially constructed panels, that can be calibrated to measure average pressure, must be incorporated in the model. In this case, meaningful pressures, shear forces, bending moments can be obtained from measurements.

Faltinsen [175] investigated the effect of varying velocity during impact (velocity time history) on pressure magnitude and distribution. He pointed out that it is very important to account for the varying velocity - that means the large retardation of the body that occurs at the end of impact. The retardation causes pressure reduction due to the "added-mass" effect. This means that drop tests require accurate velocity measurements of the model. Further, the scaling of drop tests results to full-scale pressure on a vessel is questionable when large retardations of the model occur. Since a vessel will have a smaller retardation than the drop test model, unconservative full-scale predictions for a vessel can occur as a consequence. The effect of the model retardation is illustrated in Fig. 3-30 from

[68]. This figure shows the free-surface elevation and the pressure distribution at the final time of the numerical simulation by the nonlinear boundary element method. Three different cases are presented. One case is with a symmetric body and constant downward velocity of $V_o$=4.05 m/s. The two other cases are with an asymmetric body. The geometry of the body was taken from Yamamoto paper [176]. It can be seen that the variation of velocity is more important than whether the body is symmetric or asymmetric.

The model testing can include collections of wave impact data for a range of sea, heading and speed conditions which correspond to the ship's projected operational environment. A probabilistic analysis can then be performed to determine a maximum lifetime design pressure. If a Weibull analysis is performed, the following results are given:

$$N_P = f(I_n) \tag{3-55}$$

$$p_\alpha = \frac{p_{max}\left[\ell n\left(\frac{N_p}{\alpha}\right)\right]^{1/M}}{[\ell n(N_p)]^{1/M}} \tag{3-56}$$

where:

$N_p$ = *The total number of impacts expected over the life of the vessel for the gauged locations and operating conditions;*
$I_n$ = *The frequency of impacts as determined from model tests for a specific combination of ship speed, heading and sea state;*
$M, \beta$ = *Slope and y intercept of Weibull plot;*
$p_{max}$ = *Pressure with 63.2% probability of being exceeded;*
$\alpha$ = *Probability of exceedance;*
$p_\alpha$ = *The extreme maximum pressure with a probability of exceedance* $\alpha$.

### 3.3.2 Full Scale Data

Significant full scale slamming data are available. A list of references is given under "Full Scale Measurements" in [177] and other full scale information is referenced in [178]. More recently Daidola et al [179] have prepared a bibliography supporting this SSC project which includes data for aircraft landings as well.

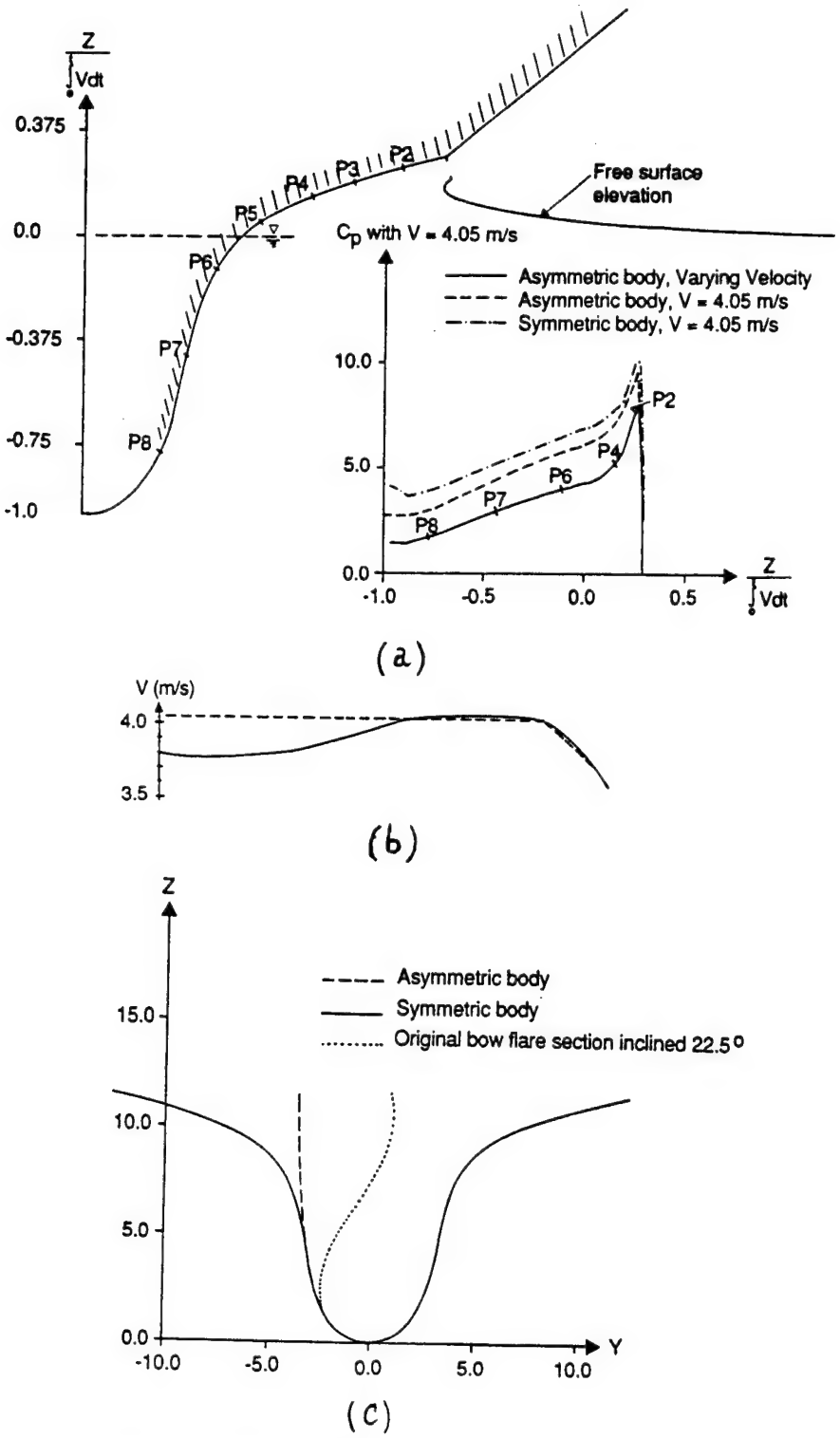


**Fig. 3-30. Effect of Velocity Time History and Body Geometry on Free-Surface Elevation and Pressure Distribution on the Cross Section With Bow Flare at Final Time of Numerical Simulation**

**(a) Results of simulation**

**(b) Impact velocity time history**

**(c) Cross sections of model used in numerical simulation**

There are two major types of slamming data collected. The first type concerns the local slamming at the bow. This includes local slamming pressure measurements and the local structural response in the slamming areas, such as information obtained from the sea trial of USCGC UNIMAK [180] and Motor Torpedo Boat YP 110 (ex PT 8) [181].

The second type of slamming data collected concerns the hull whipping stress caused either due to the bow flare slamming, such as sea trials of USS ESSEX [182], or bottom slamming, such as the sea trials of USS EDWARD MCDONNELL (DE 1043) [183] and other ships [184][185][186][187][188]. The analyses of sea trial data of USS ESSEX were performed and used to compare with the model test [189], the Seaworthiness Analog Computer [190], and the Structural Seaworthiness Digital Computer Program [120]. Their agreements were considered very good.

Data collections on bottom slamming during ship operations were attempted by several ships. The S/S WOLVERINE STATE is probably one of few where enough information to be reported [191] was obtained.

Pegg *et al.* [192] have carried out finite element predictions of measured bow flare plate stresses under dynamic loading. The analyses are based on pressures measured on the research vessel CFAV QUEST as shown in Figure 3-31.

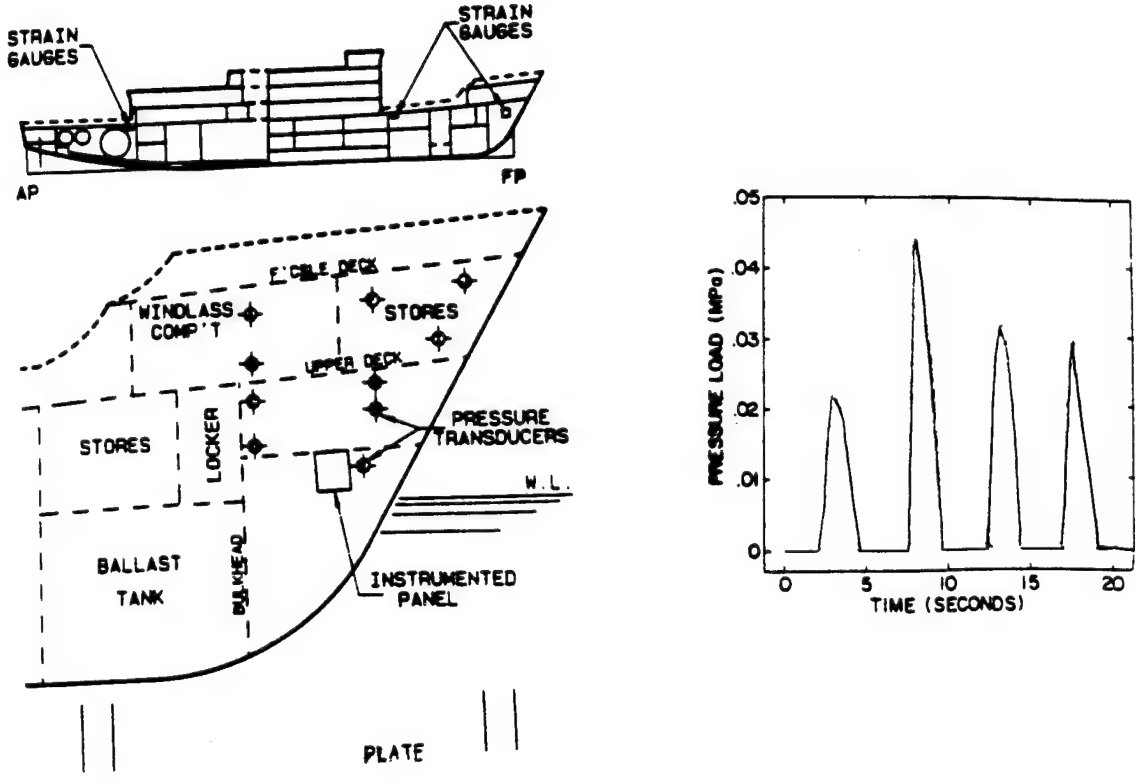


**Fig. 3-31. Bow Flare Pressure Pulses on CFAV QUEST [192]**

The sea trials of the catamaran USNS HAYES collected a considerable amount of test data on the slamming of cross structure (which bridges the twin hulls of the catamaran) [118].

Takemoto, et al [193] measured wave impact loads and hull response during sea trials with a 1,300 ton patrol vessel in severe seas with variation of heading and ship speed. Some of the results were published earlier. Further analysis showed that: (1) Bow flare slamming induced high bending stresses in the deck; (2) Bow flare slamming induced whipping vibrations; explanations of the excitation mechanism were deduced which also explain the sharp decay of whipping vibration after the strike; (3) Whipping stresses and frequencies are high when compared with normal wave bending; therefore, they can be expected to have an influence on fatigue life.

Purcell, et al [194] published a structural analysis of the forward bottom of a patrol boat. The analysis uses relatively simple assumptions for the impact load. Slamming pressure measurements on a model in irregular waves and the results of sea tests with the full-scale craft, which was driven at high speed into severe seas, causing slamming and some dishing of the plating were reported. Conclusions include recommendations for structural improvements.

Full-scale measurements of impact loads were performed by Barabanov et al [195,96] and by Rask [196]. For a 34 m patrol boat, the latter author compared the measured k-factor in the formula of equation (3-54) for impact pressure. He concluded that the k-factor varied considerably from one impact to another, depending to a great extent on the rolling motion. Analysis of full-scale results for three ships enabled the author [195] to derive a semi-empirical formula for slamming design loadings with parameters depending on ship speed, length and draft. Very strong speed and draft dependences can be identified.

Bugakov [197,198] has reported on his investigations of slamming effects and storm damages and their relations to safe sea speed and performance of hull forward bottom structures. In the case of a reefer vessel KAMCHATSKIYE GORI, damages were reported on the side shell plating after heavy weather operations. Authors of [195] and [197] reported a recorded peak slamming pressure of 4.5 MPa (654 psi) during an experimental cruise, Figure 3-32, more than twice the 2.17 MPa (315 psi) maximum pressure recorded during the sea trials of the USCGC UNIMAK. In studying several ship classes, Bugakov found that slamming damage repairs cost 2.5-3 times that of new construction and a 60-70% increase in plate strength reduces slamming damage expenses by about 75%. He concluded that, giving consideration to lost ship speed, repair and vessel availability costs during repairs, it is best to increase scantlings in the bow flare and foredeck between 0.1 and 0.2L and in the bottom plating from 0.22-0.32L aft of the forward perpendicular. Bugakov recommended use of special storm diagrams as guidance for safe sea speed, constructed to indicate permissible speed for ships being designed, built and operated. They should be included as a part of the ship's seaworthiness and strength certificate. Such diagrams were published by Aertssen [199], Tasaki et al [200], Cruikshank [201], Lipis and Remez [114].

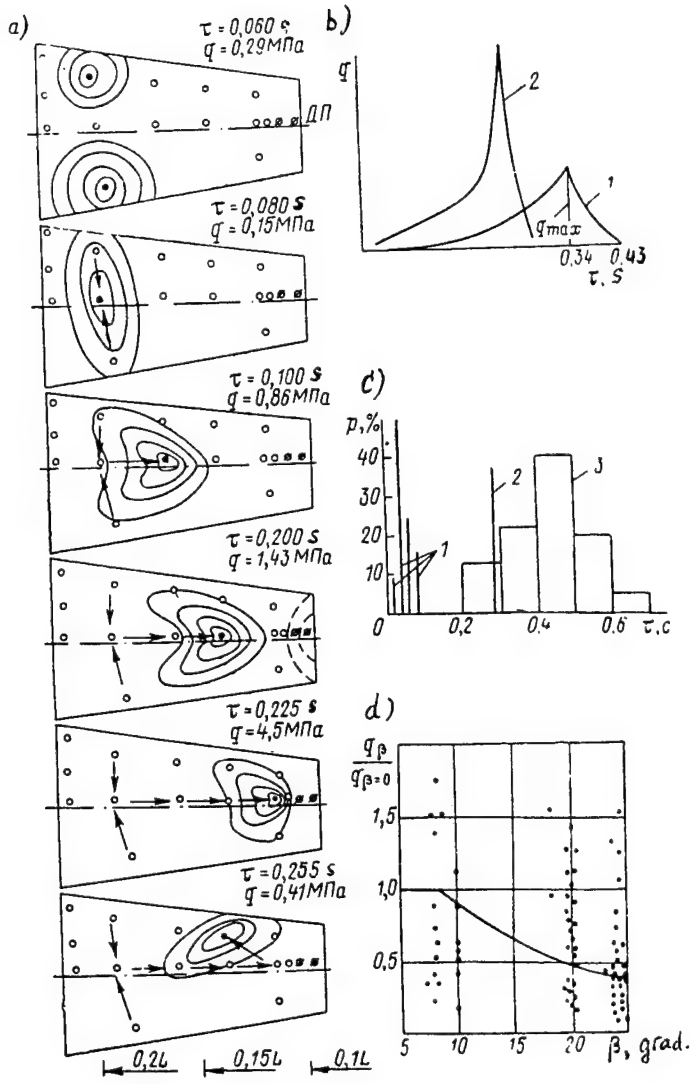


**Fig. 3-32. Full Scale Slamming Pressure Measurements on Reefer Ship "KAMCHATSKIE GORI" [197]**

(a) Loading process during most strong hit; o pressure gauges; $\phi$ pressure gauges destroyed during sea trials; —— contours of constant pressure.

(b) Typical pressure time history.

(c) Natural half of periods of fore bottom strusture (1), hull (2) and slamming pressure duration (3).

(d) Effect of deadrise angle on slamming pressure.

Solomentsev [202] points to poor seaworthiness of twin hull vessel structure mainly due to a serious underestimate of the frequency and severity of cross-structure slamming impacts. Seven passenger, ferry, fishing and research vessels are reviewed and design recommendations were made for seaworthiness improvements that will not result in substantial deterioration in the economic attributes of these vessels, e.g., fuel consumption and structural weight.

### 3.3.3 Empirical Procedures Based on Experiment

#### 3.3.3.1 k-Value Procedures

A number of empirical procedures based on experiment predominantly seek to identify the value of "$k$" in Equation (3-54).

In his earlier work Ochi [142] develops $k$-values for eight hull transverse section forms through the use of model experiment results. Later, Ochi and Motter [203] developed a technique for calculation of $k$ or $k_1$ from an equation with coefficient obtained from a three parameter mapping of a hull section:

$$\begin{aligned} k &= e^{(-3.599 + 2.419a_1 - 0.873a_3 + 9.6241a_5)} \\ k_1 &= k/\tfrac{1}{2}\rho \end{aligned} \qquad \textbf{(3-57)}$$

The authors [28] have attempted to simplify the $k$-value prediction technique by presenting them for a series of section shapes in a graphical format for a total series of 120 different hull form sections with various combinations of beam/draft ratios, sectional area and flat of bottom. Figure 3-33 gives an example of the results where the computed $k_1$ values are presented as a function of width/draft ratio, b/d, flat of bottom width ratio, b*/b, and the sectional area coefficient $C_a$ = A*/(2bd). The term b* is the half width of the flat-of-bottom and A* is the full sectional area below the one-tenth of the design draft, d, at the design beam, b. The authors conclude that the $k_1$ value appears to be a function of b*/b for any b/d value, and independent of the hull shape series A, B or C, and of the sectional area coefficient.

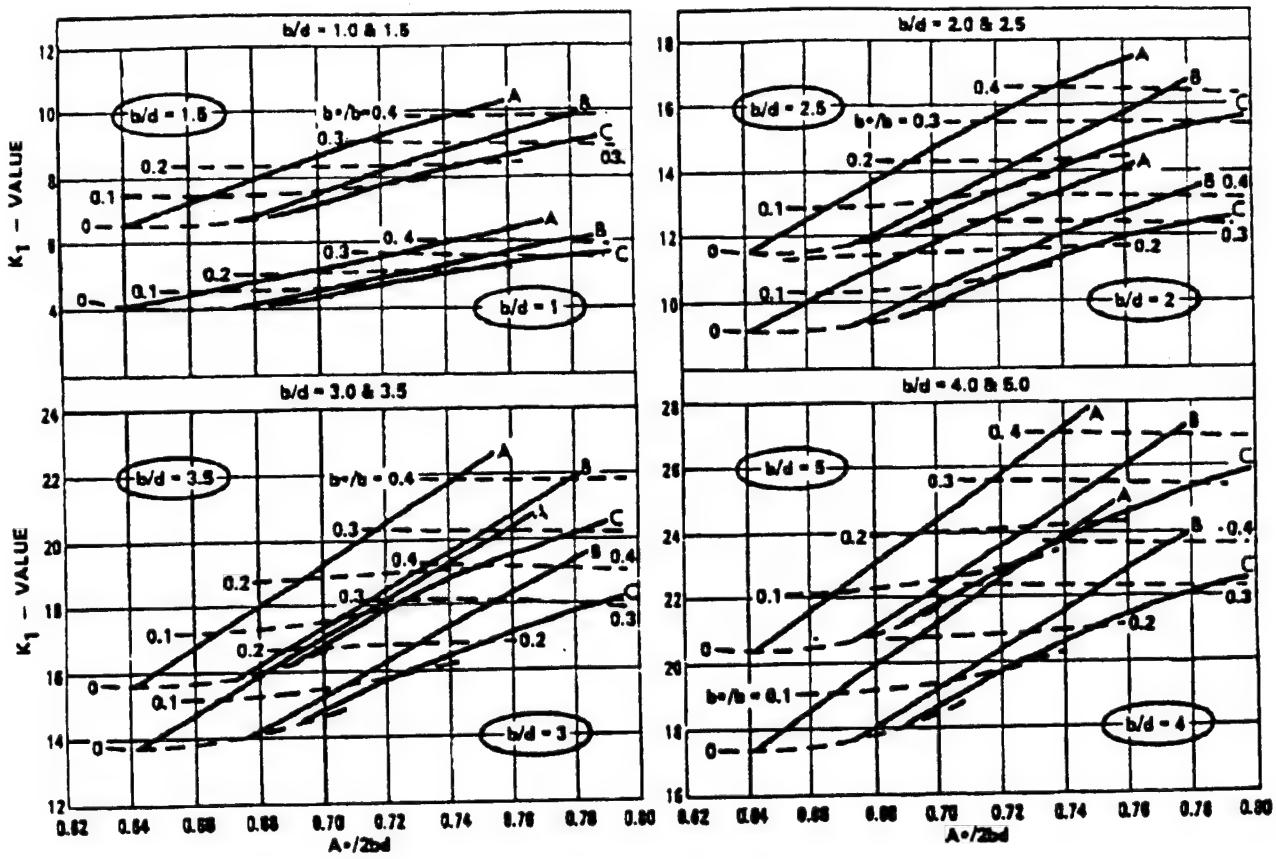


**Fig. 3-33. $K_1$-Value for Hull Shape Series [28]**

In this approach the loading is assumed to act instantaneously over the bottom one-tenth of the draught (i.e., over a dept of 0.1 T) but the pressure varies over this region, being assumed zero at 0.1 T and a maximum, $p_{max}$, at the keel. Figure 3-34(a), taken from the book by Bishop and Price [29], shows the profile of the region of interest. As a simplification, the normal pressure at any angle is assumed to be given by

$$p_n(\phi) = p_{\max} \frac{y(\phi)}{d}, \tag{3-58}$$

where d=0.1 T(x) and $p_{max}$ is deduced from equation (3-50).

The next transient force at any section can be evaluated by integrating the vertical component around the section profile. The contribution to the net vertical transient force per unit length along the hull exerted at the ith element of the section is given by

$$p_i \cos \beta_i \, \delta s_i.$$

where $\beta_i$ and $\delta s_i$ are as shown in Figure 3-34(b). The total instantaneous vertical force per unit length on section is thus

$$F(x) = 2 \sum_{i=1}^{n-1} p_i \cos \beta_i \, \delta s_i$$

But since $y_1 = d$,

$$p_i = p_{max} \frac{y_{i+1} + y_i}{2 y_1}$$

and

$$\cos \beta_i = \frac{x_{i+1} - x_i}{\delta s_i},$$

it follows that

$$F(x) = p_{max} G(x),$$

where the shape factor

$$G(x) = \frac{1}{y_1} \sum_{i=1}^{n-1} (y_{i+1} + y_i) \; (x_{i+1} - x_i).$$

Turning now to the temporal variation, we employ an assumption due to Kawakami et al [130]. It is that the transient loading is of the form

$$F(x,t) = \frac{p_{max}}{T_o} G(x) \, t \, e^{(1 - t/T_o)}, \qquad \textbf{(3-59)}$$

where $T_o$ is the time that elapses between the instant at which the bottom strikes the wave surface and the instant at which the loading reaches its maximum value.

Chuang [204] has also carried out experiments on models appropriate for high speed vehicles, studied methods for calculating slamming pressures and compared these with actual experiments [205,206]. Stavovy and Chuang [117][x] developed the earlier works of Chuang into a rational method for calculating slamming pressures which they have prepared for high-speed vehicles as well as conventional ships. The method determines the impact pressure in an infinitesimal area of the hull bottom. In that area the deadrise, buttock, trim and heel angles are determined from ship lines, body plan, ship motions and wave profile. The authors consider the sum of the pressures acting normal to the bottom as that due to slamming and planing where this is present:

$$p_t = p_i + p_p \tag{3-60}$$

where:

$p_t$ = *total pressure*
$p_i$ = *impact pressure*
$p_p$ = *planing pressure which is usually small and insignificant compared with the impact pressure*

$$p_i = k_1 V_n^2 \tag{3-61}$$

where:

$V_n$ = *relative normal velocity of impact body to wave surface on plane normal to wave surface*
$k_1$ = $0.37\,\xi/2.2 + 0.5$ ; $0 \le \xi < 2.2$ *degrees*
$k_1$ = *various other relationships* ; $2.2 \le \xi$ *degrees*
$\xi$ = *effective impact angle on plane normal to wave surface and impact surface on hull bottom, measured from wave surface to impact surface of hull bottom*

The resulting values for $k_1$ are shown in Figure 3-35 as a dashed line.

To evaluate the lateral transient force per unit length along the hull a distribution of hydrodynamic panels over the estimated slamming area is used (see, for example, Aksu et al [207]). Thus, by distributing hydrodynamic panels and defining a slam (or slams) due to the relative motion between structure and waves, the slamming pressure forces on each panel can be calculated. Figure 3-36 illustrates the application of this approach in 3-D analysis.

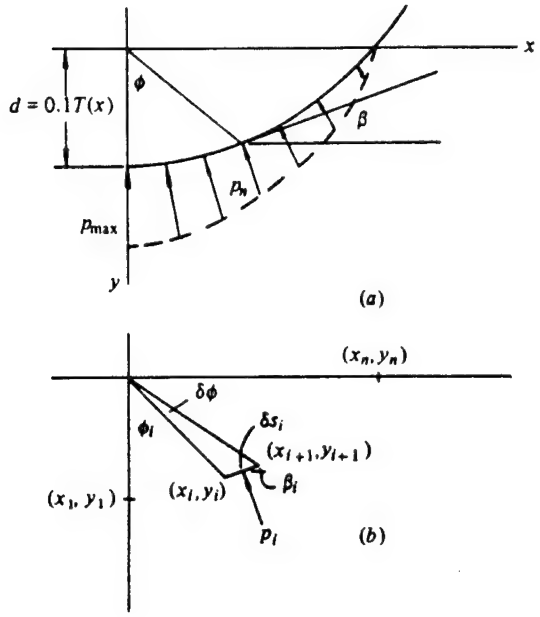


**Fig. 3-34 (a) The Distribution of normal pressure $p_n$ over the bottom one-tenth of the Draught at Any Instant.**
**(b) Notation Used in Writing Down That Contribution Made at the ith Element of the Ship's Bottom to the Total Transient Force per Unit Length.**

### 3.3.3.2 Other Procedures

Sikora and Disenbacher [157] have developed a procedure to predict maximum pressures based on model testing of a large SWATH. By instrumenting a model at several locations with pressure transducers, time histories and histograms of pressure magnitudes were developed. Based on these, cumulative probability of exceedance distribution were determined, the pressure magnitude assumed to be directly related to the square of the relative impact velocity and the pressure taken as a Rayleigh distribution for relative velocity. The expression for lifetime expected pressure becomes:

$$p(\text{max}) = \sqrt{E}\, A \ln(N/\alpha) \qquad \textbf{(3-62)}$$

where:

$p(\text{max})$ = *maximum impact pressure*
$A$ = *distribution coefficient*
$\sqrt{E}$ = *RMS of the pressure magnitues*
$N$ = *total number of impacts during the life of the vessel*
$\alpha$ = *a risk factor*

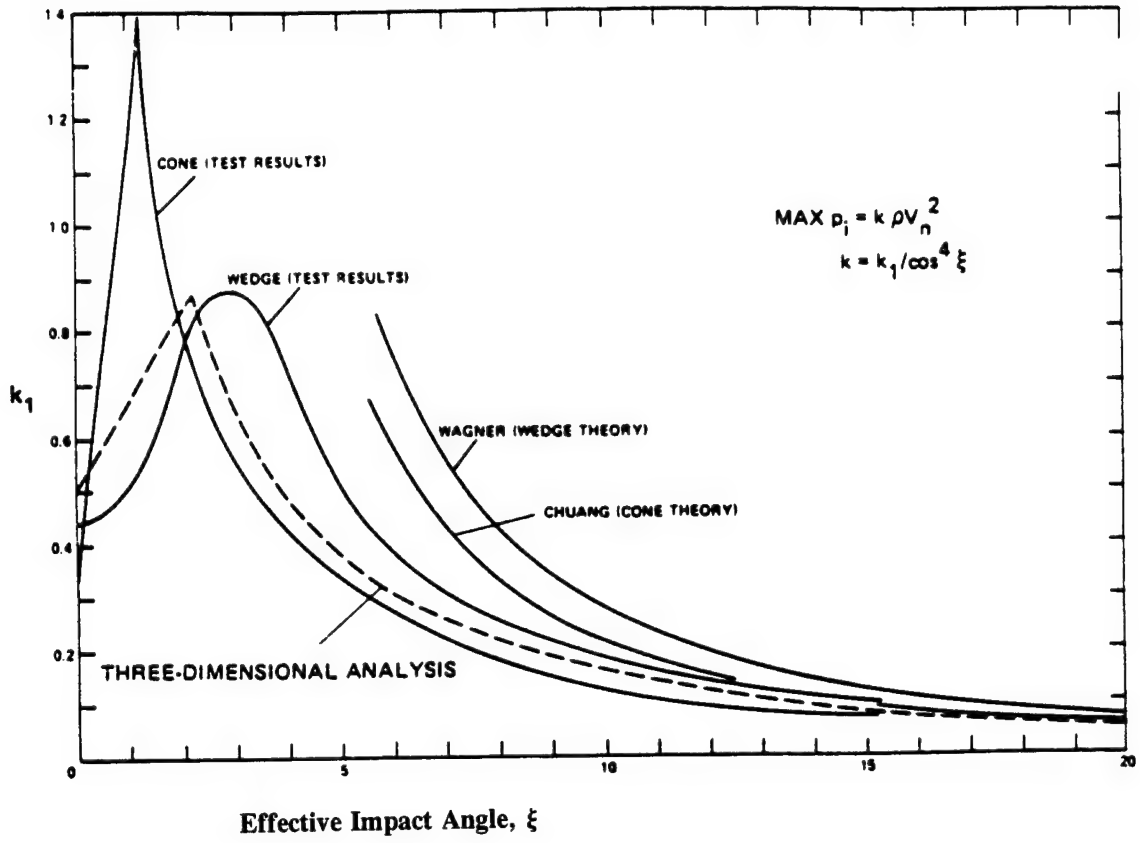


**Fig. 3-35. Comparison of $k_1$ Values [117]**

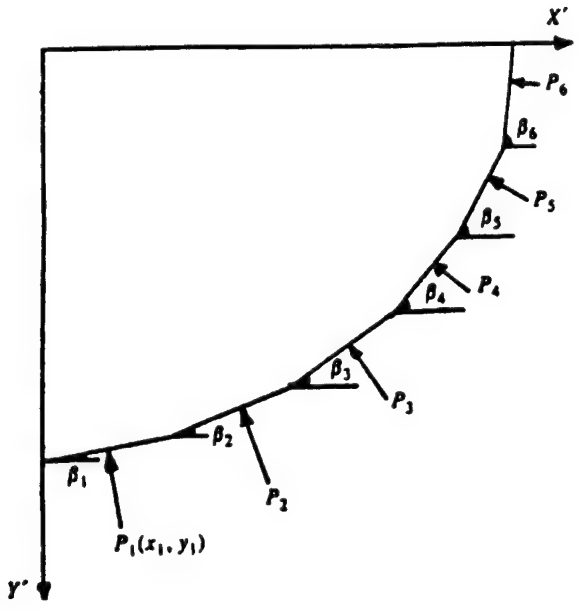


**Fig. 3-36. Idealization of Three-Dimensional Impact Forces on a Ship Section**

The total number of impacts, N, is the product of the frequency of impacts as measured in tests times the time the vessel is expected to spend at sea times the probabilities of being in those headings, speeds and wave heights in which slamming is likely to occur. The risk factor is taken as less than 1.0 and hence artificially increases the number of impacts and hence design maximum pressure. In TAGOS 19 a risk factor of 0.37 was assumed for plating, .01 for stiffeners and .0001 for girder design where any type of failure is to be avoided. For the TAGOS 19 the pressures from model tests as expressed by Equation (3-61) were for full scale panel sizes of 2 by 4 ft. The pressure modification according to area used by the authors was taken from Allen and Jones [208], Figure 3-37.

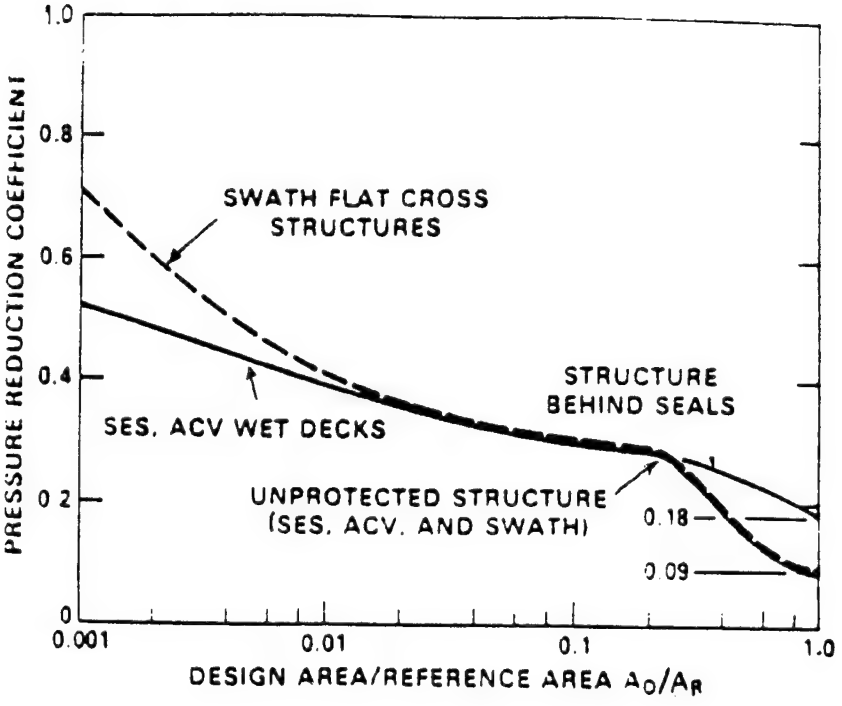


**Figure 3-37: Pressure Reduction Coefficients for SES, ACV and SWATH Vessels**

Allen and Jones [208] have developed a procedure to predict the structural design limit pressure magnitudes and distributions for slamming in a number of high performance marine vehicles. Methods are presented for planing and hydrofoil hulls, and for SES, ACV wet decks and SWATH flat cross structures. The procedures describe a simple approach to provide a designer with an equivalent uniform static pressure for each hull structural component under localized water impact load. The required input includes:

- Vehicle displacement, $\Delta$ or $w_L$
- Vehicle draft in the case of monohulls, d
- Pitch radius of gyration, $r_x$
- Impact load factor, $N_z$
- Conceptual layout of internal structure.

These are utilized to express the pressure for planing and hydrofoil hulls as:

$$p_D = 4.44 F K_D N_Z d \qquad \textbf{(3-63)}$$

where:

$p_D$ = *Equivalent uniform static design pressure, psi*
$F$ = *Longitudinal pressure distribution as a function of longitudinal location of the structural design area*
$K_D$ = *Pressure reduction coefficient as a function of the calculated values of* $A_D/A_R$
$A_D$ = *Structural design area,* $in.^2$
$A_R$ = *Impact reference area* $= \frac{25\Delta}{d}(144), in.^2$
$\Delta$ = *Full load displacement in long tons*
$d$ = *Full load static draft in feet*

The most difficult and controversial input required in the procedure is the impact load factor, $N_z$. The factor $N_z$ can be found from model tests where it would be that portion of the acceleration at the center of gravity due to impact forces (as apposed to bouyancy forces, or in the case of SES and ACV's, cushion forces). Savitsky and Brown [209] present an analytical method for determining the load factors for planing hulls.

Garcia [168][x] provides a procedure to determine the impact pressure and distribution for wave slap as a result of his testing of water waves breaking against vertical barriers as discussed in Section 3.3.2. He gives the maximum pressure as:

$$p_{max} = 50(\rho g)^{3/5} E_o^{1/5} \qquad \textbf{(3-64)}$$

where:

$$E_o = \text{wave energy} = \tfrac{1}{8}\rho g H_o^2 L_o$$

$$H_o, L_o = \text{wave height and length respectively}$$
$$y = \text{distance above or below point of maximum pressure}, p_{max}$$

with the shape of the pressure distribution above the point of maximum pressure at $y = 0$: and below:

$$p = p_{max}\left(1 - \frac{2y}{d_w}\right)^2 \qquad \textbf{(3-65)}$$

$$p = p_{max}\left(1 - \frac{1.5y}{d_w}\right)^2 \qquad \textbf{(3-66)}$$
$$d_w = \text{still-water depth at the wall}$$

The exact location of the point of maximum shock pressure was a function of the still-water depth at the wall, the deep water wave steepness and the slope of the beach in front of the wall. The maximum pressure position approaches the still water level as the beach slope increases and for a beach slope of 1:10 is within 0.9-1.1 of the still-water level.

According to the U.S. Navy Structural Design Manual [210], wave slap loads acting on vertical surfaces, such as the upper shell on most hull forms, are generally assumed as 500 psf minimum. For inclined surfaces, the following assumptions are usually made:

a. Sponson loads with medium height:
   1600 psf in the forward one-third length
   1000 psf in the after two-thirds length
b. High sponsons: 500 psf
c. Bow flare regions: 1600 psf (average)

Koelbel [211] discusses the calculation methods currently in use for predicting the hydrodynamic loads of high speed planing craft, including experimental results. With this discussion he presents the uncertainty inherent in these methods. He then recommends using the much simpler and more certain approach of picking the design vertical acceleration of the craft based on the intended service, and calculating the loads from the acceleration.

# 4. ANALYSIS TECHNIQUES AND PROCEDURES

## 4.1 General

A number of the hydrodynamic predictive approaches and data discussed in the previous sections have been presented by their respective authors in the format of an analysis technique which can be utilized to predict hydrodynamic impact loadings in design. This section addresses specific techniques which have been identified and which appear to exhibit unique features.

## 4.2 Slamming

### 4.2.1 Von Karman [32] - Monohulls

#### 4.2.1.1 General

Started the analytical analysis of slamming while trying to develop a means for determining impact loads on seaplane floats during landing. The procedure is a force and pressure formula for a 2-D section. Wagner [33] furthered the approach by considering spray during impact.

#### 4.2.1.2 Prerequisite Information

- Section shape of vessel
- Impact velocity

#### 4.2.1.3 Procedure

Force and pressure determination in accordance with Equations (3-7)-(3-9) of Section 3.2.1.

### 4.2.2 Ochi and Motter [28] - Monohulls

#### 4.2.2.1 General

The overall method developed by Ochi is depicted in Figure 4-1 and includes a number of phenomena related to slamming, among which are:

1. Frequency of Occurrence
2. Limiting Speed (Slamming Tolerable)
3. Time Interval Between Slams
4. Slamming Pressure
5. Time Before Next Slam
6. Extreme Probability Pressure

8. Extreme Pressure for Design
9. Ship Speed Free from Slamming
10. Slam Impact Force
11. Main Hull Girder Response

The hydrodynamic impact theory utilized has been addressed in Section 3. Computer programs representing parts of the method for the overall procedure are available in the literature.

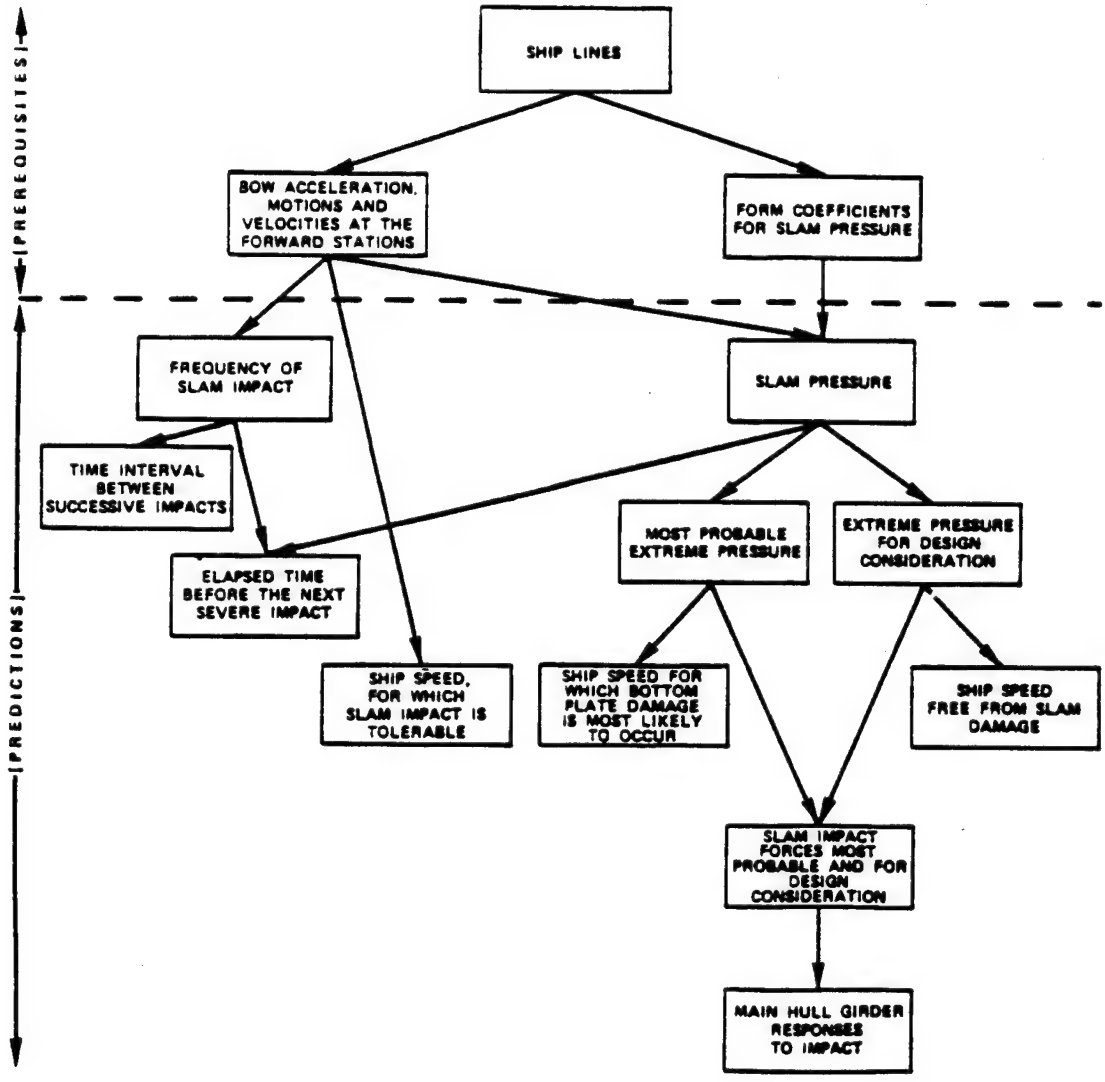


**Fig. 4-1 Flow Chart for Prediction of Slamming Characteristics and Hull Responses [28]**

#### 4.2.2.2 **Prerequisite Information**

- Vessel lines plan
- Operational Conditions
  - Draft
  - Trim
  - Speed
  - Environment (sea state)
- Statistical acceleration at bow and motions and velocities relative to waves at several forward locations (from seakeeping computer programs).
- Form coefficient for pressure term

#### 4.2.2.3 **Procedure**

*Step 1:* Frequency of occurrence of slam impact. This can be obtained from the information on ship motion and velocity relative to waves from a frequency versus time basis.

*Step 2:* Limiting speed for which slamming impact is tolerable. From results obtained in Item 1 as a function of ship speed, the limiting speed for which slam impact is tolerable is estimated as the speed for which either the probability of slam impact at Station 3 reaches a level of 0.03 or the significant amplitude of the vertical bow acceleration reaches a level of 0.4 g.

*Step 3:* Time interval between successive impacts. From results obtained in Item 1, the time interval between successive impacts can be estimated.

*Step 4:* Slamming pressure: The probability function necessary for predicting impact pressure is established utilizing the form coefficient and motion data from which the average and significant values of impact pressure can be predicted.

The average pressure (p), average of ⅓ highest pressure ($p_{⅓}$) can be obtained by the following:

$$p = k(\dot{r}_*^2 + R\dot{r}') = \tfrac{1}{2}\rho k_1(\dot{r}_*^2 + R\dot{r}') \qquad (4\text{-}1)$$

$$p_{⅓} = k(\dot{r}_*^2 + 2.10\ R\dot{r}') = \tfrac{1}{2}\rho k_1(\dot{r}_*^2 + 2.10\ R\dot{r}') \qquad (4\text{-}2)$$

Where:

$r_*$ = threshold Relative Velocity (Velocity below which no slams occur).

$Rr'$ = twice Variance of Relative Velocity, equal to area under spectral density function of relative velocity at desired location attainable via ship motion computer programs.

$k$ = form Coefficient for Slamming Pressure
= $\exp(-3.599 + 2.419a_1 - 0.873a_3 + 9.624a_5)$

$k_1$ = nondimensional form coefficient, $k_1 = 2k/\rho$.
= $\exp(1.377 + 2.419a_1 - 0.873a_3 + 9.624a_5)$

$a_1$, $a_3$, $a_5$ = constants unique to hull section shape and a function of beam, depth, sectional area and moment of inertia for which a Fortran computer code program is available [84].

The magnitude of threshold relative velocity, $r_*$, is defined as 12 feet per second for a 520 ft. vessel, and is said to be obtained empirically through model experiments and the Froude law to apply to ships of different length. In other words, the threshold relative velocity $r_* = 0.096/gL$. The source is not stated but the value has not been confirmed through full-scale trials.

*Step 5:* Elapsed time before the next severe impact. The time between one severe impact and the next at a specific location along the ship length can be estimated from the results obtained in Steps 1 and 4.

*Step 6:* Most probable extreme pressure. By applying order statistics, the magnitude of the largest impact pressure most likely to occur in a specified ship operation time in a given sea can be predicted at any location along the ship length from the results obtained in Item 4.

The magnitude of extreme pressure most likely to occur in n-observations (the most probable value) is equal to

$$\bar{p}_n = \frac{1}{2}\rho k_1 (\dot{r}_*^2 + R_i' \ln n) \qquad (4\text{-}3)$$

where:

n = Number of observations.

The magnitude of extreme pressure for which the probability of being exceeded is $\alpha$, designated by $p_n(\alpha)$

The most probable extreme pressure in "$n$" observations becomes:

$$\hat{p}_n(\alpha) = \frac{1}{2}\rho k_1 \left[\dot{r}_*^2 - R_t' \ln\left(1-(1-\alpha)^{1/n}\right)\right] \qquad (4\text{-}4)$$

where:

$\alpha$ = pre-assigned small probability specified by the designer.

Fig. 4-2 shows a pictorial sketch of the probability density function of the extreme pressure.

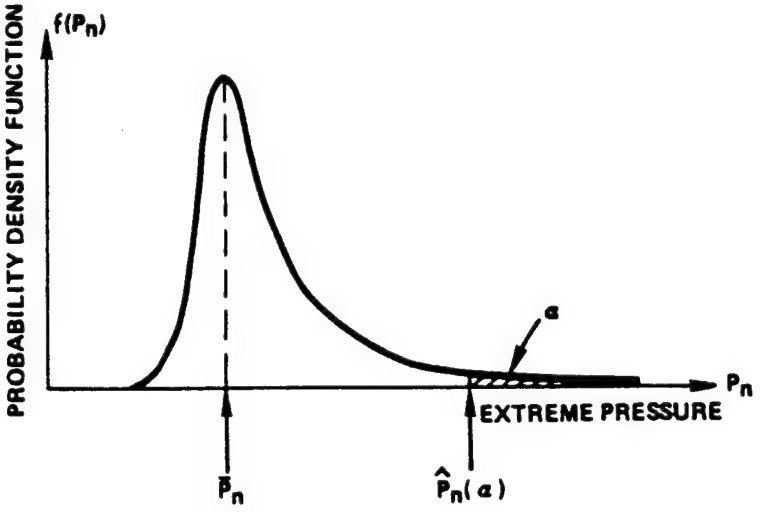


**Fig. 4-2. Explanatory Sketch of Probability Density Function of Extreme Pressure**

A Fortran Computer code for estimating extreme values of slamming pressure is available [86]. It also computes the probabilities of occurrence of bow emergence, slamming, and deck wetness.

*Step 7:* Ship speed at which bottom plate damage is most likely to occur. By equating the pressure magnitude obtained in Item 6 to that which will cause permanent set of a rectangular plate, the speed is estimated at which bottom plate damage is most likely to occur.

*Step 8:* Extreme pressure for design consideration. The magnitude of extreme pressure for design consideration can be estimated by applying order statistics to the probability function obtained in Item 4. The extreme value is controlled by a pre-assigned small probability of being exceeded that is specified by the designer.

*Step 9:* Ship speed free from slam damage. By equating the pressure magnitude obtained in Item 8 to that which will cause permanent set of a rectangular plate, the attainable (maximum) speed below which no plate damage would occur is estimated. The probability of occurrence of damage is the small number assigned in Item 8.

*Step 10:* Slam impact force. The magnitude of impact force can be estimated from Items 6 or 8, taking spatial distribution and traveling time of the pressure into consideration. The force evaluated using the extreme pressure in Item 8 is used for design consideration.

Since the slam impact pressure usually travels either forward or aft with changing magnitude, the spatial distribution of pressure on the bottom as a function of time is necessary for predicting loads.

Traveling Time: Triangular shape; assumed duration of 0.1 second for 520 foot vessel. Buy Froude's Law, the duration time of pressure $t_1$ at any point for a ship of length L in feet, is given by:

$$t_1 = 0.1 \sqrt{\frac{L}{520}} = \frac{4.4}{10^3} \sqrt{L} \qquad \textbf{(4-5)}$$

Velocity of Travel: The impact pressure travels along the ship length with changing magnitude with the following velocity:

$$V = 260 \sqrt{\frac{L}{520}} = 11.4 \sqrt{L} \qquad \textbf{(4-6)}$$

Hull Domain of Impact Pressure:

- Longitudinal: Can be found by examination of the number of impacts. The number reduces significantly with increasing distance from the F.P. The location where the number of impacts equals 1 will be the extent of longitudinal length.

- Vertical: (0.1 H, H = draft) But the pressure traveling velocity differs (in the upwards direction) at each section, due to the difference in the magnitude of relative velocity.

The impact force for a given section can now be evaluated by integrating the pressure along the girth up to a vertical limiting height determined previously. The procedure of evaluating the extreme pressure force is as follows:

a. The distance along the girth up to the limiting height for impact force consideration is extended to a straight line.

b. The most probable pressure $p_n$ obtained previously is applied uniformly on the flat bottom.

c. The pressure assumed to reduce linearly along the curved section of the hull (i.e., from the outward extent of the flat bottom to 0.1 H).

d. The cosine - component of the angle between the normal angle of the force to hull and the vertical is multiplied by the pressure ($p_n$) in order to obtain the vertical pressure component at each point along the girth, Figure 4-3.

e. Taking the pressure duration into account at each point, integration of the magnitude of pressure will then provide the most probable impact force applied to the section as a function of time, Figure 4-4.

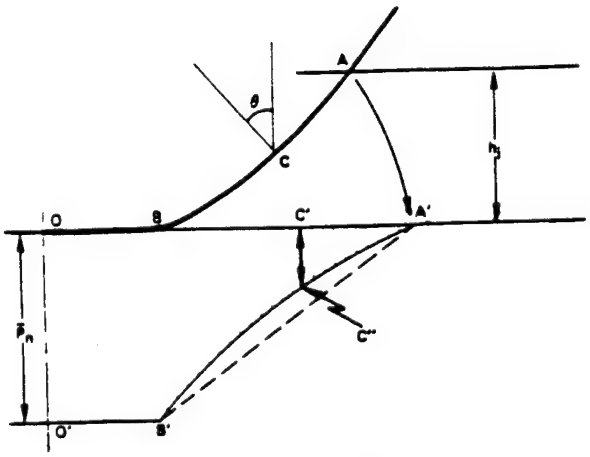


**Fig. 4-3 Explanatory Sketch of the Distribution of Extreme Pressure Along the Section Girth**

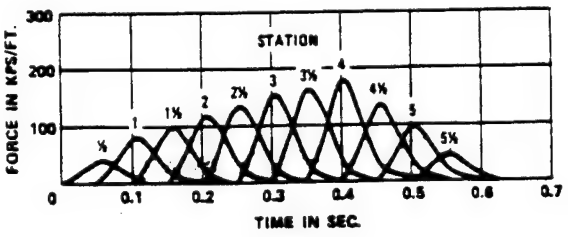


**Figure 4-4 Impact Force Applied at Various Stations as a Function of Time; Mariner, Sea State 7, Significant Wave Height 25 ft, Ship Speed 7.4 Knots, Light Draft**

*Step 11:* Main hull girder responses to impact. Using the information obtained in Item 10 as an input, the main hull girder responses such as whipping stress and deceleration due to impact are estimated by solving a mathematical model representing the hull structural characteristics. Available computer programs for dynamic response of the hull may be used with necessary alterations.

### 4.2.3 Kaplan and Sargent [125] - Monohulls

#### 4.2.3.1 General

These authors have developed a computer-based approach to predicting slam forces and the resulting bending moments and shear forces in the hull. Through the use of two-dimensional linear frequency domain, ship motion theory relative motions and frequency dependent added mass is determined. The results are used along with fluid momentum considerations in slamming to provide an initial estimate of impact forces. Then, the effects of non-linear buoyancy due to momentum changes in terms of instantaneous added mass, both due to continuing submergence of the section, are estimated. Results are fed back as corrections to the initial estimates. A time domain format of the program has been adopted as the process is transient and non-stationary. The computer program is not publicly available.

The overall approach is shown in Figure 4-5. The theoretical basis of the procedure is discussed in Section 3. The equation numbers in Figure 4-5 define those in the author's work.

#### 4.2.3.2 Prerequisite Information

- Vessel lines
- Hull weight distribution
- Heave and pitch motion frequency response including absolute motions and velocities relative to the waves in the desired sea conditions.
- 2-D added mass for different levels of immersion of a section. The authors have utilized frequency dependent added mass.

#### 4.2.3.3 Procedure

As depicted in Figure 4-5 with the prerequisite information identified the calculation sequence for the time history simulation can begin. The entire procedure is automatic with the intermediate evaluations noted.

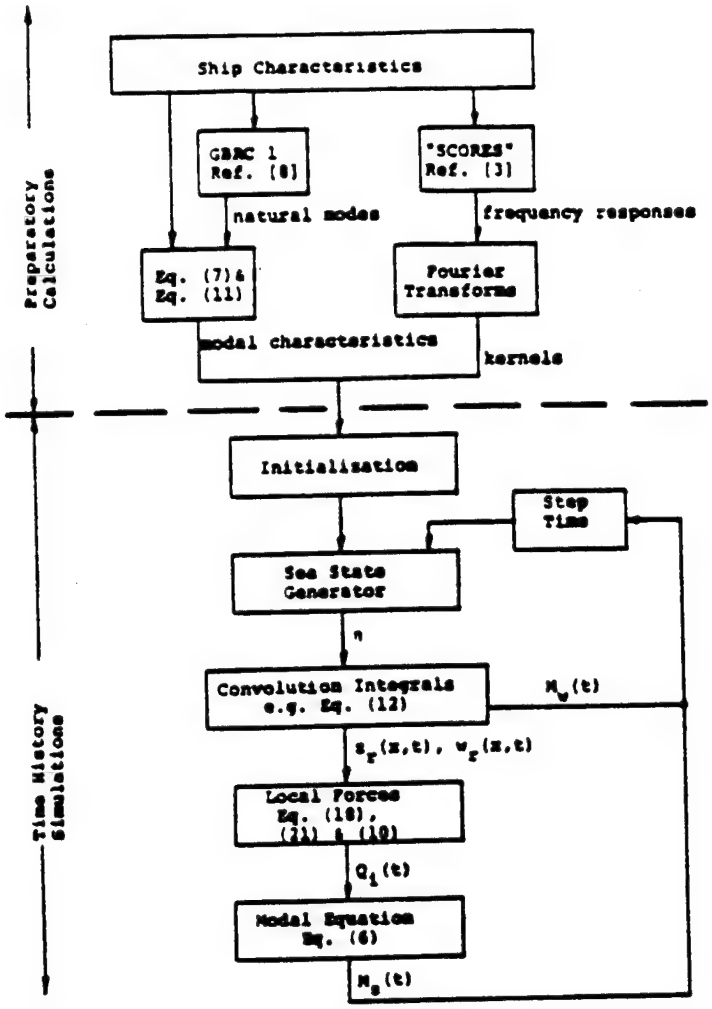


**Fig. 4-5. Flow Chart for Prediction of Slamming Characteristics and Hull Response [125]**

### 4.2.4 Kaplan [102] - Multi-hulls

A quasi-three-dimensional fluid momentum analysis has been applied to predict impacts on the water surface of the flat of bottom centerbody surfaces of multi-hulled marine craft such as SES, SWATH and catamarans. The total force developed is treated as the summation of the bow ramp, flat wetdeck between the hulls and the flare of the hulls as:

$$\text{Vertical Slam Force} = Z_{slam} = Z_{ramp} + Z_{wetdeck} + Z_{flare}$$

The method requires the prediction of the vessel response to waves from which the time and spacial relationships between the hull surface and wave profile can be obtained. The momentum relationships associated with a slam are then evaluated and modified to account for unsteady lift force generation and any buoyancy contributions of the submerging structures.

The entire calculation is carried out by computer program which is proprietary.

By comparison (author's, not shown in reference) to a set of model test results [212] for an SES it is concluded that it is possible for significant differences in the loads to manifest themselves due to small differences in the occurrence time of the vessel motions or the incident wave reference. However, for the case of irregular waves where different aspects of ship orientation and motion magnitudes cover a significant degree of change in an irregular fashion, the results should appear similar. It is suggested by the author that similar results can also be expected for catamaran hulls and SWATH due to the similarity of large flat surfaces and the same type of motion analysis procedure.

This approach is essentially identical to that for monohulls developed by Kaplan and Sargent [125] and presented in 4.2.2 except that the seakeeping analysis pertains to twin hull vessels, the slam forces due to the centerbody have been added, and hull flexure is not considered.

### 4.2.5 Troesch and Kang [3] - Monohulls

The two-dimensional and three-dimensional techniques developed by these authors appear to be equally applicable to slamming and bow flare impacts. As they were particularly concerned with bow flare impact a summary of their technique is given in Section 4.4.

### 4.2.6 Jasper and Church [119], Chuang [120]

#### 4.2.6.1 General

Figure 4-6 shows a block diagram of the structural seaworthiness digital computer program ROSAS. The "sea" subroutine is capable of simulating regular sinusoidal waves, a wave train of definite shape or simply a sinusoidal pulse at a prescribed location. The response of the ship feeds back to the hydrodynamic subroutine to produce dynamic interaction between the ship and the hydrodynamic forces. In case bow emergence occurs, a slamming subroutine compares the bottom slamming forces and adds then to the hydrodynamic forces for computing ship responses in terms of forces in the hull girder.

The computer program is available in the literature [120].

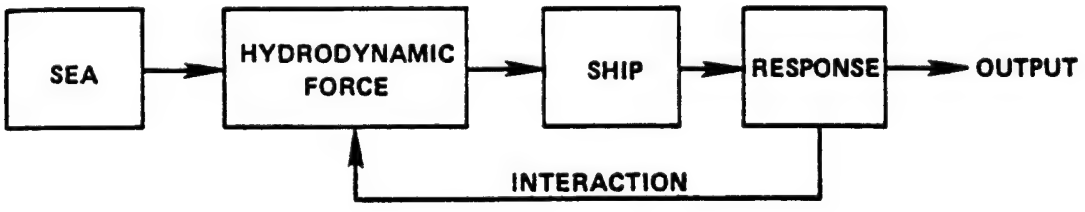


**Figure 4-6: Diagram of Structural Seaworthiness Digital Computer Program ROSAS**

#### 4.2.6.2 Prerequisite Information

- Vessel lines plan
- Operational Conditions
  - Draft
  - Trim
  - Speed
  - Simplified wave description

#### 4.2.6.3 Procedure

As depicted in Figure 4-6 with the prerequisite information identified the calculation sequence for the time history simulation due to the moving wave can begin. The entire procedure is automatic with a system of ordinary differential equations representing the equations of motion for the discretized hull and numerically integrated by the Runge-Kutta method.

### 4.2.7 Stavovy and Chuang [117]

#### 4.2.7.1 General

The authors have developed a procedure to determine the impact pressure in an infinitesimal area of the hull bottom at point A in Figure 4-7.

The basis is described in Section 3.3.3 and consists of determining the relative normal velocity of impact of body to wave surface, $V_n$, and the effective impact angle, $\xi$, on a plane normal to the wave surface and impact surface on the hull bottom. With $\xi$ known the peak pressure factor, $k_1$, can be selected from Figure 3-35. The impact pressure at point A is equal to

$$p_A = k_1 V_n^2$$

The entire calculation can be carried out by computer program which is available in the literature and demonstrated in Table 6-2.

#### 4.2.7.2 Prerequisite Information

- Vessel lines
- Sea conditions
- Vessel forward speed
- Vessel seakeeping motion characteristics

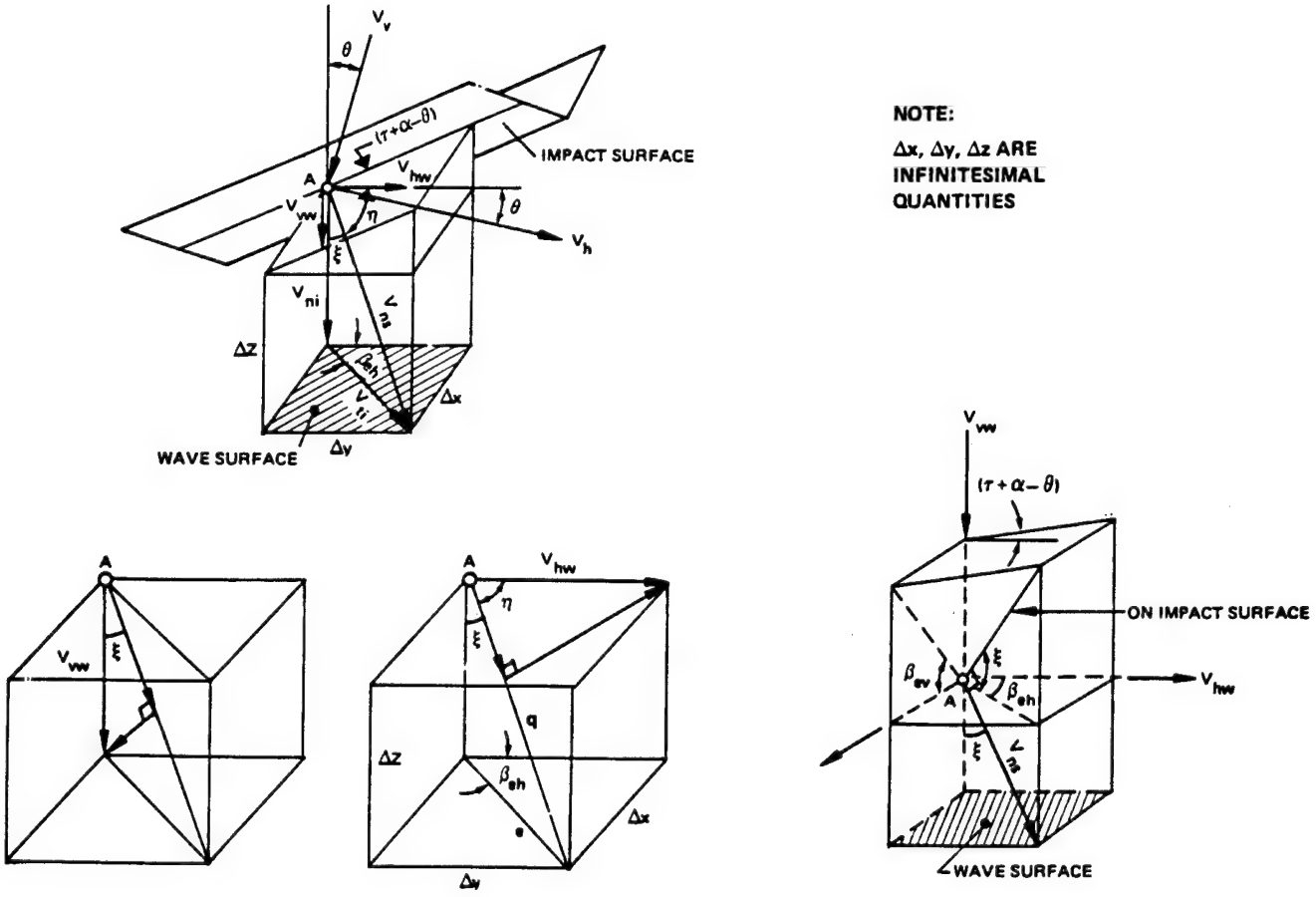


**Figure 4-7: Velocity Diagram For Impact Surface**

#### 4.2.7.3 Procedure

The procedure involves determining the impact velocity and orientation, and pressure factor for which a computerized procedure is available. The seakeeping motions of the vessel need to be superimposed.

### 4.2.8 Slam Pressure Predictions Using Scaled Models [3]

The procedure is described in Section 3.3.3. It consists of testing a hydro-elastic model of a vessel in irregular waves and measuring the response. A probabilistic Weibull analysis of the results is carried out to derive the lifetime maximum pressures.

### 4.2.9 Bishop and Price [29]

The unique features of the authors' approach are in the consideration of the hull stiffness and vibratory characteristics and the incorporation of an initial impact slam and

following momentum slam. The procedures for determining the hydrodynamic loads are adopted from others as follows:

- Impact Forces - Stavovy and Chuang [117]
- Momentum Forces - Leibowitz [128]
- Force Time Histories - Ochi and Motter [28] and Kawakami, Michimoto and Kobayaski [130]

A computerized technique is not available in the literature.

#### 4.2.10 U.S. Federal Aviation Administration [42]

In the U.S. Code of Regulations they maintain a procedure for design impact loading of seaplanes during take-off and loading. The procedure itself is directed at seaplanes. The pressure predictions utilize semi-empirical formulas similar to Von Karman [32] and Wagner [33].

#### 4.2.11 Zhao and Faltinsen [68]

##### 4.2.11.1 General

The authors have developed a procedure to determine pressure distributions over a surface of a two-dimensional body of arbitrary cross-section. The water free surface is initially calm and its depth is infinite. The solution is applicable both to slamming and bow flare impact.

The technique is described in Section 3.2.2 and is based on the solution of Laplace's equation with nonlinear free boundary condition. The numerical procedure is applied to the integral equation corresponding to a boundary value problem.

Parametric numerical solution ("similarity" solution) and an asymptotic solution are available for the wedge-like bodies.

##### 4.2.11.2 Prerequisite Information

- Vessel cross-section lines.
- Impact velocity time history.

##### 4.2.11.3 Procedure

The procedure determines the pressure distribution. The seakeeping motions of the vessel need to be superimposed.

### 4.2.12 Mitsubishi Heavy Industries (Toki et al [135]; Vulovich et al [20])

#### 4.2.12.1 General

The authors developed a time-domain numerical simulation program MSLAM and a model test technique which the authors term the "elastic backbone model" technique. Basic assumptions and theoretical formulation on which the simulation program was based include assumption of constant advance ship speed in regular of long-crested irregular waves, use of strip theory, and a nonuniform Timoshenko beam approach. The method is described in Section 3.2.4.2. The computer program of the procedure is not available in the public domain.

#### 4.2.12.2 Prerequisite Information

- Vessel lines (Bonjean data)
- Hull Weight Distribution
- Bending rigidity distribution
- Sea conditions
- Vessel forward speed

#### 4.2.12.3 Procedure

The SLAM program calculates time histories of ship vertical motions (heave and pitch), hull vertical vibration and vertical shearing force and bending moment on the hull girder. It also accounts for the effects of large bow flare, bottom emergence, bottom and bow flare slamming, and a combined effect of ship motions as a rigid body and lower-mode hull girder vibrations.

### 4.2.13 Aksu et al. [132]

#### 4.2.13.1 General

The authors have developed a time-domain simulation method to determine transient vertical and transverse responses (motion, distortion, bending moment, shear force, twist) in head and oblique waves. Slamming pressure is calculated on the basis of the Stavovy and Chuang method. The seaway is assumed to be irregular and long crested. The technique is described in Section 3.2.4.

The method can be applied to arbitrary shaped, non-beam-like structures, for example, multi-hulls. The computer program is not available in the public domain.

#### 4.2.13.2 Prerequisite Information

- Vessel lines
- Hull weight distribution
- Bending rigidity distribution
- Sea conditions
- Vessel forward speed

#### 4.2.13.3 Procedure

The simulation program calculates time histories of ship motions, hull wave and transient vibration, shearing force and bending moment on the hull girder in vertical and horizontal planes.

## 4.3 Wave Slap

### 4.3.1 Wave Slap Pressure Predictions Using Scaled Models [3]

In principal the type of approach discussed for slamming in Section 4.2.6 should be possible.

### 4.3.2 Garcia [168]

Garcia developed a procedure for breaking wave pressures, specifically for breakwaters, but which in principal can be considered for wave slap. The procedure predicts a maximum wave impact pressure based on wave characteristics and provides expressions for varying the pressure from the point of maximum impact, which is between 0.9 and 1.1 times the still-water line, herein taken as the vessel draft.

Vessel speed would have to be incorporated in application to ships and perhaps this can be incorporated as an effective wave length.

The expressions for pressure and additional discussions are provided in Sections 3.3.3.2.

### 4.3.3 U.S. Navy [210]

Pressures for various impact surface positions are presented for design.

## 4.4 Frontal Impact

### 4.4.1 Troesch and Kang [5] - Monohulls

The procedure by Troesch and Kang is based on either a two-dimensional strip theory or three-dimensional panel integral equation mathematical basis as discussed in Sections 3.2.2 and 3.2.3. It considers both bow flare and slamming impact.

The reported extent of application of the procedure has been to two ship idealizations as shown in Figure 3-18. Troesch [213] has indicated the 2-D program has been expanded to accept ship forms.

The computer program required to execute the calculations is available at the University of Michigan.

It is surmised that the calculation requires the impact velocity, vessel orientation, and geometry to be input. It is only for calm water.

### 4.4.2 Kaplan and Sargent [125] - Monohulls

The authors utilize the same procedure used for slamming and discussed in Section 4.2.2 for predicting bow flare impact.

### 4.4.3 Jasper and Church [119], Chuang [120]

The authors utilize the same method used for slamming and discussed in Section 4.2.6 except that the slam force is replaced by non-linear added mass and buoyancy.

### 4.4.4 Frontal Impact Pressure Predictions Using Scaled Models [2]

The type of approach is the same as was discussed for slamming in Section 4.2.8.

### 4.4.5 Gran et al [64]

The authors have developed an expression for the instantaneous impact force as described in Section 3.2.2. They emphasize that the immersion of the solid body will continuously change the added mass distribution, and it is therefore important to understand that their approach is based upon a quasi-stationary assumption, i.e., the water flow at each instant is taken to be identical with steady state flow. The simplified two-dimensional problem in the place of a cross-section and head waves are considered. Stress response evaluation is based on a flexible hull model.

# 5. COMPARISON OF ANALYSIS TECHNIQUES FOR APPLICATION

## 5.1 General

In this section the analysis techniques identified in Section 4. herein will be compared in order to identify those which appear to be most successful in predicting hydrodynamic impact phenomena. These will be compared further with example calculations in Section 6.

The comparison of the analysis techniques has been accomplished in the following fashion:

- Comparative tabulation of the salient characteristics of each theory including method, sea surface conditions, rigidity of impact surface, 2-D or 3-D, hull form characteristics, forward speed; Section 5.2.
- Identification of strengths and weaknesses; Section 5.3.

## 5.2 Comparative Tabulation

Tables 5-1 through 5-3 give a comparative tabulation of the analysis techniques identified in Section 4. Each table consists of three sheets to describe each method.

## 5.3 Evaluation

### 5.3.1 Slamming

#### 5.3.1.1 Von Karman [32] - Monohulls

Strengths:

- Simple.

Weaknesses:

- Does not consider waves.

Other features:

- Enhanced by subsequent researchers such as Wagner [33].

| Method | Type of Ships | Basis Formulation | 2-D/3-D | Sea Surface |
|---|---|---|---|---|
| **Von Karman [32]** | Monohulls | Hydrodynamic wedge impact theory. | 2-D | Calm. |
| **Wagner [33]** | Monohulls | Hydrodynamic wedge impact theory. | 2-D | Calm. |
| **Armand and Cointe [43]** | Pontoon-Like Mono-hulls | Hydrodynamic cylinder impact theory | 2-D | Calm. |
| **Stavovy and Chuang [117]** | All | Combination of wedge and cone theories and experimental results including 2-D/3-D. | 3-D | Regular wave from any direction. |
| **SNAME [3] Scaled Models** | All | Hydro-elastic model tests with probabilistic analysis of results. | 3-D | Waves from any direction. |
| **Bishop and Price [29]** | Monohulls | Hydro-elastic beam analysis with impact forces by others. | 2-D | Head sea waves. |

**Table 5-1: Summary of Analysis Technique Characteristics - Slamming**
**[Continues on 3 Sheets]**

| Method | Impact Surface/ Hull Rigidity | Hull Form Character-istics | Forward Speed | Theoretical/Experimental Model Description Boundary Conditions |
|---|---|---|---|---|
| **Von Karman [32]** | Rigid/ Rigid | Actual section shape. | Included in impact velocity. | Wedge impact in calm water<br>Linear free surface. |
| **Wagner [33]** | Rigid/ Rigid | Actual section shape. | Included in impact velocity | Wedge impact in calm water<br>Linear free surface |
| **Armand and Cointe [43]** | Rigid/ Rigid | Circular arc bottom. | May be included in impact velocity. | Small perturbation asymptotic model<br>Body and free surface linear. |
| **Stavovy and Chuang [117]** | Rigid/ Rigid | Actual section shape. | Included in impact velocity. | 3-D experiment. |
| **SNAME [3] Scaled Models** | Elastic/ Elastic | Actual | Yes | Exact model of full scale. |
| **Bishop and Price [29]** | NA*/ Elastic | Actual | Yes | Freely floating elastic beam representation of hull with impact forces by Stavovy and Chuang [54] and Leibowitz [60]. |

*Not applicable.

**Table 5-1: (Continued - Page 2)**

| Method | Types of Example Calculations | Correlation with Full Scale or Model Experiment | Pressure/ Force Deter-mined | Refer-ence Sec-tions |
|---|---|---|---|---|
| **Von Karman [32]** | Seaplane pontoon. | Acceptable agreement with experiments and full scale results. | Yes/ Yes | 3.2.2 |
| **Wagner [33]** | Seaplane pontoon. | Acceptable agreement with experiments and full scale results. | Yes/ Yes | 3.2.2 |
| **Armand and Cointe [43]** | 2-D circular cylinder. | Acceptable agreement with model experiment for initial stage of impact | Yes/ Yes | 3.2.2 |
| **Stavovy and Chuang [117]** | Slow to fast monohulls and catamaran cross structure. | Good correlation with monohulls and full scale catamaran results. | Yes/ No | 3.3.3.1 |
| **SNAME [3] Scaled Models** | None. | No comparisons. | Yes/ Yes | 3.3.3 |
| **Bishop and Price [29]** | Destroyer and frigates. | Reasonable agreement with full scale tests | No/ Yes | 3.2.4.2 |

Table 5-1: (Continued - Page 3)

| Method | Type of Ships | Basis Formulation | 2-D/3-D | Sea Surface |
|---|---|---|---|---|
| **Ochi and Motter [28]** | Monohull | Slamming occurrence predicted by statistical seakeeping events and pressure by empirical relationship based on test data. | 2-D integrated to product quasi 3-D results. | Irregular sea wave from any direction. |
| **Kaplan and Sargent [125]** | Monohull | Slamming occurrence predicted by changes in momentum and buoyancy utilizing 2-D seakeeping theory and response includes hull flexure. | 2-D integrated to produce quasi 3-D results. | Irregular head sea waves. |
| **Troesch and Kang [5]** | Monohull | Hydrodynamic impact boundary value theory. | 2-D and 3-D. | Calm water. |
| **Kaplan [102]** | Multi-hulls | Slamming occurrence predicted by seakeeping theory and centerbody slam forces by the Von Karman technique adopted by the author. | 3-D for centerbody. | Regular head sea waves. |
| **Jasper and Church [119]**<br><br>**Chuang [120]** | Monohull | Slamming occurrence predicted by travelling wave pressure by empirical relationship and response includes hull flexure. | 2-D discretization of hull producing quasi 3-D results. | Regular head sea wave. |

**Table 5-1a: Summary of Analysis Technique Characteristics - Slamming**
**[Continues on 3 Sheets]**

| Method | Impact Surface/ Hull Rigidity | Hull Form Character-istics | Forward Speed | Theoretical/Experimental Model Description |
|---|---|---|---|---|
| **Ochi and Motter [28]** | Rigid/ Rigid | Actual | Considered as part of sea-keeping events but deemed unimportant for pressure to 15 knots. | Not applicable as slam pressure based on tests. Seakeeping model used is based on strip theory, or experiments. |
| **Kaplan and Sargent [125]** | Rigid/ Elastic (1st Mode) | Actual | Considered as part of seakeeping events. | Per 2-D seakeeping theory except added mass and buoyancy provided at the actual waterline as opposed to the still waterline. |
| **Troesch and Kang [5]** | Rigid/ Rigid | 2-D Actual/ 3-D Ideal Cases | Included. | Body boundary and linear free surface. |
| **Kaplan [102]** | Rigid/ Rigid | Actual | Considered as part of sinusoidal wave passing hull. | 2-D Von Karman impact theory applied to centerbody in 3-D. |
| **Jasper and Church [119]**<br><br>**Chuang [120]** | Rigid/ Elastic | Actual | Considered as part of sinusoidal wave passing hull. | Discretized hull sections with 2-D section properties, including impact added mass by Wagner and buoyancy at the actual waterline as opposed to the still waterline. |

**Table 5-1a: (Continued - Page 2)**

| Method | Types of Example Calculations | Correlation with Full Scale or Model Experiment | Pressure/ Force Determined | Reference Sections |
|---|---|---|---|---|
| **Ochi and Motter [28]** | Application to a 520' LBP MARINER cargo vessel. | Pressure relation has significant correlation but overall method has not been compared to actual results. | Yes/ Yes | 3.3.3.1 |
| **Kaplan and Sargent [125]** | Containership | Containership full scale data indicates bending moment predictions high but velocities are acceptable according to authors. | No/ Yes | 3.2.4.2 |
| **Troesch and Kang [5]** | Two idealized 3-D forms | Good with experiment. | Yes/ Yes | 3.2.3 |
| **Kaplan [102]** | For an SES | Not shown in reference but author states that magnitudes of the loads are in agreement. | No/ Yes | 3.2.3 |
| **Jasper and Church [119]**<br><br>**Chuang [120]** | ESSEX aircraft carrier | Acceptable agreement with full scale experiment. | No/ Yes | 3.2.4.2 |

**Table 5-1a (Continued - Page 3)**

| Method | Type of Ship | Basis Formulation | 2-D/3-D | Sea Surface |
|---|---|---|---|---|
| **Zhao and Faltinsen [68]** | Monohulls | Hydrodynamic impact theory for arbitrary shape. | 2-D | Calm |
| **Mitsubishi Heavy Industries (Toki et al [135])** | Monohulls | Time domain simulation of ship motions. Strip theory and nonuniform beam approach. | 2-D for slamming force | Regular or irregular long crested waves. |
| **Aksu et al [132]** | Multihulls | Time domain simulation of ship motions. Stavovy and Chuang method for slamming pressure. | 3-D | Irregular long crested waves. |

**Table 5-1b: Summary of Analysis Technique Characteristics - Slamming (Continues on Three Sheets)**

| Method | Impact Surface/Hull Rigidity | Hull Form Characteristics | Forward Speed | Theoretical/Experimental Model Description / Boundary Condition |
|---|---|---|---|---|
| **Zhao and Faltinsen [68]** | Rigid/ Rigid | Actual section shape. | Included in ship motions prediction method. | 2-D hudrydynamic impact. / Non-linear boundary conditions. |
| **Mitsubishi Heavy Industries (Toki et al [135])** | Rigid/ Elastic | Actual section shape. | Included in ship motions prediction method. | 2-D slamming model based on momentum law formula. / Linear free surface. |
| **Aksu et al [132]** | Rigid/ Elastic | Actual section shape. | Included in ship motions prediction and impact velocity. | Semi-empirical Stavovy and Chuang model. |

**Table-5-1b: (Continued - Page 2)**

| Method | Types of Example Calculations | Correlation With Full Scale or Model Experiment | Pressure/ Force Determination | Reference Sections |
|---|---|---|---|---|
| **Zhao and Faltinsen [68]** | Wedge impact; bow flare section impact | Good agreement with model experiment (bow flare section) [183]. | Yes/Yes | 3.2.2 |
| **Mitsubishi Heavy Industries (Toki et al [135])** | Containership | Considerable underesti-mation of compressive stress on the foredeck; Slight over estimation of stresses on the mid portion of the deck. | No/Yes | 3.2.4.2 |
| **Aksu et al [132]** | Barge Elastic | No comparisons with experiment. | Yes/Yes | 3.2.4 |

**Table 5-1b: (Continued - Page 3)**

| Method | Type of Ships | Basis Formulation | 2-D/3-D | Sea Surface |
|---|---|---|---|---|
| **Garcia [168]** | All | Model experiments on breakwaters. | 2-D | Waves |
| **U.S. Federal Aviation Administration (FAA) [42]** | Seaplanes | Wedge impact, including bow flare sections. | 2-D with 3-D corrections | Calm. |
| **U.S. Navy [210]** | All | Design pressures for various impact surface positions. | 2-D | Waves |

**Table 5-2: Summary of Analysis Technique Characteristics - Wave Slap**
**[Continues on 3 Sheets]**

| Method | Impact Surface/ Hull Rigidity | Hull Form Character-istics | Forward Speed | Theoretical/Experimental Model Description Boundary Conditions |
|---|---|---|---|---|
| **Garcia [168]** | Rigid/ Rigid | NA* | Not included but authors wave length can be adjusted to reflect. | Regular wave striking breakwater. Body and free surface complete formulation. |
| **U.S. Federal Aviation Administration [42]** | Rigid/ Rigid | Simple shapes (wedge, un-flared and flared bottom). | Yes | Wedge impact in calm water. Linear free surface. |
| **U.S. Navy [210]** | Rigid | All ships | Not explicit. | N/A |

*Not applicable.

**Table 5-2: (Continued - Page 2)**

| Method | Types of Example Calculations | Correlation with Full Scale or Experiment | Pressure/ Force Determined | Reference Sections |
|---|---|---|---|---|
| **Garcia [168]** | None | Good correlation with model tests. | Yes/ No | 3.3.3.2 |
| **U.S. Federal Aviation Administration [42]** | None | Design loads method is based on semi-empirical formulas. Hence, loads should correlate with full scale experiment corrected by margin of safety factors. | Yes/ Yes | 3.2.2 |
| **U.S. Navy [210]** | Exclusive use in design | Routinely used in design over the years. | Yes/ No | 3.3.3.2 |

**Table 5-2: (Continued - Page 3)**

| Method | Type of Ships | Basis Formulation | 2-D/3-D | Sea Surface |
|---|---|---|---|---|
| **Troesch and Kang [5]** | Monohull | Bow flare impact; impact boundary value theory. | 2-D and 3-D. | Calm water. |
| **Kaplan and Sargent [125]** | Monohull | Bow flare impact predicted by changes in momentum and buoyancy utilizing 2-D seakeeping theory and response includes hull flexure. | 2-D integrated to produce quasi 3-D results. | Irregular head sea waves. |
| **Jasper and Church [119]**<br><br>**Chuang [120]** | Monohull | Bow flare impact predicted by changes in momentum and buoyancy utilizing sinusoidal waves and response includes hull flexure. | 2-D integrated to produce quasi 3-D results. | Regular head sea waves. |
| **Gran et al [64]** | Monohull | Bow flare impact boundary value theory. | 2-D | Waves [identified as relative impact velocity]. |
| **U.S. Federal Aviation Administration (FAA) [42]** | Seaplanes | Wedge impact, including bow flare sections. | 2-D with 3-D Corrections | Calm. |

**Table 5-3: Summary of Analysis Technique Characteristics - Frontal Impact**

| Method | Impact Surface/ Hull Rigidity | Hull Form Character-istics | Forward Speed | Theoretical/Experimental Model Description / Boundary Conditions |
|---|---|---|---|---|
| **Troesch and Kang [5]** | Rigid/ Rigid | Actual | Not considered. | Potential panel method<br>Body boundary and simplified free surface. |
| **Kaplan and Sargent [125]** | Rigid/ Elastic (1st Mode) | Actual | Considered as part of seakeeping events. | Per 2-D seakeeping theory except added mass and buoyancy provided above the still waterline as necessary. Added mass based on infinite oscillation theory. |
| **Jasper and Church [119]**<br><br>**Chuang [120]** | Rigid/ Elastic | Actual | Considered as part of seakeeping wave speed passing ships. | Discretized hull sections with added mass and buoyancy provided above and below still waterline as necessary. Added mass is based on impact momentum theory. |
| **Gran et al [64]** | Rigid/ Elastic | Actual | Yes | Consistent with 2-D impact boundary value problem with corrections for spray.<br>Simplified wave profile. |
| **U.S. Federal Aviation Administration [42]** | Rigid/ Rigid | Simple shapes (wedge, unflated and flatted bottom) | Yes | Wedge impact on calm water.<br>Linear free surface. |

**Table 5-3: (Continued - Page 2)**

| Method | Types of Example Calculations | Correlation with Full Scale or Model Experiment | Pressure/ Force Determined |
|---|---|---|---|
| **Troesch and Kang [2]** | Two idealized 3-D forms | Cylindrical shape: Good agreement with model drop test. Flared body: Good agreement with model drop test for first maxima; overpredicts the magnitude of second maxima. | Yes/ Yes |
| **Kaplan and Sargent [125]** | Aircraft carrier | Aircraft carrier model test results are in good agreement | No/ Yes |
| **Jasper and Church [119]**<br><br>**Chuang [120]** | ESSEX aircraft carrier | Aircraft carrier model test results are in good agreement. | No/ Yes |
| **Gran et al [64]** | Lewis form hull sections. | Reasonable agreement with scale stress measurements (fast cargo ship). | No/Yes |
| **U.S. Federal Aviation Administration (FAA) [42]** | None | Design loads method is based on semi-empirical formulas. Hence loads should correlate with full scale experiment corrected by margin of safety factors. | Yes/ Yes |

**Table 5-3: (Continued - Page 3)**

#### 5.3.1.2 Wagner [33] - Monohulls

Strengths:

- Simple

Weaknesses:

- Does not consider waves

Other features:

- An enhancement of Von Karman's approach wherein a refinement of the wetted surface area and hence average pressure is obtained by considering the pile-up of water at the free surface during impact.

#### 5.3.1.3 Armand and Cointe [43]

Strengths:

- Simple asymptotic formula for force valid for initial stage of impact.
- Can serve as a standard for advanced calculations and experiments.

Weaknesses:

- Applicable only for simple ship hull with circular shape.
- Actual sea state not considered.
- Utilizes only through strip theory (3-D effects not included).

#### 5.3.1.4 Stavovy and Chuang [117] - All

Strengths:

- Considers all types of vessels.
- Considers any forward speed, including high speed craft.
- Correlation to a relatively large number of models and full scale measurements.

- Computer code available in literature.
- Considers hull geometry.
- Considers simplified wave definition.
- Computer calculations of a moderate extent.

Weaknesses:

- Only considers infinitesimal area at a single point each time.
- Sea state not statistically described.

#### 5.3.1.5 SNAME [3] Scaled Models - All

Strengths:

- Considers all types of vessels.
- Considers vessel speed.
- Considers exact hull geometry.
- Considers exact wave conditions.

Weaknesses:

- Requires scaling to full scale.
- Extensive model testing required.

#### 5.3.1.6 Bishop and Price [29]

Strengths:

- Considers overall hull geometry.
- Considers sea conditions.
- Acceptable correlation with experiment.

- Strengths of impact load theories it employs (Ochi and Motter [83] or Liebowitz [60]).

Weaknesses:

- Limited application.
- 2-D approach to impact problem.

Other features:

- Computer code proprietary.

#### 5.3.1.7 **Ochi and Motter [28] - Monohulls**

Strengths:

- Provides a procedure for determining the occurrence of slamming at sea.
- Statistical description of slamming pressure is provided.
- Utilizes an extensively correlated pressure relationship.
- Considers overall hull geometry.
- Computer codes available

Weaknesses:

- Strip theory; ignores ship rolling and non head sea directions.

#### 5.3.1.8 **Kaplan and Sargent [125] - Monohulls**

Strengths:

- Considers overall hull geometry.
- Considers sea conditions.

Weaknesses:

- Limited application and correlation to tests; therefore accuracy not known. Did not correlate in one case.
- Local pressure not available.

Other features:

- Proprietary computer code

#### 5.3.1.9 Troesch and Kang [5] - Monohulls

Strengths:

- Considers significant aspects of 3-D problem.
- Good correlation to limited experiments.

Weaknesses:

- Limited application to ship hull forms and comparison to tests.
- Most likely significant computation capacity and time required for the 3-D approach.

Other features:

- Proprietary computer code.

#### 5.3.1.10 Kaplan [102] - Multi-Hulls

Strengths:

- Appears to be applicable to various multi-hull vessels
- Considers overall hull geometry
- Computer calculations of moderate extent for added force due to cross structure.

Weaknesses:

- Limited comparison to experiment.

Other features:

- Proprietary computer code.

#### 5.3.1.11 **Jasper and Church [119], Chuang [120] - Monohulls**

Strengths:

- Considers overall hull geometry.
- Considers idealized and more simplified sea state definitions.
- Computer code available in the literature.

Weaknesses:

- Limited application and correlation to tests.
- Local pressure not considered.
- Sea state not statistically described.

#### 5.3.1.12 **Zhao and Faltinsen [68]**

Strengths:

- Arbitrary cross-section, including bow-flare forms.
- Simple "similarity" and asymptotic solutions for wedges are available.
- Actual impact velocity time history can be considered.
- Good correlation to limited model experiment and other calculations.

Weaknesses:

- Actual sea state not considered.
- Utilizes only through strip theory (3-D effects not included).

Other features:

- Computer code is proprietary.

5.3.1.13 **Mitsubishi Heavy Industries (Toki et al [135])**

Strengths:

- Arbitrary cross-section of actual ship hull.
- Considers arbitrary sea state and wave directions.
- Effect of ship speed is included.

Weaknesses:

- Local pressure not considered.
- Poor correlation with stress measurements in deck.

Other features:

- Computer code is proprietary

5.3.1.14 **Aksu et al [132]**

Strengths:

- Arbitrary cross-section of actual ship hull.
- Considers arbitrary sea state and wave directions.
- Effect of ship speed is included.
- 3-D effects are considered in ship motions and slamming pressure predictions.

Weaknesses:

- More extensive comparisons with model and full scale are needed.

Other features:

- Computer code is proprietary.

### 5.3.2 Wave Slap

#### 5.3.2.1 Garcia [168] Breakwater Models - All

Strengths:

- Based on significant tests and model test correlation.
- Simple formulas for estimation provided.

Weaknesses:

- Developed for breakwaters.
- Does not explicitly consider forward speed.

#### 5.3.2.2 U.S. Federal Aviation Administration [42]

Strengths:

- An established official procedure
- Simple, engineering-oriented procedure

Weaknesses:

- Only for seaplanes.
- Does not consider waves.

Other features:

- Design loads method includes margin of safety factors.

#### 5.3.2.3 U.S. Navy [210] - All

Strengths:

- Extensive historical use in design applications.
- Pressure directly provided.

Weaknesses:

- Does not explicitly consider forward speed.

#### 5.3.2.4 SNAME [3] Scaled Models - All
See Section 5.3.1.5

### 5.3.3 Frontal Impact

#### 5.3.3.1 Troesch and Kang [5] - Monohulls/Bow Flare

Strengths:

- Considers significant aspects of 3-D problem.

Weaknesses:

- Limited application to ship hull forms and comparison to tests.
- Over-predicts experimental results.
- Does not consider sea conditions or vessel forward speed.
- Most likely significant computation capacity and time required for the 3-D approach.

Other features:

- Computer code is proprietary.

#### 5.3.3.2 Kaplan and Sargent [125] - Monohulls/Bow Flare

Strengths:

- Considers overall hull geometry.
- Considers sea conditions.
- Limited but good correlation.

Weaknesses:

- Limited application.
- Local pressure not determined.

Other features:

- Computer code is proprietary.

#### 5.3.3.3 Jasper and Church [119] and Chuang [120]
**See Section 5.3.1.10**

#### 5.3.3.4 Gran et al [126]

Strengths:

- Incorporates 2-D boundary value problem.
- Considers hull geometry.
- Sea conditions introduced in relative velocity.
- Simple formulas.

Weaknesses:

- Needs to be integrated into a seakeeping simulation for computation of instantaneous force integrated over ship length.
- Computer code proprietary.
- Local pressures not available.

#### 5.3.3.5 U.S. Federal Aviation Administration [42]

Strengths:

- An established official procedure.
- Simple, engineer-oriented procedure.

Weaknesses:

- Only for seaplanes.
- Does not consider waves.

Other features:

- Design loads method includes margin of safety factors.

#### 5.3.3.6 SNAME [3] Scaled Models - All
**See Section 5.3.1.5**

# 6. EXAMPLE CALCULATIONS

## 6.1 General

Sections 4 and 5 of this report have considered several analysis techniques on their own basis. Herein an attempt is made to consider the results of each when applied to specific examples.

As there are a significant number of techniques and some are available only in proprietary and/or lengthy computer based techniques which cannot be exercised as part of this study, a more common basis of comparison is necessary. As a result, for each of the hydrodynamic phenomena considered, a base approach for comparison has been identified. Example calculations are then performed utilizing this base technique for examples cited in other techniques and the results compared.

## 6.2 Pressure

Due to lack of computer codes in the public domain, detailed information about the techniques used, geometry, and impact velocity time history, the results regarding the 2-D and 3-D nonlinear unsteady theories cannot be obtained for cases not analyzed by the authors of these methods. For this reason only examples with simple geometries (wedge, circle, sphere, etc.) and impact calculations performed by the main contributors are discussed in this Section. As a rule, the approaches of von Karman [32], Wagner [33], Stavovy-Chuang [117], Ochi-Motter [28] and Zhao-Faltinsen [68] can be applied to all cases represented. Table 6-1 summarizes the techniques used for comparisons.

A number of investigators have utilized the pressure-velocity relationship with the factor $k_1$ as a means to evaluate the effects of slamming. As the velocity for impact can be approximated from the description of the slamming event, it has been decided that a comparison on the basis of the $k_1$ factor may be the most realistic and tangible common denominator. Stavovy and Chuang [117] have already carried out some comparisons as shown in Figure 3-35. The estimated results of others are shown in Figures 6-1 through 6-5 for the maximum pressure coefficient Cpmax:

$$C_{pmax} = p_{max}/0.5\rho V^2$$

The sections 6.2.1-6.2.4 correspond to calm water, and case 6.2.5 to a seaway.

### 6.2.1 Wedge

The comparison of maximum pressure coefficient for wedge shaped 2-D sections is shown in Figure 6-1 for different deadrise angles. The classical solutions of von Karman [32] and Wagner [33] are presented along with the "universal' approximation of

| Analysis Technique | Body | Short Solution Description |
|---|---|---|
| von Karman [32] | wedge, circle, parabola, bow flare section | 2-D theory based on momentum consideration |
| Wagner [33] | wedge, circle parabola; bow flare section | 2-D theory taking into account real wetted area; calm water |
| Armand and Cointe [43] | circle | 2-D theory based on the method of method of asymptotic expansions; calm water |
| Stavovy and Chuang [117] | wedge, circle, parabola; bow flare section | approximation of pressure-impact velocity relationship valid for 2-D 3-D bodies; calm and wave surface |
| Ochi and Motter [28] | wedge, circle, parabola; bow flare section; bow section | approximation of pressure-impact velocity relationship valid for ship hulls; calm and wave surface |
| Zhao and Faltinsen [68]: similarity solution | wedge | numerical nonlinear procedure applied to a wedge with arbitrary deadrise angle |
| boundary element | wedge; bow flare section | numerical nonlinear unsteady procedure valid for 2-D entry problem |
| SNAME method [3] | wedge, circle parabola, bow flare section | approximation of pressure-impact relationship, valid for ship hull |
| Garcia [168] | breakwaters | approximation of pressure-impact relationship on breakwaters based on tests. |
| U.S. Navy [210] | all ship sections | pressures for wave slap. |

**Table 6-1 Analysis Techniques - Pressure**

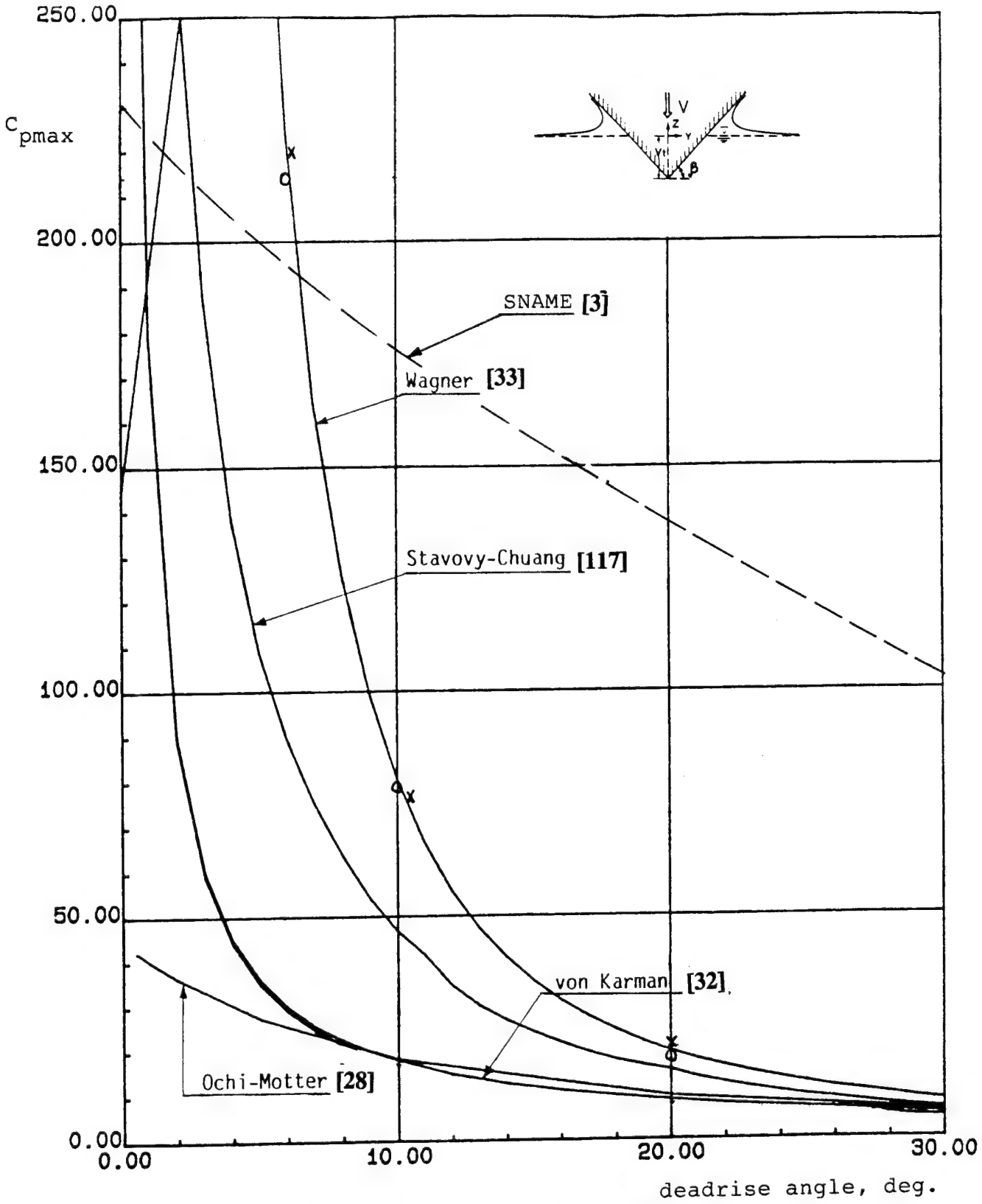


o Zhao Faltinsen (Similarity Solution) [68]
x Zhao-Faltinsen (Boundary Element Solution) [68]

**Fig. 6-1. Comparison of Maximum Pressure Coefficient for Wedge Shaped Sections as Determined by Various Methods**

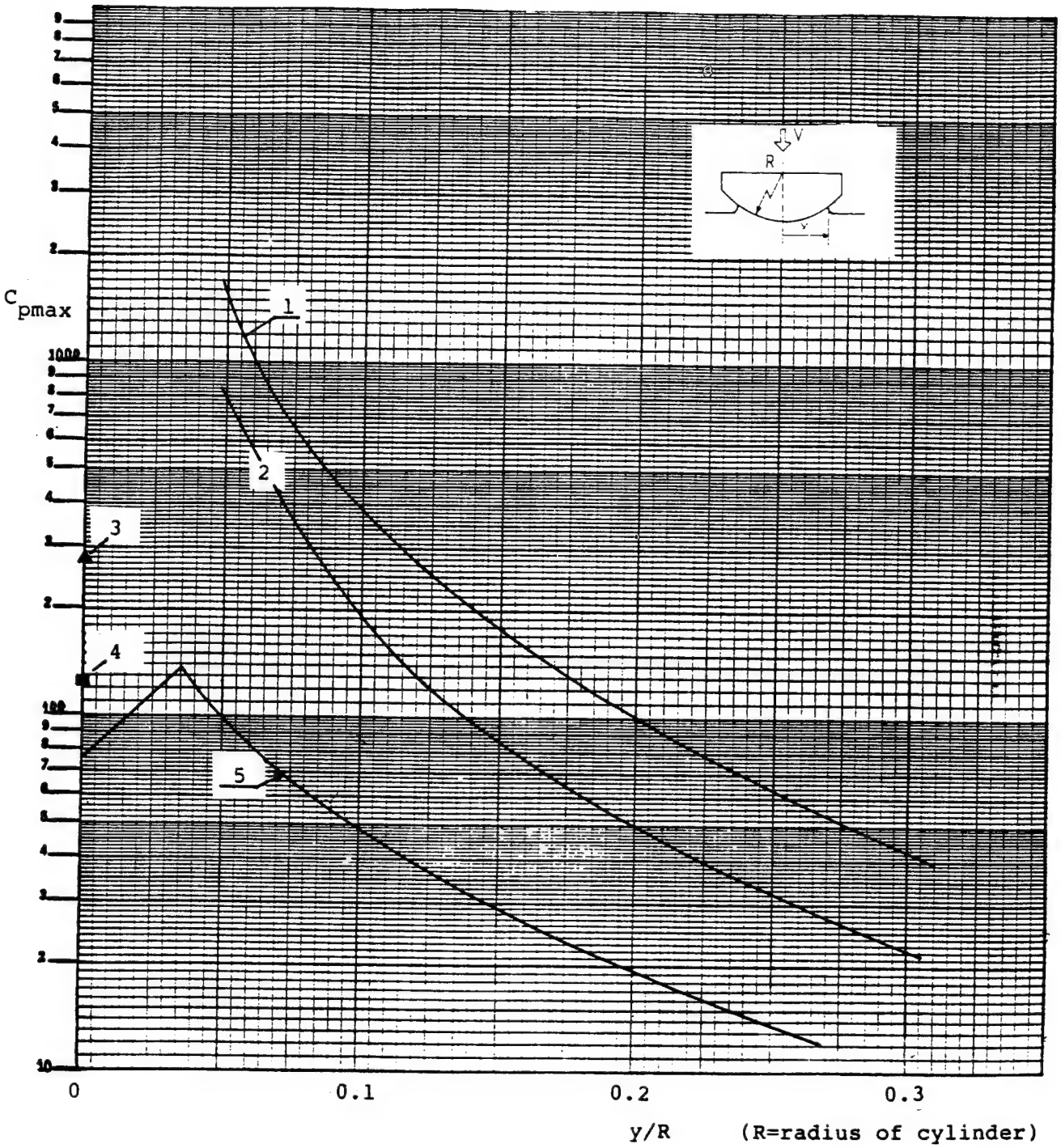


1 Wagner [33], Armand and Cointe [43]
2 von Karman [32]
3 SNAME [3]
4 Ochi and Motter [29]
5 Stavovy and Chuang [117]

**Fig. 6-2. Comparison of Maximum Pressure Coefficient for Circular Cylinder Section as Determined by Various Methods**

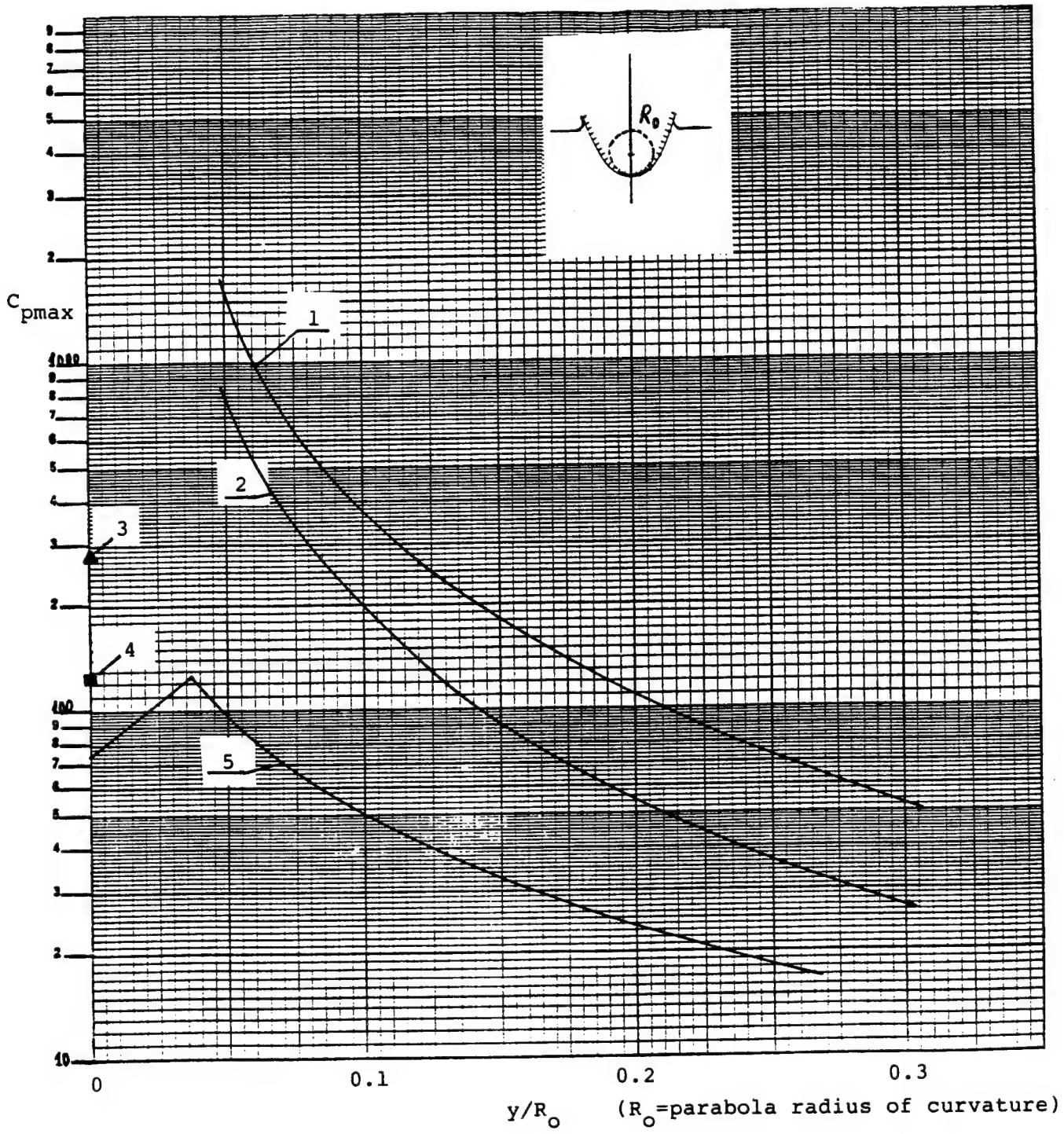


1 Wagner [33]
2 von Karman [32]
3 SNAME [3]
4 Ochi and Motter [28]
5 Stavovey and Chuang [117]

**Fig. 6-3. Comparison of Maximum Pressure Coefficient for Parabolic Section as Determined by Various Methods**

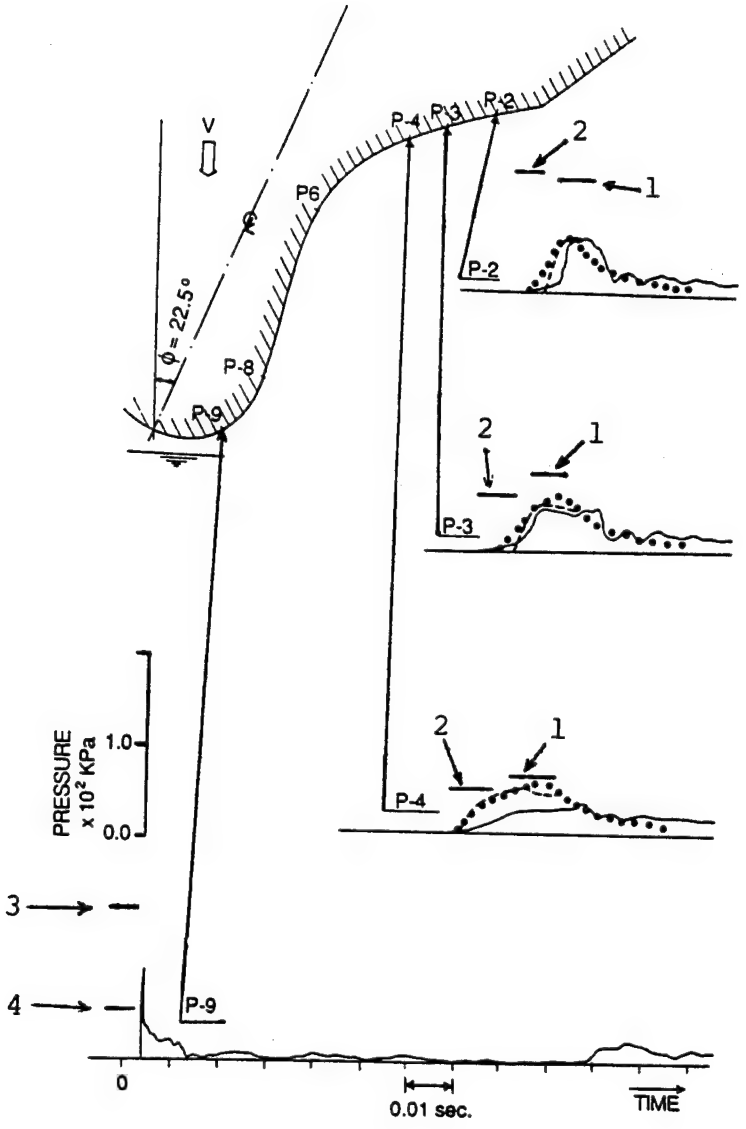


| | | |
|---|---|---|
| ——— | Drop test results by Yamamoto, et al [176] | |
| — — — | Zhao and Faltinsen [68] | } Calculations |
| • | Arai and Matsunaga [105] | |
| 1 | Stavovy and Chuang [117] | |
| 2 | von Karman [32] | |
| 3 | SNAME [3] | |
| 4 | Ochi and Motter [28] | |

**Fig. 6-4. Comparisons Between Numerical and Experimental Pressure Measurements on Bow Flare Section**

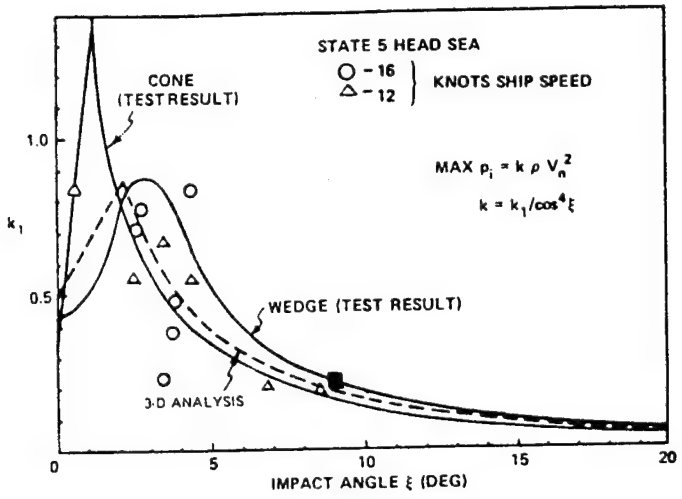


Note: $K_1$ Values Proposed by Stavovy and Chuang [117] (- - -), and Obtained From Ochi and Motter Data (■)

**Fig. 6-5. Comparison of Calculated $K_1$ Values Obtained from Different Model and Full Scale Tests**

Stavovy-Chuang [117] and other data. The difference between von Karman's and Wagner's solutions is due to correction on wetted surface length. It is known that the actual waterline width is $\sqrt{2}$ times larger than the undisturbed waterline used by von Karman. The Zhao-Faltinsen solutions [68] are reasonably close to Wagner's solution, as was indicated earlier (see Fig. 3-13). The SNAME method [3] gives moderate values for small deadrise angles and greater values for large ones.

### 6.2.2 Circle

The widely discussed case of impact of the circular cylinder is analyzed in Figure 6-2. Again the difference between von Karman's and Wagner's solutions is well pronounced. The Stavovy-Chuang method [117] exhibits conservative behavior, as well as the Ochi-Motter and SNAME methods. It should be pointed out that latter two give only maximum pressure for the initial stage of slamming.

### 6.2.3 Parabola

This 2-D form is similar to a U-shaped cross-section of a ship's hull. As a result, the methods of Stavovy-Chuang, Ochi-Motter and SNAME give close values for the maximum pressure coefficient, Figure 6-3. The von Karman and Wagner solutions overpredict the slam pressure coefficient. To allow for an easier comparison with the circle case, independent variable was constructed on the basis of parabola radius of curvature. Indeed, the curves for small y/R values are almost the same as in Figure 6-2.

### 6.2.4 Bow Flare Section

Zhao and Faltinsen presented the results of numerical modeling of impact of the bow flare 2-D section [68]. The comparison between numerical and experimental pressure measurements are shown in Figure 6-4. Reasonable agreement between test results, numerical data and the Stavovy-Chuang method is evident. The other techniques also give good results. However, a significant overestimation by the SNAME method for slamming pressure is seen (gauge P-9).

### 6.2.5 Hull Section

Consider a comparison of the experimental data presented by Ochi and Motter [28] and the results of prediction by the Stavovy-Chuang technique [117]. This case was chosen because it corresponds to a seaway. The example of "reverse" calculations was performed to determine coefficient $k_1$ for pressures used in the Stavovy-Chuang method. All steps are summarized in Table 6-2. The calculations use experimental data on pressure pick (identifier PIC) as an input information along with the geometry of ship and her kinematic parameters of motion. The result, coefficient $k_1$, is shown in Figure 6-5 (black square). As it can be seen from the last two lines of Table 6-2 and Figure 6-5, the agreement is relatively good.

Pressures due to wave slap can be determined from Garcia [168] and the U.S. Navy [210]. A comparison of allowable pressures specified by the U.S. Navy Structural Design Manual [210] and those predicted by Garcia's method [168] shows that the latter are significantly larger. It is believed the reason is that Equation (3-64) corresponds to total breaking and reflecting of waves on a wall mounted on the sea bottom. In the case of a ship only a portion of the wave is involved and the water particles can also move under the ship hull so wave diffraction and reflection are not complete as in wavebreaking wall.

## 6.3 Forces

There are two general approaches to calculate transient force acting at any section of a ship hull: (1) integrating the corresponding component of impact pressure around the section profile; (2) by using the momentum law. In the first case maximum impact pressure can be evaluated on the basis of data from Section 6.2. The pressure distribution functions for slamming, frontal impact, and for wave slap, are described in Chapter 3.

All techniques with force data available are listed in Table 6-3. Other procedures (Kaplan [102], Kaplan and Sargent [125], Jasper and Church [119], Bishop and Price [29], Federal Aviation Administration [42]) use the momentum approach and hence coincide with von Karman's theory [32] or lie between von Karman's and Wagner's theory. The problems analyzed include the impact of a wedge, Figure 6-6, circle Figure 6-7, a sphere Figure 6-8, and a cylindrical body Figure 6-9. In all examples the water was calm.

### 6.3.1 Wedge

A comparison between theoretical values of slam force coefficient of a wedge is presented in Figure 6-6. The value of Vt has been chosen as a dimensional parameter of length. The impact force itself is proportional to the time variable and equal to zero at $t=0$. The data gained by Wagner's solution and Zhao-Faltinsen's techniques are sufficiently close. At the same time Gran's theory underestimates most of the data.

### 6.3.2 Circle

The results of calculations and experiments for the well-known problem of the circle impacting on calm water is shown in Figure 6-7. According to the data presented, the experimental and theoretical results corresponding to the initial stage of impact lie between von Karman's and Wagner's solutions. For $Vt/R=0.1...0.2$ the experimental results lie between Armand & Cointe's solution and Gran's approach. It should be noted that the experimental slam force coefficient at $t=0$ equals zero, due to effects not included in the theoretical models. Armand and Cointe's technique based on the matched asymptotic expansions method demonstrates that Wagner's wetting correction is indeed valid at the instant of impact, but additional terms are required for later time and larger depths. The effect of these phenomena are seen in Figure 6-7.

### 6.3.3 Sphere

In addition to the Figure 3-17, Figure 6-8 illustrates the differences between the approaches in the problem of a sphere impact on calm water. Surprisingly good results for the very initial impact stage is provided by the von Karman theory [32], combined with the strip theory technique. Note that strip theory and nonlinear 2-D numerical modeling give worse results. For this comparison the only one value of von Karman's solution for force coefficient was used (@t=0). The numerical 3-D solution obtained by Troesch and Kang [5] is in good agreement with experiment for the range $0<z/R<0.2$ (z=vertical coordinate of the point at a bottom of the sphere).

| | | | | |
|---|---|---|---|---|
| IMPACT PRESSURE FROM DATA, PIC = | | | 83.09 PSI | |
| Vh = | 7.4 kts | 12.50 ft/sec | | |
| Vv = | | 5.97 ft/sec | | |
| Sea State | | | 7 | |
| WAVE HEIGHT, H = | | | 20 ft | |
| WAVE LENGTH, Lw = | | | 400 ft | |
| WAVE NUMBER, K = 2*pi/Lw | | | 0.016 | |
| MAX. WAVE SLOPE, (THETA)max = Kh = | | | 0.157 | |
| percent y = | | | 0 % | |
| DEADRISE ANGLE, B = | | | 0 deg = | 0 rad |
| TRIM ANGLE, T = | | | 0 deg = | 0 rad |
| BUTTOCK ANGLE, AL = | | | 0 deg = | 0 rad |
| SLOPE, WS = [360*H/(2*Lw)]*COS(2*@pi*y) = | | | 9 deg = | 0.157079 rad |
| TBEH = TAN(B)/(SIN(T-WS)+TAN(AL)*COS(T-WS))= | | | | 0 |
| TBEV = TAN(B)/(COS(T-WS)-TAN(AL)*SIN(T-WS))= | | | | 0 |
| BehO, BEHO = | | | 0 deg | 0 rad |
| SIN(T-WS)+TAN(AL)*COS(T-WS) = | | | | -0.156 |
| beh, BEH = | | | 180 deg = | 3.142 rad |
| bev, BEV = | | | 0 deg = | 0.000 rad |
| TXI = COS(BEH)*TAN(T+AL-WS)+SIN(BEH)*TAN(BEV) = | | | | 0.158 |
| IMPACT ANGLE, XI = | | | 9 deg = | 0.157 rad |
| Vw, VW - 2.26&SQRT(WL) | | | 45.20 ft/sec | |
| Von, VON - Vw*sin(WS) | | | 7.07 ft/sec | |
| Vo - K*H*Vw/2 | | | 7.10 ft/sec | |
| VOT = SQRT(VO 2-VON 2) | | | 0.64 ft/sec | |
| SIN (2*PI*Y) | | | 0.00 | |
| VOT - VOT, if sin(2pi*Y) ⟨0 | | | 0.64 ft/sec | |
| VHW = VH*COS(WS)-VV*SIN(WS)-VOT | | | 10.77 ft/sec | |
| VVW = VH*SIN(WS)+VV*COS(WS)+VON | | | 14.92 ft/sec | |
| VNS = VHW*COS(BEH)*SIN(XI)+VVW*COS(XI) | | | 13.05 ft/sec | |
| VN = VNS*COS (XI) | | | 14.74 ft/sec | |
| VT = VNS*SIN (XI) | | | 2.33 ft/sec | |
| c = PIC/(1.94*VN 2) | | | 0.23 | |
| c1 = k*(COS(XI)) 4 | | | 0.22 | |
| c1 = (from Stavovy-Chuang) | | | 0.20 | |

Notes:
1. For definitions see Figure 4-7.
2. WL = $L_w$ = wave length, ft.
3. VW = $V_w$ = $(g/K)^{1/2}$ = wave celerity

**Table 6-2. Comparison of the pressure coefficient $k_1$ found from experimental data of Ochi & Motter (Ref. 28) and proposed by Stavovy & Chuang (Ref. 117).**

| Analysis Technique | Body | Short Solution Description |
|---|---|---|
| von Karman [32] | wedge, circle, sphere *, cylindrical body * | 2-D theory based on momentum considerations |
| Wagner [33] | wedge, circle, sphere *, cylindrical body * | 2-D theory taking into account account real wetted area; calm water |
| Armand and Cointe [43] | circle | 2-D theory based on the method of asymptotic expansions; calm water |
| Zhao and Faltinsen [68]: similarity solution | wedge | numerical nonlinear procedure applied to a wedge with arbitrary deadrise angle |
| boundary element solution | wedge | numerical nonlinear unsteady procedure valid for 2-D entry problem |
| Troesch and Kang [5] | sphere; cylindrical body | numerical nonlinear unsteady procedure valid for 2-D and 3-D entry problem |
| Gran, et al [64] | wedge, circle | 2-D approach based on quasi-steady consideration of fluid momentum |

* 2-D solution applied to 3-D problem through the strip theory.

**Table 6-3. Analysis Techniques - Forces**

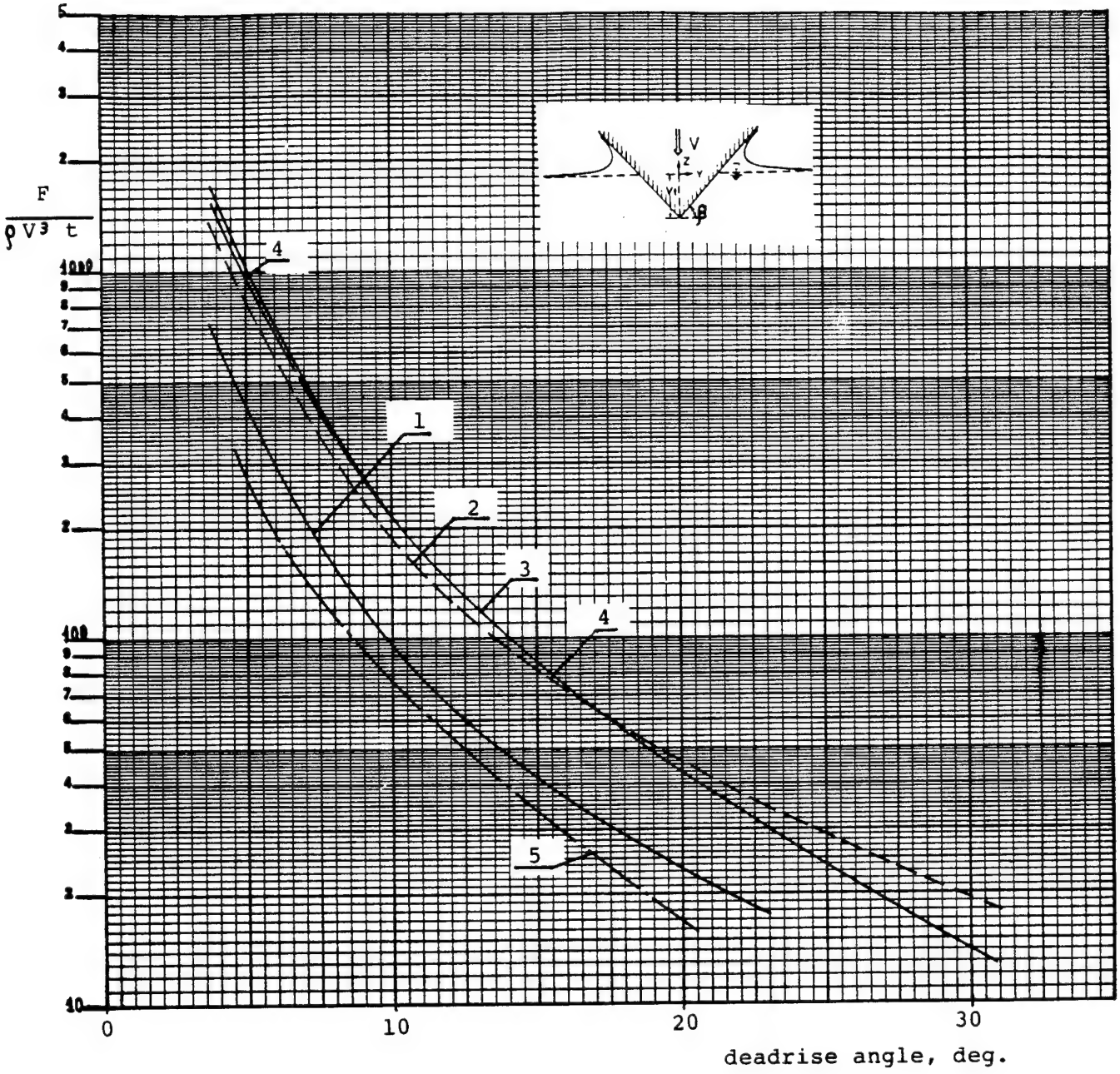


t= time variable with t=0 corresponding to initial time of impact
1 von Karman [32]
2 Wagner [33]
3 Zhao and Faltinsen (similarity solution) [68]
4 Zhao and Faltinsen (boundary element solution) [68]
5 Gran, et al [64]

**Fig. 6-6. Comparison Between Theoretical Values of Slam Force Coefficient of a Wedge Moving with Constant Downward Velocity V**

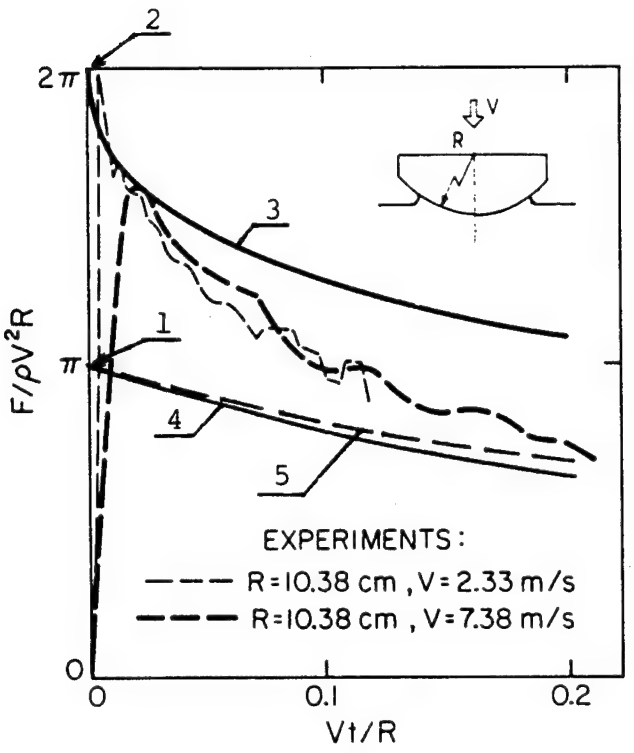


t= time variable with t=0 corresponding to initial time of impact

— —
— — experiments [43]

1 von Karman [32]
2 Wagner [33]
3 Armand and Cointe [43]
4 Gran [64]
5 Faltinsen [4]

**Fig. 6-7. Comparison Between Experimental and Theoretical Values of Slam Force Coefficient During Entry of a Circular Cylinder with Constant Downward Velocity V**

### 6.3.4 Cylindrical Body

The good agreement between experimental data and results of calculations for the cylindrical body with length-width-draft ratio 2:1:0.5 [3] is shown in Figure 6-9. For this ship hull-like body von Karman's solution plus strip theory illustrate excellent results for the maximum slam force coefficient. The force time history is predicted by the theoretical approaches very well. As in the previous case, Wagner's solution applied with strip theory overestimates the slam force coefficient at the instant of impact t=0. This is due to increased wetted area.

## 6.4 Bending Moment

The comparison between two theories based on the momentum consideration approach to bottom slamming is shown in Figure 6-10 for the ship WOLVERINE STATE in light loading. The first method developed in Russia [157], [159], uses semi-empirical formula described in Section 3.2.4.2 (formula (3-46)). Second one is developed by Kaplan and Sargent [99]. The bending moment in this method is a result of numerical simulation on analogue computer. One can see reasonable agreement with slight overprediction by Russian technique. It should be noted that these methods use different procedures for the prediction of ship motions.

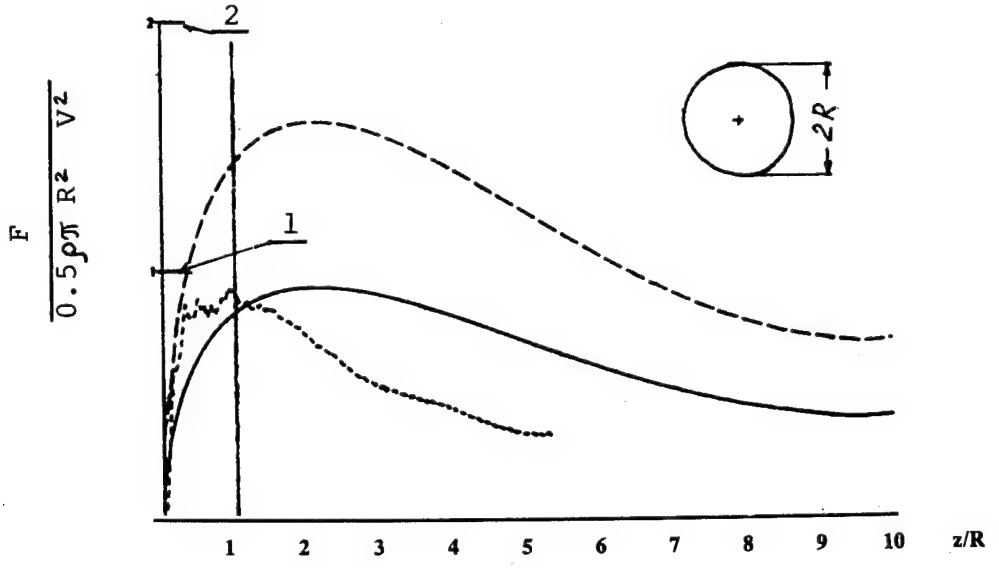


..... experiment, Troesch and Kang [210]
——— 3-D nonlinear theory, Troesch and Kang [3]
— — strip theory + 2-D nonlinear theory, Troesch and Kang [3]
1 strip theory + von Karman approach for a cylinder
2 strip theory + Wagner approach for a cylinder

**Fig. 6-8. Experimental and Theoretical Comparison of the Vertical Slam Cofficient for a Sphere**

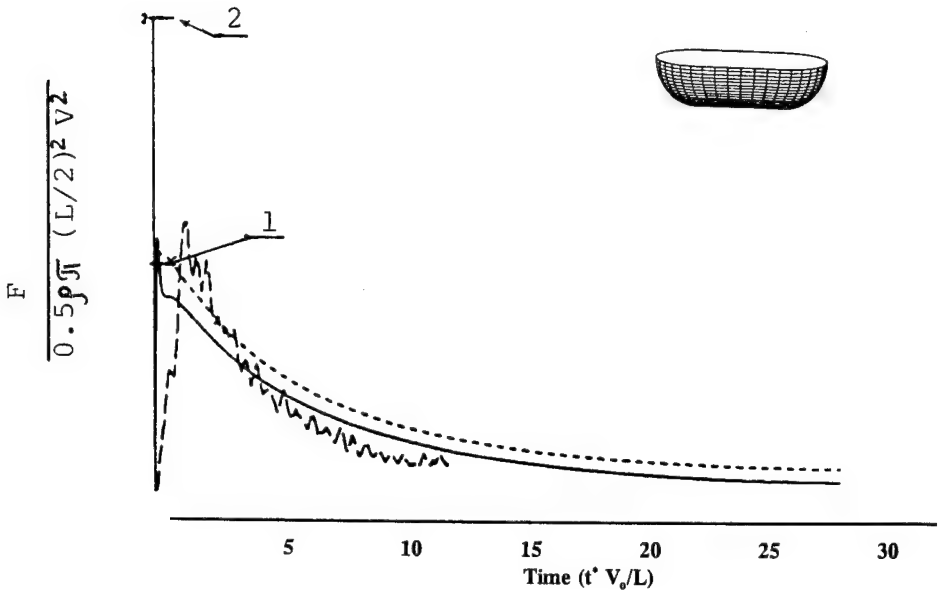


— — experiment, Troesch and Kang [214]
——— 3-D nonlinear theory, Troesch and Kang [5]
- - - - - strip theory + 2-D nonlinear theory, Troesch and Kang [5]
1 strip theory + von Karman approach for a cylinder
2 strip theory + Wagner approach for a cylinder

**Fig. 6-9. Experimental and Theoretical Comparison of the Vertical Slam Coefficient for a Cylindrical Body With L/B=2 [5]**

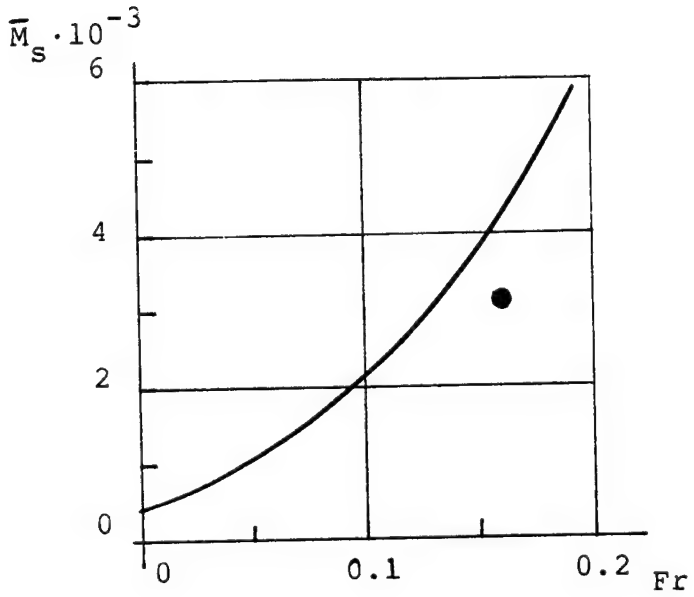


State State = 7, $h_{1/3}$ = 39 ft, Head Seas

——— Boytsov and Paliy [96], [98]

• Kaplan and Sargent [125]

**Fig. 6-10 Comparison of Theoretical Results for Bending Moments Amidship Due to Bottom Slamming of the Ship WOLVERINE STATE**

# 7. CONCLUSIONS

The results of the survey and assessment reported herein suggest the following conclusions:

- The phenomena of hydrodynamic impact are still not completely understood. More design guidance as to how these phenomena should be avoided from an operational perspective, or how their dangerous load effects should properly be repelled or absorbed in the structural design, would be extremely useful.

- In the investigation of structural systems, information on pressure, force and their spatial distribution is necessary.

- Model and full scale test results remain the most reliable source of information on pressures and forces induced by the ship hull impacting on the disturbed sea surface.

- The most accurate theoretical pressure distribution and time history can be obtained by using numerical nonlinear unsteady methods. At this time they are developed only for the case of calm water. Most of them solve the 2-D problems (Zhao and Faltinsen [175], Arai and Matsunaga [106]) and only one "exact" method is available for solution of the 3-D impact problem (Troesch and Kang [58]).

- An engineering approach for predicting impact loads can be based on simpler theories and/or semi-empirical relationships. For example, the maximum impact pressure can be satisfactorily predicted by the Stavovy-Chuang method [117], based on the generalization of 2-D and 3-D solutions, as well as experimental data obtained for ship hulls. The SNAME technique [3] and Ochi-Motter method [28] are also good for this purpose. Stavovy-Chuang's technique is most powerful because of its ability to address a variety of hull forms and sea conditions.

- In spite of rapid development of sophisticated numerical methods and codes used for modeling of the 3-D impact problem, the well known and commonly used strip theory combined with simple 2-D momentum theories (for example, von Karman [32]) remains a good source of reasonable data for impact force prediction, especially in slamming problems. Indeed, the usual quantities of interest are global hydrodynamic forces or bending moments and shear forces near the middle of the hull. These forces and moments are typically insensitive to the end effects where strip theory approximations are less valid. Frontal or bow flare impact and the resulting primary structural loads occur in areas of rapid longitudinal curvature of hull lines. The applicability of strip theory in these calculations is questionable.

- Wave slap can still only be addressed by rules for pressures which may be experienced at various locations of the hull.

- Further improvements of theoretical approaches are needed to reduce discrepancies between numerical techniques and experimental data. Some of them will be discussed in the next Section.

- Hydrodynamic impact theories and numerical fluid dynamics in general are expanding at a rapid rate. Concurrently computer technology is expanding and proliferating as well, allowing ever more complex computations to be realistically carried out. As time moves on it will be important to cross-correlate the approaches on the forefront of technology with requirements of engineering practitioners.

- A number of the potential hydrodynamic models of the future will relate to pressure. It will be important to have available structural models which will transmit the loads throughout the ship to develop proper shear and bending moments.

# 8. RECOMMENDATIONS FOR FUTURE RESEARCH

## 8.1 General

In the design of reliable and cost/weight effective ship structures operating in harsh environments, the prediction of hydrodynamic impact loadings plays an important role. As a result, in one context a structural engineer can feel the need to apply high precision prediction techniques for impact forces. This, of course, requires the availability of advanced numerical and experimental approaches, use of powerful computers, sophisticated algorithms, and software. At the same time, the reliability of complex engineering structures depends on a variety of other loadings and many factors, for example: material properties, margins of safety, and some parameters having a random nature. In this context the structural engineer must consider a myriad of analyses and needs some reasonable trade-off between time-consuming computerized "exact" (nonlinear, unsteady, and so on) solutions and simpler analytical formulas (e.g., von Karman or Wagner for impact) having clear physical meaning but, at the same time, realistic requirements for application within a design spiral. Therefore, the concept of development of an engineering method, consisting of the explicit relationships between governing parameters and proven by extensive analytical, numerical, and experimental studies, can be considered as the most important direction in future research of hydrodynamic impact loadings.

The areas of investigation which will contribute to development of the above-mentioned engineering method can be subdivided into three programs:

- Near-term program which covers years 1-2 of investigation and application of known techniques in design practice;

- Mid-term program which covers years 2-4, dedicated to improvement of existing analytical methods and approaches to make possible their application as design procedures;

- Long-term program covering the period beyond 4 years, consisting of R&D of advanced sophisticated numerical techniques without necessarily an immediate engineering application.

## 8.2 Near-term Program

During the near-term program attempts should be made to choose the most reliable engineering method from all available and applicable techniques and adjust it, as necessary, for the ship design and analysis purposes.

*Slamming*: The most promising approach for estimation of slamming pressures in actual sea conditions can be based on the Stavovy and Chuang method. The technique of Ochi and Motter also provides satisfactory results. An efficient estimate of maximum pressure can be obtained by using the method of Zhao and Faltinsen

for arbitrary wedge-like forms with any deadrise angle and the Wagner solution for small angles.

The investigation of these procedures and combination into a self-contained computer code applicable to ships is expected to require 2 person-years.

*Wave Slap*: The U.S. Navy method, providing design pressures for various impact surface positions, is believed to be the most reliable and ready-to-use technique for design practice. It enables one to assume wave slap pressures for different structural members. This method is already available although not generally known.

*Frontal Impact*: The bow flare impact force can be predicted by changes in momentum and buoyancy. The Kaplan and Sargent method can be utilized in combination with seakeeping theory to estimate hull girder forces generated by frontal impact loads. The prediction of pressure due to frontal impact can be based on the Stavovy and Chuang method.

The investigation of these procedures including extensive correlation with experimental and full scale results, and combination into a self-contained computer code applicable to ships, is expected to required 2 person-years.

### 8.3 Mid-term Program

This program will deal with further development of advanced modern techniques which have been developed mostly by R&D Centers and Universities. Two approaches are most promising in this context: the 3-D finite element analysis by Troesch and Kang and 2-D finite difference numerical solution by Zhao and Faltinsen. These methods should be developed to take into account actual ship forms (mono- and multi-hulls) and actual sea surface conditions. To suggest application of these numerical techniques in design practice, extensive experimental and full scale verification will be needed, including seakeeping and drop tests, full-scale pressure measurements with precise probes, and adequate correlation with this data.

The above-mentioned methods should equally be useful for *Slamming, Wave Slap, and Frontal Impact* loadings predictions.

The investigation of these procedures and combination into a self-contained computer code application to ships is expected to required 2 to 4 person-years for each of the methods, depending on their current state of development.

### 8.4 Long-term Program

The long-term program will cover many aspects of research activities in areas of modern Marine Hydrodynamics, Numerical Fluid Dynamics, and Computer Science

(especially in parallel and distributed computing). First this program will result in solutions to theoretical and then to practical design problems. These investigations can start in the near future and emphasize development of 3-D non-linear seakeeping predictions and a Euler solver for simulation of *Slamming and Wave Slap* loadings experienced by a ship in rough seas. Successful prediction of *Bow Flare* loads should be obtainable with the development of a Naiver-Stokes equation solver considering viscous flow separation, entrapped air, and compressibility effects.

The investigation of these procedures and combination into a self-contained computer code applicable to ships is expected to be an ongoing process for years to come. A development of the procedures into an engineering approach should be expected to take in the order of 10 person-years, but could be as high as 15 to 20 person-years.

It is also acknowledged that this approach is highly dependent on available computer technology which continues to develop rapidly and will serve to foster these types of analytical procedures.

## 8.5 General Characteristics of Research

- A new advanced 3-D theory and numerical technique should be developed to improve seakeeping predictions (ship motions), wave loads, and nonlinear forces and moments induced by hydrodynamic impact. In this context, the time domain analysis of coupled seakeeping/impact problems via computer simulation is more promising. The continuous development of increased computer capabilities should make it plausible to achieve this in the future which will result in the ability to perform rapid assessment of hydrodynamic loads on different ships for a range of operational and environmental conditions.

- Most of the recently developed numerical techniques assume that the water surface is calm and the ship does not have roll motions. A rigorous solution of the nonlinear unsteady problem with actual free surface is extremely complex; however, it can provide the researcher/engineer with a deeper understanding of the hydrodynamic impact phenomena.

- Methodologies for conventional monohull vessels which show promise should be investigated for possible extension to advanced marine vehicles, including multi-hulls, SES, SWATH, etc.

- More accurate treatment of the free surface, including jet spray, is needed in numerical analysis of the 3-D impact problems, especially in frontal and bow flare impact. This may attenuate the maximum impact force in flared bodies and reduce any overestimation resulting from existing numerical techniques.

- The nonlinear boundary element method is a useful tool for a broad class of hull forms. However, it is necessary in the future to incorporate the effect of flow separation, for instance entrapped air, and compressibility effects (where needed).

- The numerical simulation of slamming should include the actual impact velocity time history. The "added-mass" effect on the slamming pressure due to large retardation typical of a drop test model can result in optimistic slamming predictions.

- The statistical and/or probabilistic nature of hydrodynamic impact loads can be found from the analysis of time histories obtained from extensive model or full scale tests. Similar results can in principle be gained from the results of a series of computer-based Monte Carlo simulation studies.

## 9. REFERENCES


1 MacCutcheon, E.M.; Oakley, O.H.; Stout, R.D.
Ship Structure Committee Long Range Research Plan - Guidelines for Program Development
SSC Report SSC-316
1982

2 Weirnicki, C.J.
Damage of Ship Plating Due to Wave Impact Loads
SNAME, STAR Symp. pp 151
1986, May

3 Notes on Ship Slamming
Society of Naval Architects and Marine Engineers
SNAME Technical and Research Bulletin 2-30.
1993, May

4 Faltinsen, O.M.
Sea Loads on Ships and Offshore Structures
Cambridge University Press, 328 pp
1990

5 Troesch, A.W.; Kang, C.G.
Bow Impact Loads Including Effects of Flare
Final Report
UM Rpt for MarAd, Rept. No. MA-RD-840-88037, MTIF-03/8451
1991

6 Hughes, O.F.
Ship Structural Design
John Wiley and Sons
1983

7 Surface-Effect Ships
Report of Committee V.4
12th International Ship and Offshore Structures Congress, Canada
1994

8 Kaplan, P.; Dalzell, J.F.
Hydrodynamic Loads Prediction (Including Slamming) and Relation to Structural Reliability
Ship Structures Symposium, Arlington
1993, November

9 Szebehely, V.G.; Todd, M.A.
Ship Slamming in Head Seas
DTMB, Rpt. No. 913
1955, February

10 Akita, Y.; Ochi, M.K.
Investigations on the Strength of Ships Going in Waves
By Model Experiments
JZK Rpts 1-3, No. 95, 96, 97; or SNAME
1965

11 Ochi, M.K.
Model Experiments on Ship Strength and Slamming
in Regular Waves
SNAME, Transactions, Vol 66, pp 345-383
1958

12 Ochi, M.K.
Extreme Behavior of a Ship in Rough Seas - Slamming and
Shipping Green Water
SNAME, Transactions, Vol. 72
1964

13 Ochi, M.K.
Experiments on the Effect of Bow Form on Ship Slamming
DTMB, Report 1400
1962

14 Lehman, G.
Bodenschaden in Vorschiff under die Neuen Vorschriften
der Klassifications
Schiffahrt und Hafenbau, 37
1936, April

15 SNAJ
Report on the Investigation Committee on Damage of
Diesel Ships due to Slamming
Society of Naval KArchitects of Japan
1936

16 Dillon, E.S.; Lewis, E.V.
Ships with Bulbous Bows in Smooth Water and in Waves
Report S-1, SNAME T&R Symposium
1967, October

17 Ochi, M.K.
Performance of Two Hull Forms (U & V) in Irregular Waves
SNAME, Report S-1, T&R Symposium
1967

18 Lacey, P.; Edwards, R.
ARCO Tanker Slamming Study
Marine Technology, Vol. 30, No. 3
1993, July

19 Matveev, G.A.; et al
Results of Full Scale Tests of the "Krim" Class Tankers
Krylov Research Institute, Leningrad
1974

20 Vulovich, KR.; Harayama, T.; et al.
Characteristics of Hull Stresses Measured on a Large
Containership in Rough Seas
Transactions of the SNAME, Vol 97, 1989, BMT-90040786
1989, November

21 Beck, R.F.
Motions in Waves
Principles of Naval Architecture, 2nd Rev., SNAME, Vol III
1988

22 8th Int. Ship Structures Congress
1982

23 9th Int. Ship Structures Congress
1985

24 11th International Ship and Offshore Structures Congress
Report of Committee II.2, "Dynamic Load Effects", China
1991

25 Environmental Forces
Report of Committee of 10th International Ship Structures
Congress, Denmark
1988

26 Schlachter, G.
Hull Girder Loads in a Seaway Including Non-Linear Effects
Marintechnik, GmbH, Hamburg, Germany, Schiffstechnik, Vol. 36
1989, H.4

27 Mansour, A.E.; D'Oliveira, J.M.
Hull Bending Moment Due to Ship Bottom Slamming
in Regular Waves
SNAME, JSR, Vol. 19, No. 2
1975, June

28 Ochi, M.K.; Motter, L.E.
Prediction of Slamming Characteristics and Hull Responses
for Ship Design
SNAME, Transactions
1973

29 Bishop, R.E.D.; Price, W.G.
Hydroelasticity of Ships
U.K. Cambridge University Press
1979

30 Hansen, P.F.
On Combination of Slamming- and Wave-Induced Responses
Journal of Ship Research, Vol. 38, N 2
1994, June

30a Melville, W.K. and Chan, E.S.
Personal Communication, April, 1984,
as referenced in [2].

31 Green, T.
Wave Forces on Vertical Walls. An Overview of Recent Work
with Annotated Bibliography
University of Wisconsin
1989, June

31a Kawakami, M.
"On the Impact Strength of Ships Due to Shipping Green Seas-
Towing Experiments of a Ship Model in Regular Waves"
Selected Papers from the Journal of the Society of Naval
Architects of Japan, Vol. 8, pp. 1-16
1971

32 Von Karman, T.
The Impact on Seaplane Floats During Landing
NACA, Tech Note 321, SITDL TR 1854
1929, October

33 Wagner, H.
Landing of Sea Planes
NACA Tech. Memo 622, SITDL TR 2101
1931, May

34 Sedov, L.I.
Two-Dimensional Problems in Hydrodynamics and Aerodynamics
Interscience
1965

35 Fritts, M.; Comstock, E.; Lin, W.C.; Salvesen, N.
Hydro-Numeric Design: Performance Prediction and
Impact on Hull Design
SNAME Transactions, Vol. 98
1990

36 Hutchinson, B.
Seakeeping Studies: A Status Report
Transactions of the SNAME, Vol. 98
1990

37 Wang, X.D.; Huang, Z.J.; Hsiung, C.C.
Application of the Flux Vector Splitting Method to Capture
Shock Waves and Calculate Pressure in Ship Slamming
20th Symposium on Naval Hydrodynamics, Santa Barbara
1994, August

38 Maskew, B.
A Nonlinear Numerical Method for Transient Wave/Hull Problems
on Arbitrary Vessels
SNAME Transactions, Vol. 99
1991

39 Newman, J.N.
The Numerical Towing Tank - Fact or Fiction?
Schiffstechnik, Vol. 36, H.4
1989

40 Von Karman, T.
Calculation of the Pressure Distribution on Airship Hulls
U.S. Experimental Model Basin (DTMB), SITDL, TR 1856
1930, March

41 Wagner, H.
Uber Stross-und Gleitvorgange an der Oberflasche
von Flussigkeiten
ZAMM, Vol. 12, No. 4
1932

42 United States Government
Code of Federal Regulations, Title 14, Chapter 1, Federal
Aviation Administration
CFR 14, Part 25, pp. 263-267, 1980;
pp. 321-326, 1993

43 Armand, J.L.; Cointe, R.
Hydrodynamic Impact Analysis of a Circular Cylinder
5th OMAE Symp. Proceedings, Tokyo, Japan
1986

44 Hillman, A.
Vertical Impact on a Water Surface By a 60 Degree Cone
Math Tables Project, N.Y. University
1946

45 Chu, W.; Abramson, H.N.
Hydrodynamic Theories of Ship Slamming - Review and Extension
SNAME, JSR, Vol. 4, No. 4, PP-9-21, SWRI, San Antonio, Texas
1961, March

46 Henry, Jr.; Bailey, KF.C.
Slamming of Ships: A Critical Review of the Current
State of Knowledge
SSC, Rpt. No. 208, Teledyne Materials Research Co. NTIS-AD-711267
1970

47 Milwitzky, B.
A Theoretical Investigation of Hydrodynamic Impact Loads on
Scalloped Bottom Seaplanes and Comparisons with Experient
NACA, Rpt. No. 867
1947

48 Milwitzky, B.
Generalized Theoretical and Experimental Investigation of the
Motions and Hydrodynamic Loads Experienced by V-Bottom Seaplanes
During Step Landing Impacts
NACA, Tn-1516
1948

49 Milwitzky, B.
Generalized Theory for Seaplane Impact
NACA, TR 1103
1952

50 Mayo, W.L.
Analysis and Modification of Theory for Impact of Seaplanes on Water
NACA, TN-1008
1945

51 Mayo, W. L.
Theoretical and Experimental Dynamic Loads for a Prismatic Float
Having an Angle of Deadrise of 22-1/2 Degrees
NACA, Rpt. No. L-5-F-15
1945

52 Bisplinghoff, R.O.; Doherty, C.S.
A Two Dimensional Study of the Impact of Wedges on a Water Surface
MIT, Rpt.
1950

53 Bisplinghoff, R.L., Doherty, C.S.
Some Studies of the Impact of Vee Wedges on a Water Surface
Franklin Institute, Journal, Vol. 253, No. 6, pp 547-61
1952

54 Szebehely, V.G.; Brooks, S.H.
Hydrodynamics of Slamming of Ships
NTMB, Report 823
1952, July

55 Szebehely, V.G.
Hydrodynamic Approach to the Slamming of Ships
2nd Midwestern Conference on Fluid Mechanics, Proceedings
1952

56 Szebehely, V.G.; Todd, M.A.; Lum, S.M.Y.
On Slamming
DTMB, Rpt. 995, European Shipbuilding, Volumd 3-4
1956, January

57 Todd, M.A.
Slamming Due to Pure Pitching Motion
DTMB, Rpt. No. 833
1955

58 Bledsoe, M.D.
Series Investigation of Slamming Pressures
DTMB, Rpt. No. 1043
1956

59 Schnitzer, E.; Hathaway, M.E.
Estimation of Hydrodynamic Impact Loads and Pressure Distributions on Board Approximating Elliptical Cylinder and Special Reference to Water Landings of Helicopters
NACA, Report TN 2889
1953

60 Fabula, A.G.
Some Theoretical Calculations on the Impact of Circular Cylinders on Water
U.S. Naval Ordinance Test Station, China Lake, CA, TRP 111
1955

61 Fabula, A.G.
Ellipse-Fitting Approximation of Two-Dimensional Normal Symmetric Impact of Rigid Bodies on Water
5th Midwestern Conf on Fluid Mechanics, Proceedings, UOFM
1957, April

62 Fabula, A.G.; Ruggles, I.D.
Vertical Broadside Water Impact of Circular Cylinder; Growing Circular Arc Approximation
NAVROD Rpt 4947 (NOTS 1268)
1955

63 Ochi, M.K.; Bledsoe, M.D.
Hydrodynamic Impact with Application to Ship Slamming
4th ONR Symp on Naval Hydrodynamics, Vol. 3
1962

64 Gran, S.; Olsen, H.; Tellsgard, F.
Hull Response to Hydrodynamic Forces on Bow Flare
Det Norske Veritas, Norwegian Maritime Research, No. 3, Vol. 4
1976

65 Greenhow, M.
Wedge Entry Into Initially Calm Water
Applied Ocean Research, Vol. 9, No. 4
1987

66 Greenhow, M.; Lin, W.M.
Numerical Simulation of Nonlinear Free Surface Flows Generated by Wedge Entry and Wavemaker Motions
4th Int'l Conf. Numerical Ship Hydrodynamics, Proceedings, Washington, D.C. NMRC-11-2086-A7 (1991)
1985

67 Yim, B.
Numerical Solution for Two-Dimensional Wedge Slamming with a Nonlinear Free Surface Condition
4th Int'l Conf Numerical Ship Hydrodynamics, Proceedings, Washington, D.C., NMRC-11-2086/A8
1985

68 Zhao, R.; Faltinsen, O.
Water Entry of Two-Dimensional Bodies
Journal of Fluid Mechanics, Vol. 246
1993

69 Korobkin, KA.A.; Puchnachov, V.V.
Initial Stage of Water Impact
Annual Review on Fluid Mechanics, Vol. 20
1988

70 Watanabe, T.
Analytical Expression of Hydrodynamic Impact Pressure by Matched Asymptotic Expansion Technique
Trans. West-Japan Soc. Naval Architect. No. 71
1986

71 Dobrovol'skaya, Z.N.
On Some Problems of Similarity Flow of Fluid With a Free Surface
Journal of Fluid Mechanics, Vol. 36
1969

72 Cointe, R.
Free Surface Flows Close to a Surface-Piercing Body
In "Mathematical Approaches in Hydrodynamics" (ed. T. Miloh), SIAM, Philadelphia
1991

73 Howison, S.D.; Ockendon, J.R.; Wilson, S.K.
Incompressible Water-Entry Problems at Small Deadrise Angles
Journal of Fluid Mechanics, Vol. 222
1991

74 Venkat, N.K.; Spaulding, M.L.
Numerical Simulation of Nonlinear Free-Surface Flows
Generated by a Heaving Body of Arbitrary Cross Section
Journal of Ship Research, Vol. 34, N 2
1990, June

75 Toyama, Y
Two-Dimensional Water Impact of Unsymmetrical Bodies
Journal of the Society of Naval Architects of Japan, Vol. 173
1993

76 Egorov, I.T.
Udar o Schimaemuiu Zhidkost (Impact of a Compressible Fluid)
NACA, TM 1413
1958, February

77 Ogilvie, T.F.
Compressibility Effects on Ship Slamming
Schiffenstechnik, Volume 10, No. 53, pp 147-154
1963

78 Skalak, R.; Feit, D.
Impact on the Surface of a Compressible Fluid
ASME, Paper No. 65-WA/UnT-3, Columbia University Dept. of
Civil Engineering, Tech. Rpt. 31
1965, December

79 Hagiwara, K.; Yuhara, T.
Fundamental Study of Wave Impact Loads on Ship Bow
Selected Papers from the Journal of Soc. Nav. Arch., Japan, Vol. 14
1976

80 Kamel, A.M.
Shock Pressures Caused by Waves Breaking Against Coastal Structures
ACOE, Waterways and Experiment Station, MRIS-054189
1968, September

81 Weinig, F.
Impact of a Vee-Type Seaplane on Water With Reference to Elasticity
NACA, TM 810
1936

82 Meyerhoff, W.K.
Die Berechnung Hydroelasticher Stotze
Schiffstechnik, Volume 12, No. 60, 61
1965

83 Chuang, S.S.
Theoretical Investigation of Dynamic Interaction Between Ship Bottom and Fluid During Slamming
DTNSRDC Report No. 2403
1967, December

84 Sellars, F.H.
Water Impact Loads
SNAME, Chesapeake Section, MRIS-084451 and SNAME Marine Technology
1976, January

85 Shiffman, M.; Spencer, D.C.
The Force of Impact on a Cone Striking a Water Surface
Commun. Pure and Applied Math, Vol. 4
1951

86 Chuang, S.L.
Theoretical Investigation of Slamming of Cone-Shaped Bodies
SNAME, JSR, Vol. 13, No. 4, MRIS
1969, December

87 Miloh, T.
Wave Slam on a Sphere Penetrating a Free Surface
Journal of Engineering Math, Vol. 15, No. 3
1981

88 Ochi, M.K.; Motter, L.E.
Prediction of Extreme Values of Impact Pressures Associated with Ship Slamming
SNAME, JSR, Vol. 13, No. 2, MRIS-015291
1969

89 Yamamoto, Y.; Fujino, M.; Fukasawa, T.
Motion and Longitudinal Strength of a Ship in Head Sea and Effects of Non-Linearities (1st, 2nd, 3rd Reports)
Journal, Society of Naval Architects of Japan,
Vol. 143 (1978), Vol. 144 (1978), Vol. 145 (1979)

90 Belik, O.; Bishop, R.E.D.; Price, W.G.
A Simulation of Ship Responses due to Slamming in Irregular Head Waves
RINA, pp 237-253
1982

91 Oliver, J.C.
Advanced Method for Ship Motion and Wave Load Predictions
Ship Structure Committee Project, SR 1277, Giannotti and Assoc.
1983

92 Kaplan, P.; Silbert, M.N.
Impact Forces on Platform Horizontal Members in the Splash Zone
OTC Paper No. 2498, Houston, TX
1976

93 Sarpkaya, T.; Isaacson, M.
Mechanics of Wave Forces on Offshore Structures
Van Nostrand Reinhold Co., New York
1981

94 Newman, J. N.
Marine Hydrodynamics
The MIT Press, Cambridge, Massachusetts
1977

95 Dynamic Load Effects
Report of Committee of 10th International Ship Structures
Congress, Denmark
1988

96 Rabinovitch, O.N.; Rostovtsev, D.M.; Stepanov, I.V.
A Survey of the Russian/Soviet Studies, Results and Data on
Hydrodynamic Impact Load Estimation in Marine (and Non-Marine)
Structure Design Practice
St. Petersburg State Marine Technical University,
St. Petersburg, Russia
1993

97 Stepanov, I.V.
Principles of the Free Fall Life Boats Design
Ph.D. Thesis, Leningrad Shipbuilding Institute
1988

98 Boytsov, G.V.; Paliy, O.M.
Hull Strength and Structures for Ships of New Types
Leningrad, Sudostroenie Publ. House
1979

99 Chuvikovsky, KG.S.
Hull Dynamic Bending Due to Impact on Head Waves
Proc. of the Krylov Research Institute, No. 245
1968

100 Kaplan, P.; Malakhoff, A.
Hard Structure Slamming of SES Craft in Waves
AIAA/SNAME, Advanced Marine Vehicles Conference,
San Diego, CA, Paper No. 78-746
1978, April

101 Smiley, R.F.
A Semi-Empirical Procedure for Computing the Water-Pressure Distribution on Flat and V-Bottom Prismatic Surfaces During Impact on Planning
NACA Tech, Note 2583
1953, December

102 Kaplan, P.
Analysis and Prediction of Flat Bottom Slamming Impact of Advanced Marine Vehicles in Waves
ISP, Vol 34, No. 391
1987, March

103 Ohtsubo, H.; Fukumura, M.
Simplified Analysis of Impact Pressure Taking into Account of Splash
Journal of Soc. of Nav. Arch. of Japan, No. 162
1987, December

104 Tanizawa, K.
Self-Similar Solution of Wedge Entry Problem by B.E.M.
Journal of Soc. of Nav. Arch of Japan, No. 160
1987, December

105 Hughes, O.F.
Solution of the Wedge Entry Problem by Numerical Conformal Mapping
Journal of Fluid Mechanics, Vol 56
1972

106 Arai, M.; Matsunaga, A.
A Numerical and Experimental Study of Bow Flare Slamming
Journal of Soc. of Nav. Arch of Japan, No. 166
1989, December

107 Arai, M.; Matsunaga, K.
A Numerical Study of Water Entry of Two-Dimensional Ship-Shaped Bodies
PRADS
1989

108 Radev, D.
Numerical Realization of Problem for Entry of Rigid Circular Cylinder in Compressible Fluid
4th Intern. Congress Int. Marit. As. East Med., Vol. 5
1987

109 Ando, S.
Cushioning of Slamming Impact by Elastomeric Layers
Journal of Ship Research, Vol. 33, No. 3
1989

110 Watanabe, T.
Effects of Three-Dimensionality of Ship Hull on Wave Impact Pressure
Journal of Soc. Nav. Arch. of Japan, No. 162
1987, December

111 Song, J.; Dai, Y.; Li, W.
The Computation of Oscillatory Pressure and Impact Pressure for Two-Dimensional Bodies
Journal of Harbin Shipb. Engng. Inst., Vol. 9, No. 4
1988

112 Isaacson, M.; Bussiah, K.
Random Wave Slamming on Cylinders
Journal of Waterway, Port, Costal and Ocean Engng, No. 2
1993

113 Lewis, E.V.; Gerard, G.
A Long Range Research Program in Ship Structural Design
SSC Final Rpt No. SSC-124
1959, November

114 Lipis, V.B.; Remez, Y.V.
Diagrams for Safe Ship Routing in Rough Seas
Handbook, Moscow Transport Publ. House
1982

115 11th International Ship and Offshore Structures Congress
Report of Committee I.2, "Loads", China
1991

116 Kline, R.G.; Daidola, J.C.
Ship Vibration Prediction Methods and Evaluation of Influence of Hull Stiffness Variation on Vibratory Response
SSC, Rpt. No. 249
1979

117 Stavovy, A.B.; Chuang, S.L.
Analytical Determination of Slamming Pressures for
High Speed Vehicles in Waves
SNAME, JSR, Vol 20, No. 4
1976, December

118 Hadler, J.B.; Lee, C.M.; et al
Ocean Catamaran Seakeeping Design Based on the
Experiences of USNS Hayes
SNAME, Transactions
1974

119 Jasper, N.H.; Church, J.W.
Structural Seaworthiness Studies
SNAME, Transactions, Vol. 71
1963

120 Chuang, S.L.; Schroeder, E.A.; Wybraniec, S.
Numerical Analysis by Digital Computer Program ROSAS of Response
of Ship-Hull Structure at Sea
Numerical Analysis of Dynamics of Structures Proceedings of
EUROMECH Colloquim 122, Ecole Polytechnicue, Paris
1979, September 3-5

121 Chuang, S.L.
General Considerations in the Mathematical Modeling for
Three-Dimensional Computer Program ROSAS3
David Taylor Naval Ship Research and Development Center,
Rpt. 1185
1981

122 Chuang, S.L.
Numerical Modeling and Computer Programming for Program ROSAS3
David W. Taylor Naval Ship Research and Development Center,
Structural Department Report No. 1198
1958, August

123 Chuang, S.L.
Dynamic Structural Analysis in Time Domain by Digital Computer
ROSAS3 on Responses of Ship at Sea Proceedings of the International
Symposium on Marine Structures, Shanghai, China
1991, Septembaer 13-14

124 Chuang, S.L.; Birmingham, J.T.; et al
Experimental Investigation of Catamaran Cross-Structure Slamming
SITDL TR 11078, NSRDC Rpt. 4653, pp 55, MRIS-07-127751
1975, September

125 Kaplan, P.; Sargent, T.P.
Further Studies of Computer Simulation of Slamming and Other Wave-Induced Structural Loadings on Ships in Waves
SSC-231, MRIS-040601, NTIS-AD-752479
1972, July

126 Bishop, R.E.D., Clarke, J.D.; Price, W.G.
Comparison of Full Scale and Predicted Responses of Two Frigates in a Severe Weather Trail
RINA, Trans. v.126
1984

127 Belik, O.; Bishop, R.E.; Price, W.G.
Influence of Bottom and Flare Slamming on Structure Response
RINA, Vol 130, MTIF-02/10482
1988

128 Liebowitz, R.D.
Method for Predicting Slamming Forces on and Response of a Ship Hull
DTMB, Rpt. 1691
1963, September

129 Leibowitz, R.C.
Comparison of Theory and Experiment for Slamming of a Dutch Destroyer
DTMB, Rpt. 1511
1962, June

130 Kawakami, M.; Michimoto, J.; Kobayashi, K.
Prediction of Long Term Whipping Vibration Stress Due to Slamming of Large Full Ships in Rough Seas
ISP, No. 24
1977

131 Bishop, R.E.D.; Price, W.G.; Wu, Y.
A General Linear Hydroelasticity Theory of Floating Structures Moving in a Seaway
Royal Society of London Transactions, pp 375-426
1986

132 Aksu, S.; Price, W.G.; Temarel, P.
A Three Dimensional Theory of Ship Slamming in Irregular Oblique Seaway Advanced in Marine Structures - 2
Elsevier Applied Science, pp. 208-229
1991

133 American Bureau of Shipping
Estimate of Ship Bottom Slamming
ABS
1979, December

134 Ng, R.C.; Chen, H.H.
Analytical Study on Bow Flare Impact
American Bureau of Shipping: Phase I - 1979, July;
Phase II - 1980, February; Phase III - 1981, May;
Phase IV - 1982, June

135 Toki, N.; Hatakenaka, K.; Takahashi, T.; Fujii, H.
Experimental and Theoretical Approach to the Estimation of
Non-Linear Vertical Wave Loads
Journal of the Soc. Nav. Arch. of Japan
1983, November

136 Antonides, G.P.
A Computer Program for Structural Response to Ship Slamming (SLAM)
Naval Ship Research and Development Center
1975, July

137 Comparative Analysis of Analytical Predictions for
Hydrodynamic Loads in a Seaway
NAVSEA Technical Note 051-55W-TN-0094
1992

137a Beukelman, W.
Bottom Impact Pressure Due to Forced Oscillation
Delft, Netherlands, or ISP, Vol. 27
1980, May

138 Kaplan, P.; Sargent, T.P.; Raff, A.I.
An Investigation of the Utility of Computer Simulation to Predict
Ship Structural Response in Waves
SSC-197, DON, Tech Rpt.
1969, June

139 Kaplan, P.
Computer Simulation of Ship Structural Loads Due to Waves
AIAA/ASME, Structural Dynamics and Materials Conference,
San Antonio, TX, Paper No. 72-342
1972, April

140 Ochi, M.K.; Motter, L.E.
A Method to Estimate Slamming Characteristics for Ship Design
SNAME, NY Sec. Mtg.
1970

141 Ochi, M.K.
On Prediction of Extreme Values
SNAME, JSR
1973, March

142 Ochi, M.K.
Ship Slamming-Hydrodynamic Impact Between Waves and
Ship Bottom Forward
ASME, Fluid-Solid Interaction Symposium
1967, November

143 Szebehely, V.G.; Ochi, M.K.
Hydrodynamic Impact and Water Entry
Applied Mechanics Surveys, Spartan Books
1966

144 Ochi, M.D.; Schwartz, F.M.
Two Dimensional Experiments on the Effects of Hull Form
on Hydrodynamic Impact
DTMB, Rpt. 1994
1966

145 Clevenger, R.L.; Melberg, L.C.
Slamming of a Ship Structural Model
M.S. Thesis, MIT
1963, May

146 Chuang, S.L.
Slamming of Rigid Wedge-Shaped Bodies with Various
Deadrise Angles
DTMB, Rpt. No. 2268
1966, October

147 Chuang, S.L.
Experimental Investigation of Hydrodynamic Impact on
Inflatable Fabric Ship Sections
David Taylor Model Basin Report No. 2080
1965, October

148 Chuang, S.L.
Investigation of Impact of Rigid & Elastic Bodies with Water
NSRDC
1970

149 Hirano, S.; Yoshikava, S.; Himeno, Y.
Pressure Measurement on the Bottom of a Wedge-Form Planing Hull
Kansai Soc. Nav. Arch. of Japan, No. 208
1988, March

150 Hirano, S.; Uchida, S.; Himeno, Y.
Pressure Measurement on the Bottom of Prismatic Planing Hull
Kansai Soc. Nav. Arch. of Japan, No. 213
1990, March

151 Watanabe, I.; Tanizawa, K.; Sawada, H.
An Observation of Bottom Impact Phenomena by Means of
High Speed Video and Transparent Model
Journal of Soc. Nav. Arch. of Japan, No. 164
1988, December

152 Watanabe, I.; Ueno, M.; Sawada, H.
Effects of Bow Flare Shape to the Wave Loads of a Container Ship
Journal of Soc. Nav. Arch. of Japan, No. 166
1988, December

153 Chui, F.C.; Fujino, M.
Nonlinear Prediction of Vertical Motions and Wave Loads of
High-Speed Crafts in Head Seas
Intern. Shipb. Progress, Vol 36, No. 406
1989

154 Nagai, T.; Hashimoto, T.
On the Maximum Stress of Bottom Shell and Impulsive
Water Pressure of FRP High Speed Craft
West Jap. Soc. Nav. Arch., No. 79
1990, March

155 Sawada, H.; Watanabe, I.; et al
On an Elastic Model to Simulate Elastic Hull Responses of Ships
Ship Research Institute, Japan, Vol. 24, No. 2
1987

156 Paulling, R.
Strength of Ships
Principles of Naval Architecture, 2nd Rev., SNAME, Vol. I
1988

157 Sikora, J.R.; Dinsenbacher, A.L.
SWATH Structure: Navy Research and Development Applications
SNAME, Marine Technology, Vol. 27, No. 4, pp 211-220
1990, July

158 Wahab, R.; Pritcheff, C.; Ruths, L.
On the Behavior of the ASR Catamaran in Waves
Marine Technology
1971, July

159 Giannotti, J. G.; Fuller, N.R.
Slamming of High Performance Marine Vehicles
11th Annual Symp. of the Association of Senior Engineers
1974, March

160 Chuang, S.L.
Experimental Investigation of Rigid Flat Bottom Body Slamming
DTMB Rpt 2041, Sept. 1965;
SNAME, JSR, pp 1-17, 1966, March

161 Fujita, A.
Impact of Circular Plate Falling Upon a Water Surface
SNAJ, Journal
1954

162 Lewison, G.; MacLean, W.M.
The Effect of Entrapped Air Upon the Slamming of Ships Bottoms
University of California, Berkeley, CA, Rpt No. NA-66-5
1966

163 Johnson, R.S.
The Effect of Air Compressibility on a First Approximation to
the Ship Slamming Problem
SNAME, JSR
1968, March

164 Whitman, A.M.; Pancione, M.C.
Similitude Relation for Flat Plate Hydrodynamic Impact
Journal of Ship Research
1973, March

165 Gerlach, C.R.
Investigation of Water Impact of Blunt Rigid Bodies -
Size Scale Effects
Technical Report #2, Southwest Research Institute
1968, November

166 Nott, J.A.
Techniques for Simulating the Hydrodynamic Forces on Sonar Domes by Static Loads
DTMB, Rpt. 1441
1961, April

167 Lunchick, M.E.; Eibling, J.H.; Short, R.D.,Jr.
A Feasibility Study of Methods for Simulating by Static Forces the Nonuniform Hydrodynamic Pressures on Sonar Domes
DTMB, Rpt. 1134
1957, May

168 Garcia, W.J., Jr.
Experimental Study of Breaking Wave Pressures
Army Corps of Engrs., Vicksburg, MD
1968, September

169 Rose, C.W.
Shock Pressure of Breaking Waves
Fourth Conference on Coastal Engineering, Chicago
1953

170 Denny, D.F.
Further Experiments on Wave Pressures
Journal of Institution of Civil Engineers, Vol. 35, No. 4
1951, February

171 DeRouville, A.; Besson, P.; Petry, P.
Development of International Studies on Wave Force
Translation, U.S. Army Engineer Waterways Experiment Station Research Center, Vicksburg, Miss., TR N 40-13
1940, May

172 Nagai, S.
Shock Pressures Exerted by Breaking Waves on Breakwaters
ASCE Journal, Waterways and Harbors Division, Vol. 86, WW2
1960, June

173 Rundgren, L.
Water Wave Forces: A Theoretical and Laboratory Study
Transactions of Royal Institute of Technology, Institution of Hydraulics, Stockholm, Bulletin 54
1958

174 Band, E.G.U.
Predicting the Unpredictable - Development of Rational Design Loads for High Perfordmance Vessels
Band, Lavis & Assoc., Inc., High Speed Surface Craft Exhibition and Conference, Sussex, UK
1980, June

175 Faltinsen, O.M.
On Seakeeping of Conventional and High-Speed Vessels
Journal of Ship Research, Vol. 37, No. 2
1993

176 Yamamoto, Y.; Iida, K.; Fukasawa, T.; Mirakami, T.; Arai, M.; Ando, M.
Structural Damage Analysis of a Fast Ship Due to Bow Flare Slamming
Intern. Shipb. Progress, Vol. 32, No. 369
1985

177 Giannotti, J.G.
Bibliography on Slamming, Impact and Other Transient Related Phenomena
Prep. by Giannotti & Assoc., Inc. for SNAME Panel HS-2 of the Hull Structure Committee, 114 pp.
1985

178 Spinelli, L.
Theoretical Research and Experiments in Slamming
Registro Italiano Navale, Genoa, Italy
1967, February

179 Daidola, J.C.; Mishkevich, V.G.; Bromwell, A.
Bibliographic Summary on Hydrodynamic Impact Loading on Displacement Ship Hulls
M. Rosenblatt & Son, Inc., Draft Report for SSC Project SR-1342
June 1994

180 Greenspon, J.E.
Sea Tests of the USCGC UNIMAK; Part 2: Statistical Presentation of the Motions, Hull Bending Moments and Slamming Pressures for Ships of the AVP Type
DTMB Report 977
1957, April

181 Heller, S.R.; Jasper, N.H.
On the Structural Design of Planing Craft
RINA, Quarterly Transactions
1960, July

182 Jasper, N.H.; Birmingham, J.T.
Strins and Motions of USS Essex During Storms Near Capt Horn
DTMB, Rpt. No. 1216
1958, August

183 Birmingham, J.T.; Palmer, F.W.
Stresses and Motions of a Destroyer Escort in Random Seas
NSRDC, Rpt. No. 2610
1968, March

184 Palmer, F.W.; Birmingham, J.T.
Structural Seaworthiness and Hull Deckhouse Interaction
of USCG Hamilton (WHEC 715)
NSRDC, Structures Note 139
1969, June

185 Jasper, N.H.; Andrews, J.N.
Preliminary Report of Strains and Motions of USS Ranger (CVA 61)
During a Voyage Around Capt Horn
DTMB, Report No. 1289
1959, January

186 Birmingham, J.P.; Brooks, R.L.; Jasper, N.H.
Statistical Presentation of Motions and Hull Bending
Moments of Destroyers
DTMB, Rpt. No. 1198
1960, September

187 Bledsoe, M.D.; Bussemaker, O.; Cummins, W.E.
Seakeeping Trials on Three Dutch Destroyers
SNAME, Transactions, Vo. 68, pp 37-137, DTMB Rpt. 1559
1960

188 Palmer, F.W.
Structural Seaworthiness Evaluation of USS Benicia
NSRDC, Structures Note 290
1974, October

189 Andrews, J.N.; Dinsenbacher, A.L.
Response Amplitude Operators and Whipping Response of
Carrier Model in Random Waves
NSRDC, Rpt. No. 2522
1968, January

190 Andrews, J.N.; Chuang, S.L.
Seaworthiness Analog Computer
DTMB, Rpt. No. 1829
1965, August

191 Wheaton, J.W.; et al.
Analysis of Slamming Data from the S.S. Wolverine State
Teledyne Material Research Co., Rpt. No. E-116(a)
1969, December

192 Pegg, N.G.; Vernon, T.A.; Wegner, L.; et al
Force Elevation Prediction of Measured Bow Flare Plate
Stresses Under Dynamic Wave Loading
RINA, Vol. 133, MTIF-12/12164
1989

193 Takemoto, H.; Hasizume, Y.; et al
Full-Scale Measurements of Wave Impact Forces and Hull
Response of a Ship in Waves
Journal of Soc. Nav. Arch. of Japan, No. 164
1988, December

194 Purcell, E.S.; Allen, S.J.; Walker, R.T.
Structural Analysis of the U.S. Coast Guard Island Class Patrol Boat
Trans. SNAME, Vol. 96
1988

195 Barabanov, N.V.; Ivanov, N.A.; Kulesh, V.A.
External Slamming Loads and Design of Low Bottom Structures
Sudostroenie, No. 5
1985

196 Rask, I.
Slamming Pressure in Short-Crested and Oblique Seas
Chalmers Univ. of Technology, Goteborg
1986

197 Bugakov, V.N.
Analysing Hull Bottom Structures for Slamming Effects
Sudostroenie, No. 7
1986

198 Bugakov, V.N.
Storm Damage and Safe Ship Speed
Sudostroenie, No. 12
1988

199 Aertssen, G.; van Sluys, M.F.
Service Performance and Seakeeping Trials on
a Large Containership
Trans. of Royal Inst. of Naval Arch., Vol 116
1974

200 Tasaki, R.; Takerawa, S.; Takaishi, Y.
Collection and Analysis of Full Scale Data
Report of Seakeeping Committee, 14ITTC, Ottawa
1975

201 Cruikshank, J.M.; Landsburg A.C.
Guidelines for Operating at IMCO Segregated Ballast Levels
IMCO, DE XYII, London
5.1.1977

202 Solomentsev, O.I.
Consideration of the Seaworthiness Requirements on
Designing Sea-Going Catamarans
Sudostroenie, No. 4
1988

203 Ochi, M.K.; Motter, L.E.
A Method to Estimate Slamming Characteristics for Ship Design
SNAME, Marine Technology
1971, April

204 Chuang, S.L.
Impact Pressure Distribution on Wedge-Shaped Hull Bottom
of High-Speed Craft
DTNSRDC Report No. 2953
1969, August

205 Chuang, S.L.
Design Criteria for Hydrofoil Hull Bottom Plating
DTNSRDC, Report No. 3509
1975, August

206 Chuang, S.L.
Slamming Tests of Three Dimensional Models in Calm Water and Waves
NSRDC, Rpt. No. 4095, MRIS-050494, NTIS-AD-767021/9
1973, September

207 Intentionally left blank.

208 Allen, R.G.; Jones, J.R.
A Simplified Method for Determining Structural Design Limit Pressures on High Performance Marine Vehicles
AIAA/SNAME Advanced Marine Vehicle Conference
1978, April

209 Savitsky, D.; Brown, P.W.
Procedures for Hydrodynamic Evaluation of Planning Hulls in Smooth and Rough Water
Marine Technology
1976, October

210 Structural Design Manual for Naval Surface Ships,
Naval Ship Engineering Center, Dept. of the Navy
1976, December

211 Koelbel, J.
Comments on the Structural Design of High Speed Craft
SNAME Chesapeake Section
1993, November

212 Brown, P.O.; Fridsma, G.; Klosinski, W.E.
Performance and Seakeeping Tests and Analysis of a Structural Loads Model of a L/B=6 Ruotant Sidewall SES
Division Laboratory, Rpt. No. 2137
2981, March

213 Troesch, A.
Private Communication
1993, July 13

214 Troesch, A.W.; Kang, C.-G.
Hydrodynamic Impact Loads on Three-Dimensional Bodies
16th Symposium on Naval Hydrodynamics, Berkeley
1986

215 Ochi, M.K.
Prediction of Occurrence and Severity of Ship Slamming at Sea
5th Symp. of Naval Hydrodynamics, ONR
1964

216 Ochi, M.K.; Motter, L.E.
Prediction of Extreme Ship Responses in Rough Seas
of the North Atlantic
Int'l Symp. on the Response of Marine Vehicles and Structures
in Waves, University College
1974, April

217 Chuang, S.L.
Experimental Investigation of Hydrodynamic Impact on Inflatable
Fabric Ship Sections
Model Basin Report No. 2080
1965, October

218 Kawakami, M.; Tanaka, K.
On Shipping Impact of Green Seas & Whipping Vibrations
of a Large Full Ship
WJSNA, Transactions, No. 50
1975, August

219 Dalzell, J.F.
A Note on Structural Loads Analysis in the Reliability Context
David Taylor Research Center, DTRC/SHD-1374-01
1991, November

220 Lin, W.M.; Yue, D.K.P.
Numerical Solutions for Large-Amplitude Ship Motions
in the Time Domain
18th Symposium on Naval Hydrodynamics, Ann Arbor
1990, August

221 Maskew, B.; Troesch, A.; Wang, M.
Comparison of Calculated and Measured Loads on a Flared Body
Oscillating in a Free Surface
20th Symposium on Naval Hydrodynamics, Santa Barbara
1994, August

222 Aksu, KS.; Price, W.G.; Temarel, P.
A Comparison of Two-Dimensional and Three-Dimensional
Hydroelasticity Theories Including the Effect of Slamming
Proc. of Ins. of Mech. Engrs., vol. 205, N 1
1991

# PROJECT TECHNICAL COMMITTEE MEMBERS

The following persons were members of the committee that represented the Ship Structure Committee to the Contractor as resident subject matter experts. As such they performed technical review of the initial proposals to select the contractor, advised the contractor in cognizant matters pertaining to the contract of which the agencies were aware, and performed technical review of the work in progress and edited the final report.

| | |
|---|---|
| Mr. Alan Engle | Naval Sea Systems Command |
| Dr. Walter Maclean | U.S. Merchant Marine Academy |
| Mr. James White | U.S. Coast Guard |
| Mr. Richard Dai | U.S. Coast Guard |
| Dr. Subrata Chakrabarti | Chicago Bridge and Iron |
| Mr. Raymond Ng | American Bureau of Shipping |
| Mr. William Siekierka | Naval Sea Systems Command,<br>Contracting Officer's<br>Technical Representative |
| Dr. Robert Sielski<br>Mr. Alex Stavavoy | National Academy of Science,<br>Marine Board Liaison |
| Cdr. Steve Sharpe | U.S. Coast Guard, Executive Director<br>Ship Structure Committee |

## COMMITTEE ON MARINE STRUCTURES

Commission on Engineering and Technical Systems

National Academy of Sciences – National Research Council

The COMMITTEE ON MARINE STRUCTURES has technical cognizance over the interagency Ship Structure Committee's research program.

John Landes, University of Tennessee, Knoxville, TN
Howard M. Bunch, University of Michigan, Ann Arbor, MI
Bruce G. Collipp, Marine Engineering Consultant, Houston, TX
Dale G. Karr, University of Michigan, Ann Arbor, MI
Andrew Kendrick, NKF Services, Montreal, Quebec
John Niedzwecki, Texas A & M University, College Station, TX
Barbara A. Shaw, Chairman, Pennsylvania State University, University Park, PA
Robert Sielski, National Research Council, Washington, DC
Stephen E. Sharpe, Ship Structure Committee, Washington, DC

### DESIGN WORK GROUP

John Niedzwecki, Chairman, Texas A&M University, College Station, TX
Bilal Ayyub, University of Maryland, College Park, MD
Ovide J. Davis, Pascagoula, MS
Maria Celia Ximenes, Chevron Shipping Co., San Francisco, CA

### MATERIALS WORK GROUP

Barbara A. Shaw, Chairman, Pennsylvania State University, University Park, PA
David P. Edmonds, Edison Welding Institute, Columbus, OH
John F. McIntyre, Advanced Polymer Sciences, Avon, OH
Harold S. Reemsnyder, Bethlehem Steel Corp., Bethlehem, PA
Bruce R. Somers, Lehigh University, Bethlehem, PA

## RECENT SHIP STRUCTURE COMMITTEE PUBLICATIONS

Ship Structure Committee Publications – A Special Bibliography

SSC-386 Ship's Maintenance Project R. Bea, E. Cramer, R. Schulte-Strauthaus, R. Mayoss, K. Gallion, K. Ma, R. Holzman, L. Demsetz 1995

SSC-385 Hydrodynamic Impact on Displacement Ship Hulls – An Assessment of the State of the Art J. Daidola, V. Mishkevich 1995

SSC-384 Post-Yield Strength of Icebreaking Ship Structural Members C. DesRochers, J. Crocker, R. Kumar, D. Brennan, B. Dick, S. Lantos 1995

SSC-383 Optimum Weld-Metal Strength for High Strength Steel Structures R. Dexter and M. Ferrell 1995

SSC-382 Reexamination of Design Criteria for Stiffened Plate Panels by D. Ghose and N. Nappi 1995

SSC-381 Residual Strength of Damaged Marine Structures by C. Wiernicki, D. Ghose, N. Nappi 1995

SSC-380 Ship Structural Integrity Information System by R. Schulte-Strathaus, B. Bea 1995

SSC-379 Improved Ship Hull Structural Details Relative to Fatigue by K. Stambaugh, F. Lawrence and S. Dimitriakis 1994

SSC-378 The Role of Human Error in Design, Construction and Reliability of Marine Structures by R. Bea 1994

SSC-377 Hull Structural Concepts For Improved Producibility by J. Daidola, J. Parente, and W. Robinson 1994

SSC-376 Ice Load Impact Study on the NSF R/V Nathanial B. Palmer by J. St. John and P. Minnick 1995

SSC-375 Uncertainty in Strength Models for Marine Structures by O. Hughes, E. Nikolaidis, B. Ayyub, G. White, P. Hess 1994

SSC-374 Effect of High Strength Steels on Strength Considerations of Design and Construction Details of Ships by R. Heyburn and D. Riker 1994

SSC-373 Loads and Load Combinations by A. Mansour and A. Thayamballi 1994

SSC-372 Maintenance of Marine Structures: A State of the Art Summary by S. Hutchinson and R. Bea 1993

SSC-371 Establishment of a Uniform Format for Data Reporting of Structural Material Properties for Reliability Analysis by N. Pussegoda, L. Malik, and A. Dinovitzer 1993

SSC-370 Underwater Repair Procedures for Ship Hulls (Fatigue and Ductility of Underwater Wet Welds) by K. Grubbs and C. Zanis 1993

SSC-369 Reduction of S-N Curves for Ship Structural Details by K. Stambaugh, D. Lesson, F. Lawrence, C-Y. Hou, and G. Banas 1993